



universität  
wien

# DIPLOMARBEIT

Titel der Diplomarbeit

Interactions between the peripheral and local immune system and tumor proliferation – clinical relevance for patients with epithelial ovarian cancer

Verfasserin

Anna Bachmayr-Heyda

angestrebter akademischer Grad

Magistra der Naturwissenschaften (Mag.rer.nat.)

Wien, 2012

Studienkennzahl lt. Studienblatt:

A 441

Studienrichtung lt. Studienblatt:

Diplomstudium Genetik - Mikrobiologie

Betreuerin / Betreuer:

Univ-Prof. Dr. Thomas Decker



## **Preamble**

I wrote the following diploma thesis in the Molecular Oncology Group of the Department of Obstetrics and Gynecology (Medical University of Vienna) which coordinates the OVCAD consortium (OVCAD—Ovarian Cancer: Diagnosis of a silent killer, [www.ovcad.eu](http://www.ovcad.eu)). In the course of the diploma thesis I participated in the data generation and writing of manuscripts for three research articles which have recently been submitted by members of our group and are attached to the diploma thesis. As some data of the diploma thesis were used for these manuscripts, parts of the data and results overlap with the following work.

Anna Bachmayr-Heyda



# Tables of Contents

<b>1</b>	<b>Introduction .....</b>	<b>1</b>
1.1	Ovarian cancer .....	1
1.2	Blood markers for EOC .....	5
1.2.1	Diagnostic 13 gene panel .....	6
1.2.2	Prognostic seven gene panel .....	7
1.2.3	Which are the major immune cells involved in these two gene panels? .....	9
1.3	Tumor proliferation .....	9
1.4	Tumor immunology .....	10
1.4.1	Cytotoxic T lymphocytes .....	12
1.4.2	Regulatory T cells (Tregs).....	13
1.4.3	Myeloid derived suppressor cells (MDSCs) .....	14
1.4.4	Macrophages .....	14
1.4.5	The immunosuppressive microenvironment of ovarian cancer .....	16
1.5	Aim of this study .....	17
<b>2</b>	<b>Materials and methods .....</b>	<b>19</b>
2.1	Study population and patients' materials.....	19
2.2	Cell separation from whole blood.....	20
2.3	Isolation of a “high density” blood leukocyte fraction from whole blood .....	22
2.4	RNA extraction.....	23
2.5	cDNA synthesis .....	23
2.6	qPCR.....	24
2.7	Evaluation of RT-qPCR data.....	25
2.8	Immunohistochemical and -fluorescent staining .....	25
2.9	Image digitalization .....	27

2.10	Quantification of the immunohistochemical staining using HistoQuest .....	27
2.11	Quantification of the immunofluorescent staining using TissueQuest .....	29
2.12	Evaluation and statistical analyses.....	29
<b>3</b>	<b>Results .....</b>	<b>32</b>
3.1	Study population and patients' material .....	32
3.2	Blood cell gene signatures .....	34
3.2.1	Diagnostic panel: heterogeneous expressions and significant differences between patient groups .....	34
3.2.2	Prognostic panel: peaks in the fractions CD14 and CD25 .....	43
3.2.3	Principal Component Analysis of expression patterns in the blood fractions.....	44
3.3	Tumor microenvironment.....	47
3.3.1	Immunohistochemical staining .....	47
3.3.2	Immunofluorescent staining .....	51
3.3.3	Correlation of TAMs and the prognostic blood cell signature .....	54
3.3.4	RT-qPCR CD8 relative expression values .....	54
3.3.5	Correlation with clinicopathological factors .....	54
3.3.6	Survival analyses.....	55
<b>4</b>	<b>Discussion.....</b>	<b>61</b>
4.1	Blood cell gene signatures .....	61
4.1.1	Diagnostic panel.....	61
4.1.2	Prognostic panel .....	63
4.1.3	Principal Component Analysis.....	64
4.1.4	Limitations and outlook .....	64
4.2	Tumor microenvironment.....	66
4.2.1	Study population .....	66
4.2.2	Immunohistochemical staining .....	66

4.2.3	Immunofluorescent staining.....	68
4.2.4	Correlation of TAMs and the prognostic blood cell signature.....	68
4.2.5	RT-qPCR CD8 relative expression values .....	70
4.2.6	Correlation with clinicopathological factors .....	70
4.2.7	Survival analyses.....	71
4.2.8	Trouble shooting and limitations.....	76
4.3	Conclusion .....	78
<b>5</b>	<b>List of Abbreviations .....</b>	<b>80</b>
<b>6</b>	<b>Abstract.....</b>	<b>83</b>
<b>7</b>	<b>Zusammenfassung.....</b>	<b>84</b>
<b>8</b>	<b>References .....</b>	<b>85</b>
<b>9</b>	<b>Acknowledgements.....</b>	<b>92</b>
<b>10</b>	<b>Curriculum Vitae .....</b>	<b>93</b>





# 1 Introduction

## 1.1 Ovarian cancer

Ovarian cancer is one of the most deadly malignancies in women with 226,000 new cases and 140,000 deaths worldwide per year (Jemal et al., 2011). Despite increasing knowledge in the etiology of ovarian cancer and improvements in surgery and chemotherapy there has been little change in mortality. Delayed diagnosis due to a lack of specific symptoms and a lack of routinely used screening methods leads to diagnosis of about 75% of patients at advanced stages (III and IV). Five year survival rates decrease dramatically for these patients from over 90% for International Federation of Gynecology and Obstetrics (FIGO) stage I to less than 40% for FIGO stages III and IV (Holschneider and Berek, 2000). Thus, markers for early detection of ovarian cancer to improve overall survival (OS) are urgently needed.

Risk factors for ovarian cancer are a positive family history of ovarian cancer, null parity, refractory infertility and prior history of pelvic inflammatory disease, polycystic ovary syndrome and endometriosis. The major known hereditary predispositions for ovarian cancer are BRCA1 and BRCA2 mutations as well as familial nonpolyposis colorectal cancer syndrome (also known as lynch II syndrome) caused by mutations in DNA mismatch repair genes. Protective factors for ovarian cancer are multiparity, the use of oral contraceptives, tubal ligation and hysterectomy. Currently valid prognostic factors include the patients' performance status, age, stage of disease (classified according to the FIGO classification), tumor grade representing the degree of differentiation and the debulking status after cytoreductive surgery (Holschneider and Berek, 2000).

FIGO classification for ovarian carcinoma consists of four stages (Odicino et al., 2008):

stage I: growth limited to the ovaries

stage II: growth involving one or both ovaries with extension limited to the pelvis

stage III: growth involving one or both ovaries with histologically confirmed peritoneal implants outside the pelvis and/or positive retroperitoneal or inguinal nodes; superficial liver metastases equals stage III.

stage IV: growth involving one or both ovaries with distant metastases; if pleural effusion is present, there must be positive cytology to allot a case to stage IV; parenchymal liver metastasis equals stage IV.

The degree of differentiation is usually scored by a three-tier tumor grading scheme:

1 – low grade: well-differentiated tumors with well-structured papillae and few necrotic areas; cells exhibit low mitotic activity.

2 – intermediate grade

3 – high grade: poorly-differentiated tumors often forming solid masses with necrosis, hemorrhage and slit-like spaces; cells exhibit nuclear atypical phenotypes such as pleomorphic nuclei, nuclear enlargement, prominent nucleoli and high mitotic activity.

Ovarian carcinomas are a heterogeneous group of distinct histological subtypes. 90% of ovarian cancers are of epithelial origin. Non-epithelial ovarian cancers comprise sex-cord-stromal tumors, germ-cell tumors and indeterminate tumors. Borderline (i.e. low malignant potential) tumors account for 10% to 20% of epithelial ovarian cancer (EOC). In invasive EOC, on which this study was confined, the following histological subtypes are the most important ones: serous (about 75% to 80%), mucinous (about 10%) and endometrioid (about 10%). Clear cell, small cell, undifferentiated and mixed cell are less common EOC histological subtypes (Holschneider and Berek, 2000). Generally, the histological subtypes of ovarian cancer differ considerable in their origin, epidemiology and mutation status. The term ovarian cancer mainly defines the location of dissemination (Vaughan et al., 2011).

Two main genetic molecular pathways in serous tumorigenesis are known. i) Type I EOC: the low grade pathway describes the development of low grade carcinomas from benign cystadenomas through the transition state of borderline tumors. This pathway is characterized by mutations of the oncogenes BRAF and KRAS and microsatellite instability. Rare events in low grade carcinoma are p53 mutations leading to high grade carcinoma. ii) Type II EOC: the high grade pathway represents a de novo development of high grade carcinoma. EOCs of this type frequently have mutations causing genetic instability (Lax, 2009).

In a recently published study by The Cancer Genome Atlas Research Network including hundreds of high grade serous EOC samples, which account for about 70% of ovarian cancer deaths, p53 mutations have been reported in 96% of tumors, BRCA1/2 germline or somatic mutations in about 20% and lost BRCA1 expression via promoter hypermethylation in 11%. Furthermore, the authors have described somatic mutations including the genes RB1, NF1, CSMD3, CDK12, BRAF, PIK3CA, KRAS and NRAS with a lower prevalence of 2% to 6%. More than 100 significant DNA copy number aberrations including amplifications encoding for CCNE1, MAPK1, KRAS and MECOM have been found in at least 10% of tumor samples. Deletions encoding for known tumor suppressor genes such as PTEN, RB1 and NF1 have been

found in at least 2% of tumor samples. Reduced expression of more than 150 genes including *AMT*, *CCL21*, *SPARCL1*, *RAB25* and *BRCA1* due to increased promoter methylation in tumors have been reported. Pathway analyses have indicated defective homologous recombination in about half of the studied cases and altered *FOXO1* signaling in nearly 90% (TCGA, 2011).

The question of the origin of ovarian cancer is still difficult to answer, especially because most tumors are diagnosed at advanced stages. Recent findings suggest that many ovarian cancer types derive from non-ovarian tissues (Vaughan et al., 2011). Prophylactic removing of the ovaries in high-risk patients revealed premalignant phenotypes or early stage carcinoma in numerous patients. Diagnosed tumors in these patients were all of the high grade type and localized in the area of the fallopian tubes indicating them as probable source of high grade tumors (Holschneider and Berek, 2000; Lax, 2009; Vaughan et al., 2011).

However, two different models about the origin of serous ovarian carcinoma coexist: i) In the transformation theory, adenomas and cystadenomas develop from ovarian surface epithelia and from inclusion cysts of ovarian surface epithelia which undergo transformations causing malignant cell behavior. This theory is favored by the fact that inclusion cysts and ovarian carcinoma are associated with frequent ovulations (see below factors leading to ovarian carcinogenesis). ii) The transport theory postulates that serous carcinoma, mostly of the high grade type, arise from epithelial cells from the fallopian tubes which further metastasize to the ovary (Lax, 2009). According to latest publications, mucinous ovarian cancer often derives from the gastrointestinal tract, while endometrioid and clear cell ovarian cancer arises from endometriosis (Vaughan et al., 2011). The different origins of the histological subtypes of ovarian cancer are depicted in Figure 1.

Until recently, the most favored theories about factors leading to ovarian carcinogenesis proposed that incessant ovulation causing repetitive disruption and repair of the ovarian epithelium bears a higher risk of spontaneous mutations leading to ovarian cancer. Consistently, women using oral contraceptives have a reduced risk of ovarian cancer. Alternatively, excessive gonadotropin stimulation and/or pelvic contaminants and carcinogens were believed to increase the risk of ovarian cancer (Holschneider and Berek, 2000). However, in light of new data indicating the fallopian tubes as probable origin of high grade serous EOC these theories have to be re-evaluated.

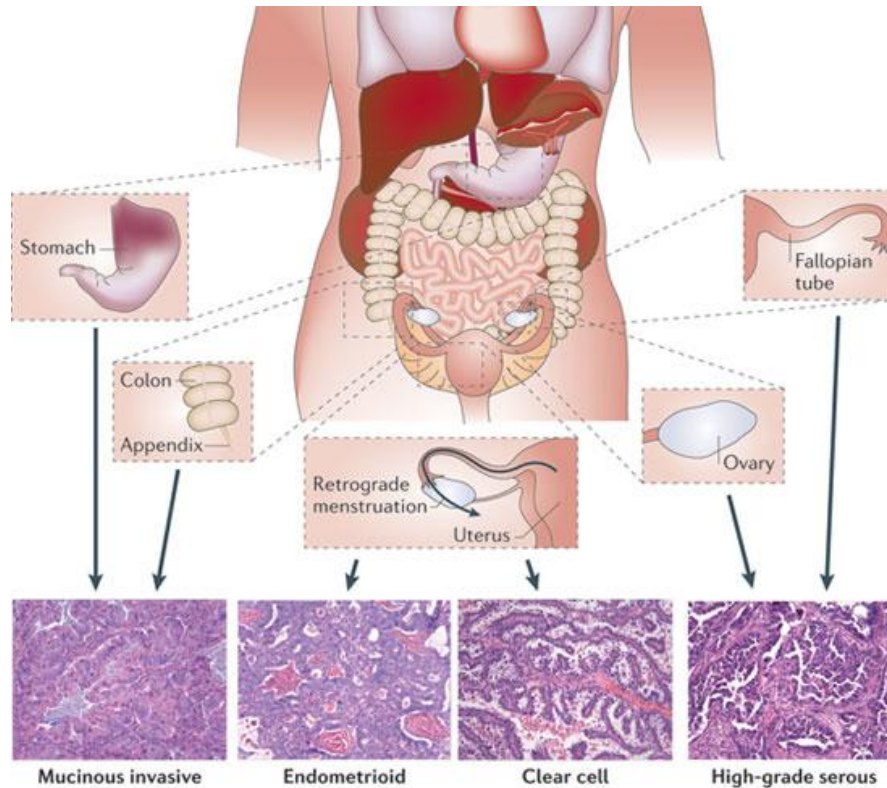


**Figure 1.** The origins of the histological ovarian cancer subtypes. Mucinous ovarian cancers are believed to derive from the gastrointestinal tract. Endometrioid and clear cell cancers are likely to have their origins in endometriosis. High grade serous ovarian cancers derive either from the ovarian surface or from the fallopian tubes (Vaughan et al., 2011).

Residual tumor after cytoreductive surgery is one of the most important prognostic factors in EOC patients. However, several cut-off values for optimal surgical cytoreduction are in use. Most clinicians use cut-off values of macroscopic visibility, 1 or 2 cm for the presence of residual tumor load. A survival benefit of patients with residual disease  $\leq 1$  cm compared to patients with residual disease  $>1$  cm has been reported. However, there is growing evidence that patients with no macroscopically visible residual tumor have better survival compared to women with visible residual disease  $\leq 1$  cm (Chang and Bristow, 2012). A study comprising only FIGO stage IV EOC patients has even described similar survival for patients with residual tumor of 0.1 to 1 cm and for patients with residual tumor  $>1$  cm, while macroscopically complete resection has been associated with improved survival compared to both categories of residual tumor load (Wimberger et al., 2010). Together, these results support the current surgical approach aiming not only to reduce the tumor load, but to remove all macroscopically visible lesions.

However, this cytoreductive surgery approach for EOC patients is complicated and involves risks. Not all patients might benefit to the same extent from this extensive surgery.

Thus, markers predicting patients' survival benefit from the debulking surgery could help to decide to which extent aggressive cytoreductive surgery should be conducted in patients in whom optimal debulking is difficult and risky to achieve.

## **1.2 Blood markers for EOC**

The poor prognosis of ovarian cancer and the lack of specific symptoms in early stages have caused great effort to establish screening programs to detect patients at early stages. Screening attempts include pelvic examinations, tumor marker measurements and ultrasonography. However, results are not satisfying and still, no additional screening marker for ovarian cancer is currently sensitive and specific enough for routine applications. The most widely used serum biomarker for ovarian cancer is cancer antigen 125 (CA125) with increased levels in more than 80% of ovarian cancer patients. However, the sensitivity for early stages is below 60%. Furthermore, the specificity of CA125 is limited since several benign gynecological (e.g. endometriosis) and medical conditions as well as other malignancies such as endometrial cancer and pancreatic cancer are characterized by increased CA125 levels. Additionally, higher CA125 levels are found in pre-menopausal women compared to women in post-menopause. Due to the impaired sensitivity and specificity of CA125 as an ovarian cancer biomarker many other serum markers have been evaluated in combination with CA125 such as leptin, prolactin, osteopontin, insulin-like growth factor II (IGF-II), macrophage migration inhibitory factor (MIF), human epididymis protein 4 (HE4), soluble mesothelin-related peptide (SMRP), CA72-4, human epidermal growth factor receptor 2 (HER-2/neu), inhibin and activin. But even the combination of several serum biomarkers do not reach required sensitivities and specificities (Moore et al., 2010).

In the search for blood biomarkers for the diagnosis of cancer, besides serum proteins, also gene expression analyses of blood cells have been performed. As cancer interacts with the immune system, infiltrating leukocytes can be found in the tumor microenvironment and also the peripheral immune system reacts to the cancer. Therefore, the evaluation of peripheral immune cell gene expressions can serve as an indicator for a malignancy. However, most data about the systemic immune response to cancer have been published for mouse models, breast cancer and non-gynecological cancers, while the interaction of ovarian cancer with the systemic immune system remains to be further elucidated. For breast cancer, gene expression profiling of peripheral blood cells has been described for early detection (Aaroe et al., 2010; Sharma et al., 2005).

Furthermore, blood biomarkers are of increasing scientific interest regarding their applicability as prognostic indicators for patients with a diagnosed malignant disease and to deduce therapeutic implications. There is evidence that a systemic inflammatory state is associated with a poor outcome in patients with malignant diseases including ovarian cancer (Hefler et al., 2008). Moreover, a link between the peripheral immune system and prognosis in human stroke (Urrea et al., 2009) and tumor development in mice (Augier et al., 2010) has been established. However, the role of the peripheral immune system in chemotherapy response and (fatal) side effects is poorly understood.

Recently, our working group has developed two molecular immune response signatures in blood leukocytes in the course of the EU-project OVCAD (OVCAD–Ovarian Cancer: Diagnosis of a silent killer, [www.ovcad.eu](http://www.ovcad.eu); coordinator Prof. Zeillinger, data not published). One of the gene signatures has been developed with the aim to detect EOC at early stages. The other gene signature has been developed with the aim to describe a prognostic signature for OS and death within two years after diagnosis in EOC patients. The gene names, function and corresponding Assay-on-demand TaqMan<sup>®</sup> probes of the genes comprised in the diagnostic and the prognostic gene signatures as well as the used housekeeping genes are summarized in Table 1, 2 and 3, respectively.

### **1.2.1 Diagnostic 13 gene panel**

The 13 gene panel for early detection of EOC includes the genes CFP, NOXA1, NEAT1, BC037918, DIS3, ZNF419, CCR2, B4GALT1, PAPOLG, PRIC285, AP2A1, C1orf63 and OSM (Table 1). A linear combination of the single expression values with coefficients listed in Table 1 is a measure of the relative risk of EOC and reaches a specificity of 99% and a sensitivity of 88%.

The panel was developed by means of a whole genome transcriptomics microarray approach comparing expressions of 29,000 genes in a “high density” blood leukocyte fraction (see 2.3) from 44 EOC patients and 19 controls comprising healthy blood donors and patients with cystadenoma, a subsequent significance analysis of the microarray data and reverse transcriptase quantitative PCR (RT-qPCR). Finally the 13 gene panel was validated with 239 EOC patients and 104 controls (healthy blood donors and patients with cystadenoma and low malignant potential tumors). In addition, abundances of six previously described plasma proteins were determined for 224 EOC patients and 65 controls: leptin, prolactin, osteopontin, IGF-II, MIF and CA125 (Visintin et al., 2008). The combined analysis of blood cell gene

expression and plasma protein based biomarkers in one model increases sensitivity and specificity which could allow earlier diagnosis.

**Table 1.** Gene names and functions of the 13 genes of the diagnostic signature, corresponding Assay-on-Demand TaqMan® probes, regulation in ovarian cancer patients and coefficients of the combined diagnostic model.

Gene symbol	TaqMan® probe	Gene name	Function	Regulation <sup>a</sup>	Co-efficients
CFP	Hs00175252_m1	complement factor properdin	Alternative pathway for complement activation	Down FC: -0.25	0.28
NOXA1	Hs01017917_m1	NADPH oxidase activator 1	Activates NADPH oxidases	Down FC: -0.49	-0.38
NEAT1	Hs01008264_s1	non-protein coding RNA 84	Non-coding RNA	Up FC: 1.53	0.26
BC037918	Hs00860048_g1	(no ORF in transcript BC037918)	Non-coding RNA	Up FC: 1.07	0.34
DIS3	Hs00209014_m1	DIS3 mitotic control homolog ( <i>S. cerevisiae</i> )	RNase, part of the exosome complex	No (FC: 0.01)	0.63
ZNF419	Hs00226724_m1	zinc finger protein 419	Zinc finger protein	No (FC: -0.07)	0.05
CCR2	Hs00356601_m1	chemokine (C-C motif) receptor 2	Chemokine receptor	Up FC: 0.34	0.26
B4GALT1	Hs00155245_m1	UDP-Gal:betaGlcNAc beta 1,4-galactosyltransferase, polypept. 1	Galactosyltransferase	No (FC: -0.21)	0.15
PAPOLG	Hs00224661_m1	poly(A) polymerase gamma	Poly(A) polymerase	Down FC: -0.69	-0.56
PRIC285	Hs00375688_m1	peroxisomal proliferator-activated receptor A interacting complex 285	Nuclear transcriptional coactivator for several nuclear receptors	Down FC: -1.12	-1.34
AP2A1	Hs00367123_m1	adaptor-related protein complex 2, alpha 1 subunit	Clathrin coat assembly	Down FC <sup>b</sup> : -0.52	-0.18
C1orf63	Hs00220428_m1	chromosome 1 ORF 63	Unknown	Down FC: -1.36	0.64
OSM	Hs00171165_m1	oncostatin M	IL-6 family cytokine	Down FC: -1.14	-1.05

<sup>a</sup>Significant down- or up-regulation in blood cells of EOC patients compared to healthy blood donors (T-test, corrected for multiple testing).

<sup>b</sup>FC are actually log<sub>2</sub>-FC values.

### 1.2.2 Prognostic seven gene panel

The second gene signature has been described to predict OS and death within two years after diagnosis (with or without recurrence) in advanced stage EOC patients independently of other clinical parameters. It comprises the seven genes SRC, GUCY1B3, TUBB1, GUCY1A3,

TUBA8, EGF and TRIM14 (Table 2). For patients who died within two years after EOC diagnosis, one can assume that rather lethal side effects of the chemotherapy than the cancer per se caused the death. As described for the 13 genes, the seven gene panel derived from microarray data from 48 EOC patients' "high density" blood leukocyte fractions (see 2.3) and was validated with RT-qPCR including 218 EOC patient samples. The seven genes were highly correlated with each other and most of them are involved in the gap junction pathway. Principal Component Analysis (PCA) was performed to reduce the complexity of the gene expression data. This analysis revealed that Principal Component 1 (PC1) (standing for 82% of data variance) and PC2 (standing for 9% of data variance) were indicators for OS and death within two years, respectively.

According to published microarray data, among six key immune cell types (T cells, natural killer (NK) cells, B cells, monocytes and macrophages, dendritic cells (DCs) and neutrophils) SRC is mainly expressed in monocytes (Abbas et al., 2005). This finding and the high correlation of the seven genes with each other suggest that the genes of this panel are basically expressed by monocytes and its derivatives.

**Table 2.** Gene names and functions of the seven genes of the prognostic signature, corresponding Assay-on-Demand TaqMan® probes and involved pathways.

Gene symbol	TaqMan® probe	Gene name	Function	Pathway
SRC	Hs00178494_m1	Proto-oncogene tyrosine-protein kinase Src (short for sarcoma)	Cell communication, embryonic development	Gap junction
GUCY1B3	Hs00168336_m1	Guanylate cyclase soluble subunit beta-1	Main receptor for nitric oxide	Gap junction
TUBB1	Hs00258236_m1	Tubulin beta-1	Mitosis, morphogenesis, platelet formation	Gap junction
GUCY1A3	Hs01015570_m1	Guanylate cyclase soluble subunit alpha-3	Main receptor for nitric oxide	Gap junction
TUBA8	Hs01026795_m1	Tubulin alpha-8	Mitosis, cell movement, development of neural structures.	Gap junction
EGF	Hs01099999_m1	Epidermal growth factor	Cellular proliferation, differentiation, and survival	Gap junction
TRIM14	Hs00207648_m1	Tripartite motif containing 14	Development and cell growth	



**Table 3.** Gene names of the three housekeeping genes and corresponding Assay-on-Demand TaqMan<sup>®</sup> probes.

Gene symbol	TaqMan <sup>®</sup> probe	Gene name
RPL21	Hs03003806 _g1	Ribosomal protein L21
RPL9	Hs01552541 _g1	Ribosomal protein L9
SH3BGRL3	Hs00606773 _g1	SH3 domain-binding glutamic acid-rich-like protein 3

### 1.2.3 Which are the major immune cells involved in these two gene panels?

There are two major possibilities describing the origin of the two gene signatures comprising gene expressions in a “high density” blood leukocyte fraction which is isolated using a density gradient (see 2.3): On the one hand, the expression characteristics could be due to differences in the relative amounts of certain immune cell types with constant expression levels; on the other hand, differences could be a result of altered gene expressions in a certain leukocyte population with a constant ratio; or a mixture of the two described possibilities. In both cases the causative leukocytes could comprise only one or several types of immune cells.

Routine applications of the blood cell gene signatures require a more simple method than the density gradient to isolate the blood cell fraction which is used for the evaluation of the gene signatures. Such methods could base on a filtering system or on an immune magnetic separation of different blood cell fractions. To establish such an alternative method, for both described gene panels blood cell fractions have to be identified which permit the discrimination of EOC patients and healthy controls with the diagnostic panel and of EOC patients with favorable prognosis and those with a worse clinical outcome with the prognostic panel, respectively. Respective cell fractions isolated from the blood could overlap with cells present in the “high density” fraction or distinct blood cell types than the majority of cells in this fraction could be found to be more suitable for the determination of the gene signatures. If the latter is the case, a remodeling of the discriminative model could be necessary to reach required specificity and sensitivity.

## 1.3 Tumor proliferation

The proliferative ability of tumor cells, determined mostly by biomarkers such as Ki67, has been reported to have a different impact on prognosis in various malignancies. The protein Ki67 is located in the cell nucleus and is expressed during all active phases of the cell cycle, but

absent in resting cells. Ki67 immunohistochemical staining is used to determine the fraction of proliferating cells.

On the one hand, high proliferation has been correlated with occurrence of metastases and subsequent worse clinical outcome (Gimotty et al., 2005). On the other hand, it has also been associated with improved OS and relapse-free survival (Fluge et al., 2009; Lee et al., 2010). In ovarian cancer Ki67 proliferation index has been associated with advanced stage, high grade and complete responsiveness to first-line chemotherapy (Aune et al., 2011; Liu et al., 2012; Sengupta et al., 2000). Moreover, Ki67 has been found to be an independent prognostic factor for poor OS (Liu et al., 2012) and disease progression (Sengupta et al., 2000). Nevertheless, data are inconsistent and there are lacking data about the interaction of local immune processes and ovarian cancer growth.

### **1.4 Tumor immunology**

The immune system of vertebrates consists of the innate and the adaptive immunity and is the major weapon in the defense against pathogens and foreign substances. The innate immunity with its instant anti-microbial mechanisms, including the skin barrier, proteins of the complement system and phagocytes, provides the early line of defense, while the adaptive branch combats infections with more advanced and specific armaments including lymphocytes and antibodies. In addition, the important role of the immune system in tumor destruction has become evident in recent years.

Studies in mice have shown that immunodeficient animals spontaneously develop tumors and that they are much more susceptible to chemically induced tumorigenesis than immunocompetent animals. Moreover, the host immune status has been reported to be crucial for the immunogenicity of tumors since tumors from immunodeficient mice were more immunogenic than tumors from immunocompetent mice (Schreiber et al., 2011; Vesely et al., 2011).

Observations like this led to the development of the cancer immunoediting hypothesis consisting of three phases of tumorigenesis: elimination, equilibrium and escape. Elimination is the phase of cancer immunosurveillance when highly immunogenic transformed tumor cells are suppressed by the host's innate and adaptive immune system. Tumor specific CD8+, CD4+ and  $\gamma\delta$  T cells, NK and NKT cells, DCs and pro-inflammatory, anti-tumoral M1 polarized macrophages accomplish the elimination of tumor cells (Schreiber et al., 2011). The

polarization of macrophages and the associated functions are discussed in one of the following sections.

In the second phase, equilibrium, anti-tumoral immune responses, on the one hand, and genetic instability and/or immunoselection of the tumor cells, on the other hand, lead to a balanced state of cancer persistence. This phase can last for years or decades. Immunoselection includes the killing of immunogenic cells by the immune system, whereas immunoresistant, poorly immunogenic and immunosuppressive tumor cells survive the immune attack and continue the malignant growth. A precondition for immunoselection is the genetic instability leading to mutations and an immunoresistant phenotype (Vesely et al., 2011). Experiments including the depletion and functional blocking of T and NK cells have shown that the immunological tumor control is most probably accomplished by the adaptive immunity. When T cells were affected, tumor progression was observed, while the blocking of NK cells had no effect on tumor growth. Besides the immunological control, tumor growth is restricted by apoptotic events and angiogenic limitations (Teng et al., 2008).

The final escape phase is characterized by chronic inflammation, recruitment of immunosuppressive leukocytes and cancer progression. These immunosuppressive leukocytes inhibit inflammatory and cytotoxic effector functions of CD8<sup>+</sup> T cells, NK cells and M1 polarized macrophages. Moreover, down-regulations of proteins from the antigen processing and presentation machinery as well as up-regulations of apoptosis inhibitors have been described as characteristics for the tumor escape phase. Another mechanism of the tumor to evade immunosurveillance is the expression of molecules inducing the killing of T cells such as programmed death-1 ligand (PD-L1, also known as B1-H1) and Fas ligand (Schreiber et al., 2011; Vesely et al., 2011).

The multistage process of tumorigenesis includes the development of a tumor microenvironment providing a special ambience which favors the recruitment of immunosuppressive leukocytes and the inhibition of immune effector functions. Angiogenesis and the formation of lymphoid tissue-like structures which recruit and maintain immunosuppressing leukocytes are crucial steps in this process (Zindl and Chaplin, 2010). Such immune cells with suppressive functions are myeloid derived suppressor cells (MDSCs), regulatory T cells (Tregs), M2 polarized macrophages, T helper type 17 (Th17) cells, plasmacytoid DCs and immature tolerogenic DCs (Apetoh et al., 2011; Vesely et al., 2011; Zindl and Chaplin, 2010; Zou and Restifo, 2010). Chemokine and cytokine modulations cause the attraction of immune cells to the tumor site and can alter their polarization and inhibit their function. Among the most important molecules involved are interleukin-10 (IL-10), transforming growth factor- $\beta$  (TGF- $\beta$ ), IL-1 $\beta$ , vascular endothelial growth factor (VEGF),

prostaglandin E2 (PGE2), granulocyte macrophage colony-stimulating factor (GM-CSF), CCL21 and CCL22 (Flavell et al., 2010; Vesely et al., 2011; Zindl and Chaplin, 2010). Moreover, inhibitory B7 molecules expressed by immune cells and by some tumors have immunosuppressive and protective functions (Zou and Chen, 2008).

In humans, indications for tumor immunosurveillance are that immunosuppressed transplantation recipients and patients with AIDS have elevated risk for tumor development, whereby virus-associated malignancies predominate. More evidence for the interaction between the host immune response and malignancy provides the correlation between tumor disease and paraneoplastic autoimmune disorders due to cross-reactivity between the anti-tumoral immune response and neurologic antigens. Furthermore, signs of human immunosurveillance are antibody responses in the blood serum of patients against numerous tumor associated antigens and the presence of tumor infiltrating lymphocytes (TILs). Lymphocyte infiltrations have been described in cases of spontaneous tumor regression and correlated with the control of tumor outgrowth and improved patients' survival (Vesely et al., 2011).

Immune responses against malignancies as well as immune reactions during a microbial infection have to be balanced between immune-activating and immunosuppressing events. This balance is necessary to accomplish the elimination of transformed tumor cells and pathogens, respectively, while limiting host tissue destruction. However, many human tumors have been reported to alter the balance in favor of immune regulatory cells by remodeling the stromal tumor microenvironment and by secreting proteins promoting immunosuppressive cells and inhibiting effector T cell responses (Zindl and Chaplin, 2010). In the following sections the most frequently mentioned anti- and pro-tumoral leukocytes and their effector functions are discussed.

### **1.4.1 Cytotoxic T lymphocytes**

Cytotoxic T lymphocytes belong to the adaptive immune system and are among the major weapons of cellular immunity against infected cells. Furthermore, they play a crucial role in tumor immunosurveillance. Cytotoxic T cells are characterized by a CD3<sup>+</sup> (T cells)/CD8<sup>+</sup> (cytotoxic T cells)/CD4<sup>-</sup> (T helper cells, regulatory T cells) phenotype. They recognize processed antigenic peptides presented in the class I major histocompatibility complexes (MHC-I) – in humans known as human leukocyte antigen (HLA) – of infected cells, allograft cells and tumor cells. The killing of the antigen presenting target cell is accomplished by the

release of the cytotoxic molecules perforin and granzymes A and B which enter the target cytosol and activate caspases that subsequently induce apoptosis. Moreover, killing by cytotoxic T cells can be induced by Fas/Fas ligand mediated apoptosis (Abbas et al., 2007).

TILs are frequently found in tumor tissues indicating an ongoing host immune response. The prognostic value of host lymphocytes has been assessed in a variety of cancer entities (Galon et al., 2006; Gao et al., 2007; Zhang et al., 2003). Most studies have shown survival advantage associated with the presence of tumor infiltrating T cells (CD3+) and cytotoxic T cells (CD8+) (Gooden et al., 2011), while few studies revealed a non-significant prognostic value of CD3+ and/or CD8+ T lymphocytes (Gao et al., 2007; Noshio et al., 2010; Sorbye et al., 2011).

Despite the established anti-tumoral effect of T lymphocytes, these cells mostly fail to eliminate tumor mass. Tumors can even induce T cell tolerance. When naïve T cells recognize tumor associated antigens in the MHC complex on a tumor cell without a secondary costimulatory signal which is usually only provided by mature antigen presenting cells (e.g. DCs), they become anergic. Another mechanism to defang T cells is to induce their apoptosis by repetitive antigenic stimulation. Moreover, cytotoxic T cells are only one component of tumor infiltrating immune cells and are exposed to other immune cells exhibiting suppressive functions such as MDSCs, Tregs and M2 polarized macrophages (Yigit et al., 2010).

#### **1.4.2 Regulatory T cells (Tregs)**

The main phenotype of Tregs is CD4+/CD25+/FoxP3+. Tregs are capable of suppressing a wide range of immune cells such as T and B lymphocytes, NK, NKT and professional antigen presenting cells. Under non-pathogenic conditions they prevent autoimmunity by suppressing the activation of self-reactive T cells (Abbas et al., 2007). In various human cancer entities they have been described as a negative predictor of survival (Bates et al., 2006; Gao et al., 2007). Tregs occur naturally and can be induced. Both subtypes suppress effector T cell functions; the former ones in a cell-dependent manner (e.g. via the expression of immunoinhibitory cell surface molecules such as cytotoxic T lymphocyte antigen 4 (CTLA-4) and PD-L1) as well as a cytokine-dependent manner (mainly IL-10 and TGF- $\beta$ ); the latter ones suppress other cells via cytokines. They are recruited to the tumor site via CCL22 secreted by tumor cells and tumor associated leukocytes such as macrophages and DCs (Yigit et al., 2010).

### **1.4.3 Myeloid derived suppressor cells (MDSCs)**

MDSCs are a heterogeneous group of immature cells of the myeloid lineage with negative regulatory functions of immune responses in human cancer and other diseases. They comprise precursors of macrophages, DCs and granulocytes. They affect the adaptive immune system by suppressing different types of T cells as well as innate immune responses by modulating the cytokine profile of macrophages. One of their suppressive effects is the depletion of arginine which is essential for T cells. Its shortage inhibits T cell proliferation. Arginine is a substrate for the enzymes inducible nitric oxide synthase (iNOS) and arginase, both expressed in high levels by MDSCs. Moreover, nitric oxide (NO), a product of iNOS activity, affects T cell functions by inhibiting janus kinase 3 (JAK3) and signal transducer and activator of transcription 5 (STAT5) signaling, inhibiting MHC-II expression and inducing apoptosis. Other important mediators of the immunosuppressive mechanisms of MDSCs are reactive oxygen species (ROS) and peroxynitrite. Peroxynitrite causes nitration of the T cell receptor which leads to CD8 unresponsiveness to antigen-specific stimulation, while T cells remain responsive to non-specific stimulation. Furthermore, MDSCs have been reported to induce Tregs. In addition, MDSCs are involved in non-immunological, pro-tumoral mechanisms such as tumor angiogenesis, invasion and metastasis (Gabrilovich and Nagaraj, 2009). In murine studies MDSCs have been described in ovarian cancer tissues (Yigit et al., 2010).

### **1.4.4 Macrophages**

Macrophages are cells of the innate immune system. They arise from circulating monocytes, which differentiate into tissue macrophages or closely related DCs. Tissue macrophages are a heterogeneous cell population and differentiate into distinct polarization stages depending on the environmental stimuli. Among their numerous functions are contribution to host defense, inflammation, tissue remodeling and immunosuppression. They maintain tissue homeostasis by removing apoptotic cells and repairing tissue after inflammation (Gordon and Martinez, 2010; Gordon and Taylor, 2005; Sica et al., 2002).

Corresponding to the Th1 and Th2 cell polarization of T cells, two distinct activation states for macrophages have been described: i) the M1 or classically activated macrophages polarized by lipopolysaccharide (LPS) and interferon- $\gamma$  (IFN- $\gamma$ ) and ii) the M2 or alternatively activated macrophages polarized by IL-4 and IL-13.

M1 macrophages play an important role in the defense against viral and microbial infection, antigen presentation and tissue damage. They can release reactive nitrogen, ROS and

pro-inflammatory cytokines such as IL-12, IL-23 and tumor necrosis factor (TNF). Moreover, they recruit and stimulate other immune cells (e.g. Th1, NK cells). In contrast, M2 macrophages participate in allergy, parasitic infections, dampening of inflammation, tissue remodeling and angiogenesis and accomplish immunoregulatory functions (Biswas and Mantovani, 2010; Gordon and Martinez, 2010). M2 macrophages are characterized by an IL-12<sup>low</sup>/IL-10<sup>high</sup>/IL-1 decoyR<sup>high</sup>/IL-1ra<sup>high</sup> phenotype and high expression of scavenger and mannose receptors. Furthermore, M2 macrophages differ from M1 macrophages in their chemokine expression (e.g. CCL17, CCL22) (Mantovani et al., 2009).

Macrophages can switch between the two functional stages. Intermediate or overlapping phenotypes have been observed during several diseases such as sepsis, cancer and obesity. M2-like forms of macrophage develop in response to e.g. glucocorticoids, TGF- $\beta$  and IL-10. IL-10 stimulates the T cell inhibitory receptor PD-L1 on macrophages which mediates inhibition of T cell immunity (Biswas and Mantovani, 2010; Mantovani et al., 2009).

Tumor associated macrophages (TAMs) are a prominent component of the leukocyte infiltrate in solid tumors (Gordon and Martinez, 2010; Sica et al., 2002). They mainly derive from circulating monocytes and are attracted by chemokines such as CCL2 produced in the tumor microenvironment (Mantovani et al., 2002). Moreover, tumor cells promote M2-like polarization and can inhibit classical macrophage effector functions such as cytotoxicity via cytokines including TNF, IL-10 and TGF- $\beta$ . On the one hand, M1-like TAMs can prevent the establishment and spread of tumor cells and are characterized by tumoricidal activity. TAMs can also produce anti-angiogenic molecules such as plasminogen activator inhibitor type 2 (PAI-2) and thrombospondin 1 (TSP1). On the other hand, M2-like TAMs can support tumor progression and dissemination by suppression of cells of the adaptive immunity such as Th1 cells and cytotoxic T lymphocytes, remodeling of the extracellular matrix and expression of angiogenic factors such as VEGF and epidermal growth factor (EGF). Moreover, they contribute to metastasis and invasion through cathepsin B and S and recruit other hematopoietic cells through chemokines (Biswas and Mantovani, 2010; Gordon and Martinez, 2010; Sica et al., 2002). M2-like TAMs also promote cancer-related inflammation, an event which has recently been added to the hallmarks of cancer and which promotes tumorigenesis and tumor progression (Hanahan and Weinberg, 2011). These diverse functions reflect the phenotypic heterogeneity of TAMs with M1- and M2-like properties.

TAMs have many properties of M2-like macrophages (Gordon and Martinez, 2010). However, this cannot be generalized for all tumor types and substantially different macrophage phenotype compositions can even be found in different areas within the same tumor. Moreover,

the M2-like phenotype of TAMs is reversible: Classical activation can be achieved by IFN- $\gamma$ , activation of toll-like receptor 9 (TLR-9) and blocking of IL-10 (Biswas and Mantovani, 2010). In concordance with the described functions of M2-like TAMs, TAMs have been associated with a poor prognosis in various cancer entities (Biswas and Mantovani, 2010; Mantovani et al., 2009; Mantovani et al., 2002; Pollard, 2004).

Given the limited number of published studies regarding human macrophages, a consensus of markers for M1 and M2 polarization has not been established so far (Gordon and Martinez, 2010). For M1 high expression of CD16, CD32, CD64, CD80, CD86, HLA-DR and iNOS has been reported, whereas M2 are characterized by up-regulation of mannose and scavenger receptors, CD163, CD23 and arginase (Escorcio-Correia and Hagemann, 2010; Mantovani et al., 2002). However, M1 and M2 polarization represents the extremes of a continuum of possible polarization states, while TAMs can present characteristics of both (e.g. simultaneous expression of iNOS and arginase) (Escorcio-Correia and Hagemann, 2010).

#### **1.4.5 The immunosuppressive microenvironment of ovarian cancer**

In contrast to many other cancer entities, ovarian cancer disseminates by metastasizing the peritoneal cavity whose special immunosuppressive environment protects the cancer from immune destruction. Distant metastases are rare and – if detectable – they do not significantly contribute to mortality in ovarian cancer patients.

A variety of tumor infiltration leukocytes and their impact on the outcome have been studied in ovarian cancer patients. Intraepithelial CD8<sup>+</sup> TILs in ovarian tumor tissues have been described to play a major role in anti-tumoral activity and survival (Leffers et al., 2009). In contrast, no significant correlation of stromal CD8<sup>+</sup> cells and survival has been reported (Hamanishi et al., 2007; Milne et al., 2009; Sato et al., 2005). A currently published meta-analysis has also confirmed the prognostic significance of TILs (CD3<sup>+</sup> and CD8<sup>+</sup>) in ovarian cancer patients (Hwang et al., 2012). Nevertheless, the tumor is rarely eradicated efficiently, but it manages to escape from immune elimination supported by immunosuppressive cells. In ovarian cancer Tregs have been shown to suppress anti-tumoral T cell immunity and have been associated with a worse clinical outcome (Curiel et al., 2004). TAMs in ovarian cancer have already been subject of several studies which have indicated an immunosuppressive M2-like polarization (Kawamura et al., 2009; Wang et al., 2010). Moreover, ovarian cancer TAMs expressing B7-H4 have been described to inhibit T cell immunity and to have a negative impact on patients' outcome (Kryczek et al., 2007; Kryczek et



al., 2006). However, further information about the prognostic value of M1 and M2 polarized TAMs in ovarian cancer patients is needed.

As a result of this immunosuppressive milieu in the peritoneal cavity ovarian cancer is able to grow and able to metastasize the abdomen. Thus, effective immune therapies should consist of a combination of immune activating strategies and the limitation of immunosuppressive mechanisms, for instance targeting Tregs, M2 polarized macrophages and MDSCs and/or the suppressive cytokines involved.

## **1.5 Aim of this study**

The work in the course of my diploma thesis aimed at the question of the relationship between the peripheral immune system, the tumor proliferative activity and tumor immune cell infiltration in EOC patients and the clinical relevance of these factors.

The peripheral immune system was represented by the two blood cell gene expression signatures recently developed in our group, one for early diagnosis of EOC and one for prognosis of OS and death within two years after diagnosis in EOC patients. A more simple methods than the described density gradient such as a filtering system or an immune magnetic separation system for whole blood would render the determination of the two described gene signatures more suitable for routine use. To facilitate the protocol applying such a method, the panels require further analysis to identify the most important blood cells involved. Therefore, the expression patterns of the genes comprised in the two panels were determined in different blood cell fractions (monocytes, monocyte derived immune cells, granulocytes, B and T lymphocytes, NK cells etc.) from 23 patients using RT-qPCR. The analysis of the diagnostic gene panel included the comparison of the expression values of each gene in each blood cell fraction between patients according to the disease in order to find cell fractions presenting significant differences between EOC patients and controls. The characterization of the prognostic gene signature was approached by comparing the gene expression values in the different blood cell fractions. The aim of this primary, rough analysis of the different blood cell fractions was to search a candidate cell fraction or a combination of cell fractions which permit the discrimination of i) EOC patients and controls with the diagnostic panel and of ii) EOC patients with a favorable outcome and those with reduced survival time with the prognostic panel. The next step would be to establish a possibly short and simple separation protocol to isolate the respective cell type(s) which can substitute the density gradient for the determination of the respective gene signature. Furthermore, confining or identifying the cell type(s) involved

could improve specificity and sensitivity of the diagnostic gene signature and strengthen the predictive value of the prognostic gene signature.

Besides the peripheral immune system of EOC patients, the tumor microenvironment in ovarian cancer patients was another target of interest of this work. The tumor proliferative activity, a marker for intrinsic tumor aggressiveness and velocity of growth, was assessed. Moreover, tumor infiltrating leukocytes which indicate an ongoing host immune response against the cancer were analyzed. The obtain information about a broad range of leukocytes, infiltration levels of cytotoxic T cells as representatives of the adaptive immune system, of macrophages as representatives of the innate immune system and of leukocytes in general were determined in more than 200 EOC tumor samples using immunohistochemical staining techniques. Interactions between tumor proliferation and immune cells were assessed. Special focus of the diploma thesis was the association of the proliferation status and the different leukocyte infiltrations with clinical outcome parameters such as survival time and chemotherapy response.

In addition, the systemic and local immune reactions were linked by assessing the interaction of the prognostic gene panel and TAMs in patients with the lowest and highest risk to die and risk of death within two years after EOC diagnosis (according to the prognostic blood cell gene expression panel). The number of macrophages in the tumor tissue and their polarization were determined using immunofluorescent staining techniques. Correlation analysis of the TAM data and the parameters from the prognostic gene signature should help to understand if the risk to die and the risk of death within two years after diagnosis of EOC patients measured by blood cell gene expression values are also reflected in the macrophage population (number and/or polarization) in the tumor tissue.

The major goal of this diploma thesis was to assess different aspects of host immune responses to ovarian cancer patients with special attention on survival analyses and possible implications for clinical purpose such as markers for early diagnosis and prognosis as well as therapy and surgery of EOC patients.

## 2 Materials and methods

### 2.1 Study population and patients' materials

*Blood:* Pre-operative blood from ten patients with suspicion of EOC and 13 female controls, comprising patients with benign gynecological diseases and healthy persons, were enrolled in the study. Patients have been recruited between March 2011 and January 2012 in the Department of Obstetrics and Gynecology, Medical University of Vienna, Austria. EOC could not be confirmed before histological examination. Therefore, some of the patients with suspicion of EOC were subsequently re-diagnosed and summarized in a separate patient cohort.

*Tumor tissue:* Patients derived from the OVCAD cohort. Only EOC patients with FIGO stage II, III and IV were enrolled in the study. They have been recruited from 2005 to 2008 in the Department of Gynecology at Charité, Campus Virchow-Klinikum, Medical University Berlin, Germany; Department of Obstetrics and Gynecology and Gynecologic Oncology, University Hospital Leuven, Belgium; Department of Gynecology, University Medical Center Hamburg-Eppendorf, Germany; Department of Obstetrics and Gynecology, Medical University of Vienna, Austria; Department of Gynecology and Obstetrics, Innsbruck Medical University, Austria. A broad and well-described tumor bank and database consisting of clinical and histopathological data as well as follow-up data were established.

Patients with other malignancies were excluded. All EOC patients were treated according to standardized protocols with cytoreductive surgery combined with a platinum/taxane based chemotherapy for six courses. Operable patients were treated with adjuvant chemotherapy after cytoreductive surgery, while initially inoperable patients were treated with neoadjuvant chemotherapy to reduce tumor load prior to surgery, followed by cytoreductive surgery and subsequent adjuvant chemotherapy. Residual tumor load was defined as negative if macroscopically absent.

Despite the impaired sensitivity and specificity of pre-operative CA125 level as a diagnostic marker, it is a well-established measurement for progression of disease and treatment response. The disease progression was determined according to the RECIST criteria (Rustin, 2003). Briefly, nadir serum CA125 levels  $\leq 35$  U/mL in the course of first-line adjuvant chemotherapy were defined as negative. Following control examinations were performed every three months during the first two years and subsequently every six months until five years after first-line therapy for patients without clinical complaints. Patients with complaints were

additionally examined. Disease progression was defined as CA125 values  $>70$  U/mL documented on two occasions for patients with negative CA125 after first-line chemotherapy or as a doubling of the nadir CA125 documented on two occasions for patients with values  $>35$  U/mL. The time point of disease progression was the first date of CA125 elevation. Besides serum CA125, radiological techniques were used to assess disease progression. Disease progression during first line platinum-based therapy or within four weeks after the last chemotherapy cycle was defined as refractory disease (Friedlander et al., 2011). OS was defined as the time interval between diagnosis of ovarian cancer and tumor-related death. Progression-free survival (PFS) was defined as the time between cytoreductive surgery and progression of disease. Patients with refractory disease were excluded from PFS analyses since the time point of progression of disease could not be reliably determined. Patients were censored at their last follow-up or after death from tumor-unrelated causes.

Informed consent for the scientific use of biological material was obtained from all patients and healthy blood donors in accordance with the requirements of the ethics committee. Experienced gynecological oncologists and pathologists of the participating universities performed the clinical and histopathological evaluation.

A total of 209 patients were included in the immunohistochemical study of tumor infiltrating leukocytes and tumor proliferation. Tissue microarrays (TMAs) comprising tumor tissues of these patients were used for the immunohistochemical staining.

A number of 19 patients, mainly overlapping with the 209 patients from the immunohistochemical study, were included in the study analyzing TAMs with immunofluorescent staining. They were selected according to their expression values of genes from the prognostic signature that had been developed recently in our working group. As outlined in the introduction, PCA performed with gene expression data of this signature revealed PC1 and PC2 as indicators of OS and death within two years after EOC diagnosis, respectively. 19 patients with extreme high or low PC1 and PC2 values were selected. Whole tissue sections (WTSSs) were used for the immunofluorescent staining.

### **2.2 Cell separation from whole blood**

Cell separation from pre-operative whole blood was performed with the Pluriselect technology using provided protocols and reagents (pluriBead® Kit Cascade, Cell lysis protocol,

pluriSelect, Germany). Per patient approximately 12 mL EDTA-anticoagulated whole blood were used for the Pluriselect cell separation with 62  $\mu$ m-bead-coupled antibodies against CD3 (T cells), CD15 (granulocytes and monocytes) and CD44 (tissue cells, leukocytes and erythrocytes) and 32  $\mu$ m-bead-coupled antibodies against CD14 (monocytes), CD19 (B cells) and CD25 (activation marker for several immune cells, predominantly of the lymphoid lineage). CD14<sup>+</sup> and CD15<sup>+</sup> cells were enriched without a second antibody, whereas the enrichment of CD3<sup>+</sup> and CD19<sup>+</sup> cells as well as of CD25<sup>+</sup> and CD44<sup>+</sup> cells was performed in the same reaction tube by adding 62  $\mu$ m-bead-coupled antibodies for the capture of one cell type and 32  $\mu$ m-bead-coupled antibodies for the capture of the other cell type. About 3 mL whole blood were used for the enrichment of the different cell fractions: CD14, CD15, CD3/CD19 and CD25/CD44. Before the enrichment of CD14<sup>+</sup> cells soluble CD14 was removed from the plasma by washing the whole blood twice with the double volume of wash buffer (300 g, without break, 10 minutes). The sample material was transferred to mixing containers provided in the kit and 40  $\mu$ L bead-labeled antibody suspension (concentration not designated) per mL whole blood were added. The samples were mixed for 45 minutes at room temperature on a horizontal roller mixer (pluriPlix®, pluriSelect, Germany).

Microscopic examination of the blood samples that had been simultaneously incubated with antibodies against CD3/CD19 and CD25/CD44, respectively, was performed to rule out the binding of antibodies coupled to different sized beads to the same cells.

The cell strainers corresponding to the size of the beads coupled to the antibodies were attached to the mixing containers. For the simultaneous enrichment of cells captured with 62  $\mu$ m-bead-coupled antibodies and cells captured with 32  $\mu$ m-bead-coupled antibodies two cell strainers were attached onto each other, whereby the 57  $\mu$ m-cell strainer for the 62  $\mu$ m-beads was the first in the cascade followed by the 27  $\mu$ m-cell strainer for the 32  $\mu$ m-beads. The mixing containers with the strainers were inverted and attached to a 50 mL tube. The mixing container and the strainers were extensively washed with wash buffer to remove unbound cells and to forward the smaller beads onto the second strainer. For the simultaneous enrichment of two cell types the cell strainers were separated from each other, attached to 50 mL tubes and washed again. The principle of the multi-target cell separation is depicted in Figure 2.

Finally, the strainers were attached to fresh 50 mL tubes with connector rings. Twice 350  $\mu$ L RLT lysis buffer (QIAGEN, Netherlands) were applied to each cell strainer, lysates were collected from the tubes and stored at -20°C.

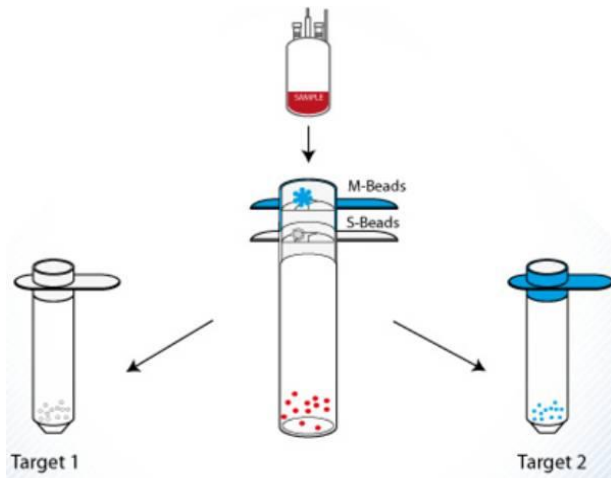


**Figure 2.** The principle of simultaneous separation of two target cells with one sample (figure taken from <http://pluriselect.com/multi-target-separation.html>; 20.06.2012).

### 2.3 Isolation of a “high density” blood leukocyte fraction from whole blood

A “high density” (HD) blood leukocyte fraction (density greater than 1.077 g/mL) depleted from the majority of peripheral blood mononuclear cells (PBMCs) and possibly present circulating tumor cells (CTCs) was obtained by performing a density gradient using 5 mL EDTA-anticoagulated whole blood, largely according to Brandt and Griwatz (Brandt and Griwatz, 1996). The granulocyte- and lymphocyte-rich HD fraction above the erythrocytes pellet and below the CTC/PBMC fraction was aspirated and washed twice with PBS (Figure 3). Washed cell pellets were lysed in 400  $\mu$ L RLT lysis buffer (QIAGEN, Netherlands).

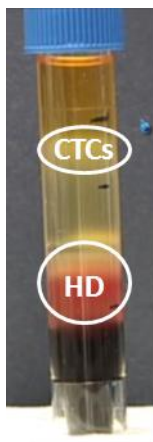


**Figure 3:** Blood gradient used to isolate a “high density” (HD) blood leukocyte fraction (density greater than 1.077) depleted from circulating tumor cells (CTCs) and peripheral blood mononuclear cells (PBMCs).

## 2.4 RNA extraction

*Blood cell fractions:* Total RNAs from lysates of fractions of enriched CD3+, CD14+, CD15+, CD19+, CD25+ and CD44+ cells and from the HD fraction lysates were isolated using the RNeasy Micro kit and the RNeasy Mini kit (QIAGEN, Netherlands), respectively, according to the manufacturer's instructions. RNA concentrations were measured spectrophotometrically.

*Tumor tissues:* About 30 mg fresh frozen tumor tissue of the 160 available tumor samples were homogenized by beadbeating at 2000 rpm for 90 seconds, using a Mikro-Dismembrator U (B. Braun, Biotech International) and lysed in 1 mL Nucleic Acid Purification Lysis Solution (Applied Biosystems, Life Technologies, USA). Total RNA from the lysates was isolated with the ABI PRISM 6100 Nucleic Acid PrepStation using provided protocols and reagents (Tissue RNA isolation, Applied Biosystems, Life Technologies, USA) and quantified spectrophotometrically. The quality of RNA was assessed with an Agilent 2100 Bioanalyzer. RNA with an RNA Integrity Number (RIN) >5 was used for the study.

## 2.5 cDNA synthesis

*Blood cell fractions:* The following protocol was used for cDNA synthesis with up to 500 ng RNA in a total reaction volume of 25  $\mu$ L: For samples with RNA amounts less than 500 ng, the available RNA amount was used. RNA and the random nonamer primer were incubated for 5 minutes at 70°C and quick-chilled on ice.

15.56 $\mu$ L	RNA ( $\leq$ 500 ng)
2.5 $\mu$ L	Random-Nonamer (100 $\mu$ M)
18.01 $\mu$ L	→ 5 min 70°C, $\infty$ 4°C

The following reagents were added to the RNA-nonamer-mixture and the reaction mix was incubated for 15 minutes at 25°C, for 50 minutes at 45°C and for 10 minutes at 55°C.

18.01 $\mu$ L	RNA-nonamer-mixture	
5 $\mu$ L	5x M-MLV RT 5x Buffer	Promega, USA
0.625 $\mu$ L	dNTP Mix (20 mM)	GE Healthcare, Life Sciences, UK
0.3125 $\mu$ L	RNasin® Plus RNase inhibitor (40 U/ $\mu$ l)	Promega, USA
1 $\mu$ L	M-MLV RT, RNase H(-) Point Mutant (200 units/ $\mu$ L)	Promega, USA
25 $\mu$ L	→ 15 min 25°C, 50 min 45°C, 10 min 55°C, $\infty$ 4°C	

*Tumor tissues:* The cDNA synthesis was performed with the Omniscript Reverse Transcription Kit (QIAGEN, Netherlands) with 500 ng RNA according to manufacturer's instructions. Random hexamer primers and RNasin® Plus RNase inhibitor (40 U/μl) (Promega, USA) were used.

## 2.6 qPCR

qPCR was performed according to the following scheme:

2 μL	cDNA sample*	
0.4 μL	20x TaqMan Gene Expression Assay	Applied Biosystems, Life Technologies, USA
4 μL	2x TaqMan Gene Expression MasterMix	Applied Biosystems, Life Technologies, USA
1.6 μL	H <sub>2</sub> O	
<hr/>		
8 μL		

\* cDNA dilution: *blood cell fractions*: 1:8 ; *tumor tissue*: 1:2

The reaction mixture was pre-incubated at 50°C for two minutes and at 95°C for ten minutes, followed by 50 cycles of two step incubation at 95°C for 15 seconds and at 60°C for one minute. Each PCR was performed in duplicates.

*Blood cell signatures:* TaqMan gene expression assays for the 13 genes from the diagnostic panel, CFP, NOXA1, NEAT1, BC037918, DIS3, ZNF419, CCR2, B4GALT1, PAPOLG, PRIC285, AP2A1, C1orf63 and OSM, and the seven genes from the prognostic panel, SRC, GUCY1B3, TUBB1, GUCY1A3, TUBA8, EGF and TRIM14, were used with the cDNA samples from the patients' seven blood cell fractions. The three stably expressed housekeeping genes RPL21, RPL9 and SH3BGRL3 were used as reference. In Table 1, 2 and 3 the TaqMan gene expression assays are summarized.

*Tumor tissues:* The qPCR was performed with the CD8A TaqMan Gene Expression Assay (Hs00233520\_m1, Applied Biosystems, Life Technologies, USA) according to the manufacturer's instructions. The housekeeping gene GAPDH (Hs99999905\_m1, Applied Biosystems, Life Technologies, USA) was used as reference.

A calibrator consisting of a mixture of cDNAs from HD blood leukocyte fractions and tumor cell lines was used.



## 2.7 Evaluation of RT-qPCR data

The mean value of the duplicate RT-qPCR expression values (Ct values) was calculated: for the analysis of the two blood cell signatures the 23 gene expression assays (13 genes of the diagnostic panel, seven genes of the prognostic panel and three housekeeping genes) in 161 blood fraction samples (23 patients with each seven fractions) and in the calibrator sample; for the analysis of CD8 gene expression in the tumor tissues the CD8A and the GAPDH assays in 160 tumor samples and in the calibrator sample. When the standard deviation was greater than 1, only the smaller Ct value was used assuming that deviations occurred due to pipette errors resulting in lower cDNA volumes and consequently higher Ct values. The geometric mean of the mean Ct values of the three housekeeping genes (blood samples) and the mean Ct value of the reference gene GAPDH (tumor tissue samples) were calculated for each sample and normalized with the mean calibrator Ct value (calibrator normalized mean of the reference). The mean Ct values were normalized with the mean calibrator Ct value of the corresponding assay and with the calibrator normalized mean of the reference. Finally the normalized Ct values were multiplied by -1 to be interpretable as  $\log_2$ -expression values (relative expression values).

## 2.8 Immunohistochemical and -fluorescent staining

Primary tumors were fixed in formalin and embedded in paraffin using standardized procedures. Per patient a representative tumor block was selected. TMA were assembled using two 1 mm cores per patient.

If not otherwise indicated described procedures were performed at room temperature. Four  $\mu\text{m}$  sections were put onto highly adhesive slides (Thermo Scientific SuperFrost Ultra Plus, Thermo Fisher Scientific, USA), deparaffinized and rehydrated. After antigen heat retrieval by microwaving the slides in EDTA (1mM, pH 8) for 15 minutes slides were cooled to room temperature. In the immunohistochemistry (IHC) protocol next endogenous peroxidase activity was quenched by incubation the samples with 3%  $\text{H}_2\text{O}_2$  in methanol for ten minutes. In the immunofluorescence (IF) protocol the blocking step directly followed the antigen heat retrieval omitting the peroxidase quench. Blocking solution (Ultra V Block; TA-015HP, Thermo Fisher Scientific, USA) was applied to the samples for seven minutes before incubation with monoclonal antibodies overnight at 4°C.

Lymphoid tissues samples (lymph node, tonsil, spleen) served as positive control for the leukocyte markers. Normal colon tissue served as positive control for the cell proliferation

marker Ki67. Mouse IgG<sub>1</sub> (1:50; Negative Control Mouse IgG<sub>1</sub>, code X0931, Dako, Denmark) was used as mouse isotype control. As for rabbit antibodies no useful isotype control was available, primary antibody was omitted as negative control.

**IHC:** After blocking antibodies against the cytotoxic T cell marker CD8 (1:1000, clone C8/144B, source mouse, isotype IgG<sub>1</sub>, Dako, Denmark), against the macrophage marker CD68 (undiluted, clone KP1, source mouse, isotype IgG<sub>1</sub>, ThermoScientific, USA), against the panleukocyte marker CD45 (1:8000, clone E19-GDB, source rabbit, DB Biotech, Slovakia) and against the cell proliferation marker Ki67 (1:75, clone MIB-1, code M7240, source mouse, isotype IgG<sub>1</sub>, Dako, Denmark) were applied. For detection the UltraVision detection system (Thermo Fisher Scientific, USA) and the Dako LSAB System (Dako, Denmark) were used according to the manufacturers' protocols. The UltraVision detection system was used for the detection of bound antibodies against CD8, CD68 and CD45. Bound antibody against Ki67 was detected using the Dako LSAB System (Dako, Denmark). Sections were incubated either with Primary Antibody Enhancer (TL-015-PB, Thermo Fisher Scientific, USA) for ten minutes and subsequently with horseradish peroxidase (HRP) Polymer (HRP Polymer; TL-015-PH, Thermo Fisher Scientific, USA) for 15 minutes or with Dako Biotinylated Link (K0675, Dako, Denmark) for 15 minutes followed by Dako Streptavidin-HRP (K0675, Dako, Denmark) for 15 minutes. Slides were stained with diaminobenzidine (DAB) (DAB Chromogen 1:50 in DAB Substrate Buffer, K0673, Dako, Denmark) for two minutes. For counterstaining, the slides were dipped into hematoxylin for 25 seconds. Slides were mounted with Eukitt® (O. Kindler, Germany).

**IF:** A double staining with primary monoclonal antibody against the macrophage marker CD68 (1:15, clone KP1, source mouse, isotype IgG<sub>1</sub>, ThermoScientific, USA) and primary antibody against the M2 polarization marker macrophage scavenger receptor 1 (MSR1) (1:200, HPA000272, source rabbit, Sigma, USA) was performed. The fluorescence labeled secondary antibodies goat anti-mouse (1:1000, AlexaFluor® 568 F(ab') fragment of goat anti-mouse IgG (H+L), Invitrogen, Life Technologies, USA) and goat anti-rabbit (1:1000, AlexaFluor® 647 F(ab') fragment of goat anti-rabbit IgG (H+L), Invitrogen, Life Technologies, USA) were incubated for one hour. For nuclear counterstaining, slides were incubated with DAPI (0.5 µg/mL) for five minutes. Slides were mounted with Fluoromount-G™ (Southern Biotech, USA).

In addition test staining for CD68 in combination with potential M1 macrophage markers (and the M2 marker MSR1) was performed. Monoclonal primary antibodies against CD80

(1:300, clone EP1155Y, source rabbit, Abcam, UK), against iNOS (1:200, clone K13-A, source rabbit, DB Biotech, Slovakia) and against HLA-DR (1:300, clone LN3, source mouse, isotype IgG<sub>2b</sub>, ThermoScientific, USA) were tested for their applicability for M1 macrophage detection. In the test staining primary rabbit antibodies (anti-CD80 and anti-iNOS) were detected with secondary goat anti-rabbit antibody (1:1000, AlexaFluor® 488 F(ab') fragment of goat anti-rabbit IgG (H+L), Invitrogen, Life Technologies, USA). Mouse anti-CD68 antibody in combination with rabbit antibodies was detected with secondary goat anti-mouse antibody (1:1000, AlexaFluor® 568 F(ab') fragment of goat anti-mouse IgG (H+L), Invitrogen, Life Technologies, USA). In a triple staining with mouse anti-CD68 IgG<sub>1</sub> antibody, mouse anti-HLA-DR IgG<sub>2b</sub> antibody and rabbit anti-MSR1 the primary antibodies were detected with the secondary antibodies, goat anti-mouse IgG<sub>1</sub> (1:1000, AlexaFluor® 568 goat anti-mouse IgG<sub>1</sub> (γ1), Invitrogen, Life Technologies, USA), goat anti-mouse IgG<sub>2b</sub> (1:1000, AlexaFluor® 647 goat anti-mouse IgG<sub>2b</sub> (γ2b), Invitrogen, Life Technologies, USA) and goat anti-rabbit (1:1000, AlexaFluor® 488 F(ab') fragment of goat anti-rabbit IgG (H+L), Invitrogen, Life Technologies, USA), respectively. Immunofluorescent staining procedures were performed as described above.

## 2.9 Image digitalization

The stained WTS and TMA slides were digitalized with the TissueFAXS system (version 2.0.4.0147, TissueGnostics, Austria) using an x20 objective lens. The images had 1392x1024 pixels (96 DPI, 24 bit color) per field of view (FOV). For the WTSs the whole tumor tissue was scanned ranging from 300 to 1500 FOVs (corresponding to approximately 100 to 500 mm<sup>2</sup>).

The slides from the immunofluorescent test staining were analyzed with a Zeiss laser scanning microscope LSM 700 (Carl Zeiss AG, Germany) using an x40 objective lens. The images had 1024x1024 pixels (96 DPI, 24 bit color) per FOV.

## 2.10 Quantification of the immunohistochemical staining using HistoQuest

All sections were coded and analyzed by observers blinded for the clinical data.

The HistoQuest software (version 3.0.3.0161, TissueGnostics, Austria) was used for the detection and quantification of the immunohistochemically stained CD8+, CD68+ and CD45+ cells. For CD8, two regions were analyzed in each TMA core: i) a 0.78 mm<sup>2</sup> region of interest (ROI) comprising the whole TMA core without discriminating between cancer epithelium and

adjacent stromal areas (CD8 whole core) and ii) a ROI of all cancer epithelium within the TMA core, comprising mainly tumor cells and only small inclusions of stromal areas within the tumor cells, varying in size according to the amount of cancer epithelium (CD8 cancer epithelium). As the CD8 whole core and CD8 cancer epithelium data correlated highly (see 3.3.1) and resulted in very similar prognostic values in survival analyses (see 3.3.6), for CD68 and CD45 only a 0.78 mm<sup>2</sup> area comprising the whole core was analyzed.

Using the HistoQuest software, two markers were created for each staining: DAB as master marker (CD8, CD68 and CD45, respectively) and hematoxylin as non-master marker (nucleus). Each DAB master marker profile was generated optimizing options such as color picker, single reference shade, intensity, merging rules and compactness. For the assessment of positive cells scattergrams were created for each ROI allowing the visualization and control of corresponding positive cells in the source ROI using the backward connection feature. To correct false events, specific gates according to cell size and intensity of staining were defined and applied to all analyzed samples. Positive cells were quantified according to the selected marker and gate. Representative examples for CD8+, CD68+ and CD45+ cell detection with HistoQuest is shown in Figure 4. For each patient the CD8+ cell densities (cells/mm<sup>2</sup>) in the whole core and cancer epithelium were obtained as well as the cell densities of CD68+ and CD45+ cells in the whole core.

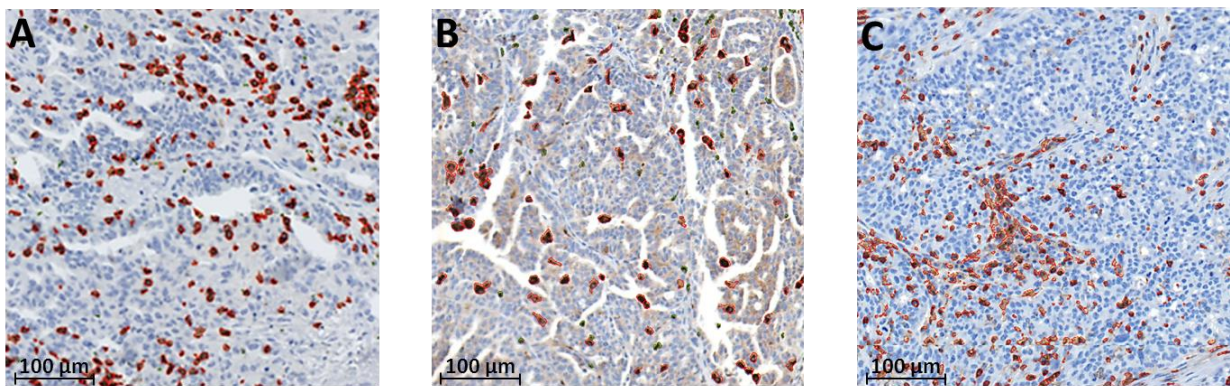


**Figure 4.** Representative example of immunohistochemically stained CD8+, CD68+ and CD45+ cells in epithelial ovarian cancer detected with the HistoQuest software using the backward connection feature; **A** CD8; **B** CD68; **C** CD45; optical magnification x200; images acquired with the TissueFAXS/HistoQuest system.

Scoring of the Ki67 was performed manually by two independent observers determining the labeling index defined as percentage of positively labeled tumor cells of the total tumor cells.

## 2.11 Quantification of the immunofluorescent staining using TissueQuest

All sections were coded and analyzed by observers blinded for the clinical data.

The TissueQuest software (version 3.0.0138, TissueGnostics, Austria) was used for the detection and quantification of the immunofluorescent CD68 MSR1 double staining. Eight FOVs per WTS comprising mainly cancer epithelium were analyzed corresponding to approximately 2.7 mm<sup>2</sup>.

Using the TissueQuest software, three markers were created: DAPI as master marker (nucleus), Alexa568 (CD68) and Alexa647 (MSR1) as non-master markers. The parameters nuclei size, discrimination by area and discrimination by grey for the nuclear marker and the ring mask parameters interior radius and exterior radius for CD68 and MSR1 were adjusted to achieve optimal cell detection. For the assessment of positive cells scattergrams were created for each FOV, allowing the visualization of corresponding positive cells in the source ROI using the real-time back gating feature. To correct false events, specific gates according to cell size and intensity of staining were defined and applied to all analyzed samples. Positive cells were quantified according to the selected marker and gate. The percentage of CD68+ cells of the total cells (DAPI positive) (CD68+/DAPI) and the percentage of double positive MSR1+CD68+ cells of total CD68+ cells (MSR1+CD68+/CD68+) was obtained for each patient.

## 2.12 Evaluation and statistical analyses

Statistical analyses were performed with the SPSS software (version 19, SPSS, Chicago, USA) and R (version 1.14).

*Blood cell signatures:* To obtain complete data sets, gene expressions below the RT-qPCR detection sensitivity were imputed using the minimum of the gene expression values of the respective assay and fraction of all patients and subtracting it by 1.

**Diagnostic 13 gene panel:** Significant up- and down-regulations of gene expression of the diagnostic 13 gene panel in the seven fractions (HD, CD3, CD14, CD15, CD19, CD25 and CD44) between the means of the three patient groups comprising EOC patients (OC group), patients with other predominantly malignant diseases except ovarian cancer (M group) and controls (B group) were assessed by analysis of variance (ANOVA) followed by correction for multiple testing with the Bonferroni testing and the Holm-Bonferroni method. ANOVA was

also used to compare the relative risk values of EOC of the combined diagnostic model between the patient groups. The relative risk of EOC is a linear combination of the single expression values with coefficients listed in Table 1.

**Principal Component Analysis (PCA):** PCA was performed to assess the influence of the two gene panels on the clustering of the analyzed blood cell fractions including the 20 gene expressions (13 genes of the diagnostic panel and seven genes of the prognostic panel) as variables. PCs of the mean-centered and scaled gene expression values were calculated and the first three of them were illustrated with the Eigenvectors with R.

*Tumor microenvironment:*

**IHC:** For the statistical analyses raw CD8+ (determined in the TMA whole core and in cancer epithelium), CD68+ and CD45+ cell density values (both determined in the TMA whole core) were log<sub>2</sub>-transformed to achieve an approximately normal distribution. The mean values of the two cores were calculated for CD8, CD68, CD45 and Ki67 for each patient.

**IF:** The 19 patients were dichotomized into PC1\_low and PC1\_high with the cut-off values at the median.

**Correlations:** Correlation of continuous variables with approximately normal distribution (CD8+ cell density in whole core and cancer epithelium, CD68+ cell density, CD45+ cell density, percentage of Ki67+ tumor cells, CD8 relative expression values, PC1, PC2 and age) was assessed by Pearson's correlation coefficients. Correlation of continuous non-normally distributed variables (CD68+/DAPI and MSR1+CD68+/CD68+) was assessed by Spearman's correlation coefficients. Continuous variables with approximately normal distribution were compared between groups by ANOVA and T-test as appropriate. Continuous non-normally distributed variables were compared between two-categorized groups by Mann-Whitney-U-test. Categorized variables were immune cell clusters (present, absent), FIGO stage (II, III, IV), grade (1, 2, 3), histology (serous, non-serous), residual tumor (yes, no) and PC1 (PC1\_low, PC1\_high). The association of categorical variables was evaluated by Chi square and by Fisher's exact tests as appropriate. The Holm-Bonferroni method was used to correct for multiple testing.

**Survival:** Univariate and multivariable Cox proportional hazards regression analyses were used to evaluate the marginal and adjusted associations of CD8+ (whole core and cancer epithelium), CD68+ and CD45+ cell density, percentage of Ki67+ tumor cells, immune cell

clusters, CD8 relative expression values and the clinicopathological factors age, histology, FIGO stage and residual tumor with survival (Cox, 1972). For multivariable survival analyses, the multivariable fractional polynomial approach was used to evaluate possible non-linear effects of the continuous variables CD8+ (whole core and cancer epithelium), CD68+ and CD45+ cell density, percentage of Ki67+ tumor cells, CD8 relative expression values and age on survival by a set of parsimonious transformations (Royston and Sauerbrei, 2008). For non-linear associations of the assessed factors with survival, the respective factors were transformed according to the shape of non-linearity. Because of the relatively low number of outcome events (58), FIGO stage was modeled as an ordinal rather than a categorical variable, assuming the same hazard ratio (HR) between FIGO IV and III as between FIGO III and II. This strategy saves one degree of freedom and hence provides more stable results than with categorical modeling of FIGO stage. Pairwise interactions between variables were tested by assessing significance of corresponding product terms. Backward stepwise exclusion of factors with inclusion criterion of  $p \leq 0.05$  and exclusion criterion of  $p \geq 0.10$  was applied for multivariable analyses.

Cumulative survival probabilities were calculated by the Kaplan-Meier method and the log-rank test. The study population was dichotomized into CD45\_low and CD45\_high, CD8\_low and CD8\_high and into Ki67\_low and Ki67\_high with the cut-off values at the respective medians as well as into Ki67- and Ki67+ with the cut-off value according to the shape of the non-linearity.

Two-sided  $p$  values  $< 0.05$  were considered statistically significant in all analyses.

### 3 Results

#### 3.1 Study population and patients' material

*Blood cell signatures:* A total of 23 women were included in the blood cell signature study whose clinical and pathological characteristics are summarized in Table 4.

**Table 4.** Characteristics of the blood cell signature cohort.

Patient groups	N (%)	Characteristics			Relative risk of EOC*
Ovarian cancer N = 4		Histology	FIGO	Grade	
EOC	4 (100.0)	serous	I	2	2.9
		serous	III	3	3.5
		mucinous	III	2	7.5
		undifferentiated	III	3	3.5
Other malignancies except ovarian cancer N = 6		Histology			
Krukenberg tumor	2 (33.3)	adenocarcinoma			2.5
					2.9
Signet ring cell carcinoma	1 (16.7)	adenocarcinoma with signet ring cells			3.6
Borderline tumor	1 (16.7)	serous cystadenoma, borderline morphology			4.8
Lymphoma	1 (16.7)	follicular lymphoma			5.7
Teratoma	1 (16.7)	dermoid cyst			0.3
Benign diseases and healthy individuals N = 13					
Hypermenorrhea	1 (7.7)				-4.9
Fibroma	1 (7.7)				-2.0
Myoma	2 (15.4)				-1.4
					2.2
CIN I, HPV-HR positive	3 (23.1)				-3.9
					-2.7
					1.5
CIN II, HPV-HR positive	1 (7.7)				1.5
CIN II, HPV-HR negative	1 (7.7)				4.3
Abortion	1 (7.7)				-6.6
Healthy individuals	3 (23.1)				-2.0
					-1.8
					-0.8

EOC: epithelial ovarian cancer; CIN: cervical intraepithelial neoplasia; HPV-HR: human papilloma virus – high risk

\* The relative risk of EOC is a linear combination of the gene expression values of the diagnostic gene panel with coefficients listed in Table 1. The gene expressions were assessed in the “high density” blood leukocyte fraction.

In the group of ten patients with suspected EOC only four patients were finally diagnosed with EOC (OC group). Six patients had other predominantly malignant diseases including



Krukenberg tumor, signet ring cell carcinoma, borderline tumor, lymphoma and teratoma. They were summarized in a separate patient group (M group). The control group comprised three healthy blood donors and ten patients with benign gynecological diseases such as hypermenorrhea, myoma, fibroma and cervical intraepithelial neoplasia (CIN) (B group).

For each woman the relative risk values of EOC according to the diagnostic gene panel assessed in the HD fraction are given in Table 4.

In the microscopic examination of the blood samples that had been incubated simultaneously with two types of antibodies coupled to different sized beads no double binding of different bead-linked antibodies to the same cell was observed.

*Tumor microenvironment:* Clinical and pathological characteristics of the tumor samples of the 209 patients included in the immunohistochemical analysis of tumor proliferation and leukocyte infiltration and of the tumor samples of the 19 patients selected for the immunofluorescent analysis of TAMs are depicted in Table 5. Patients predominantly presented with cancer at advanced stages (96% and 84% FIGO III/IV in the 209 and in the 19 patient cohort, respectively) and of serous histology (88% and 79%, respectively).

**Table 5.** Characteristics of EOC of the tumor microenvironment cohort.

	N = 209	N = 19
Characteristics	N (%)	N (%)
<b>Histology</b>		
Serous	184 (88.0)	15 (78.9)
Non-serous	25* (12.0)	4** (21.1)
<b>FIGO</b>		
FIGO II	9 (4.3)	3 (15.8)
FIGO III	164 (78.5)	13 (68.4)
FIGO IV	36 (17.2)	3 (15.8)
<b>Grade</b>		
Grade 1	9 (4.3)	
Grade 2	46 (22.0)	4 (21.1)
Grade 3	153 (73.2)	15 (78.9)
unknown	1 (0.5)	
<b>Residual tumor</b>		
no	146 (69.9)	8 (42.1)
yes	63 (30.1)	11 (67.9)

\* Endometrioid, 9; Mixed epithelial, 9; Mucinous, 1; Undifferentiated carcinoma, 4; Clear cell carcinoma, 2;

\*\* Endometrioid, 2; Mixed epithelial, 2;

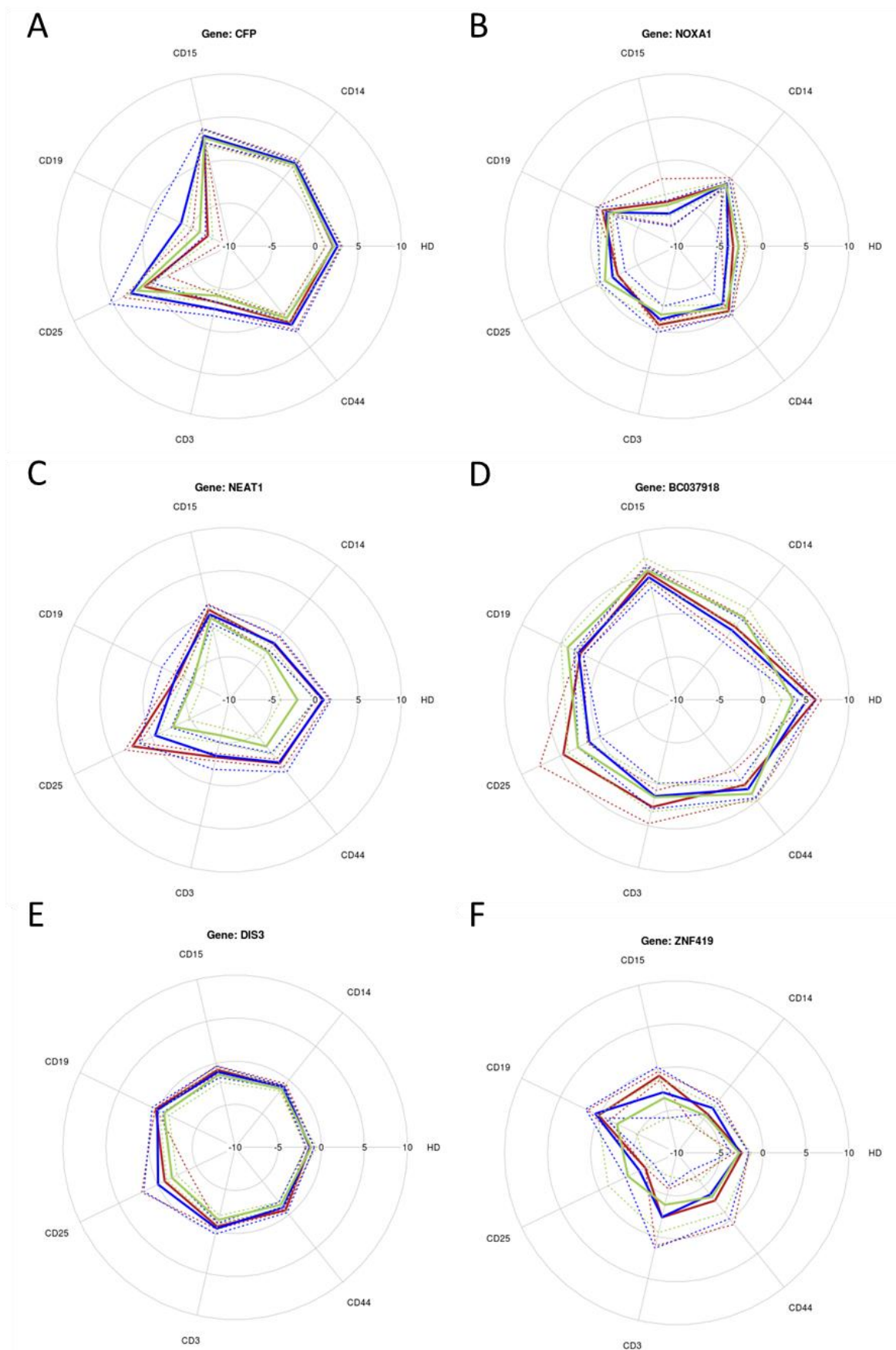
The median age of the 209 patient cohort and of the 19 patient cohort was 56 years (range 18-85 years) and 58 years (range 18-81 years), respectively. 22 patients out of the 209 patients (11%) had refractory disease. These patients were excluded for PFS analyses since the exact time point of progression of disease could not be determined. The median PFS was 18 months (range 6-48 months) and 13 months (range 5-41 months) in the 209 patient cohort and in the 19 patient cohort, respectively; the median OS was 24 months (range 1-49 months) and 21 months (range 5-41 months), respectively. The follow-up time ranged from 1 to 49 months with a median of 30 months in the 209 patient cohort and ranged from 5 to 41 months with a median of 28 months in the 19 patient cohort. 58 out of the 209 patients (28%) and 4 out of the 19 patients (21%) died within the observation period.

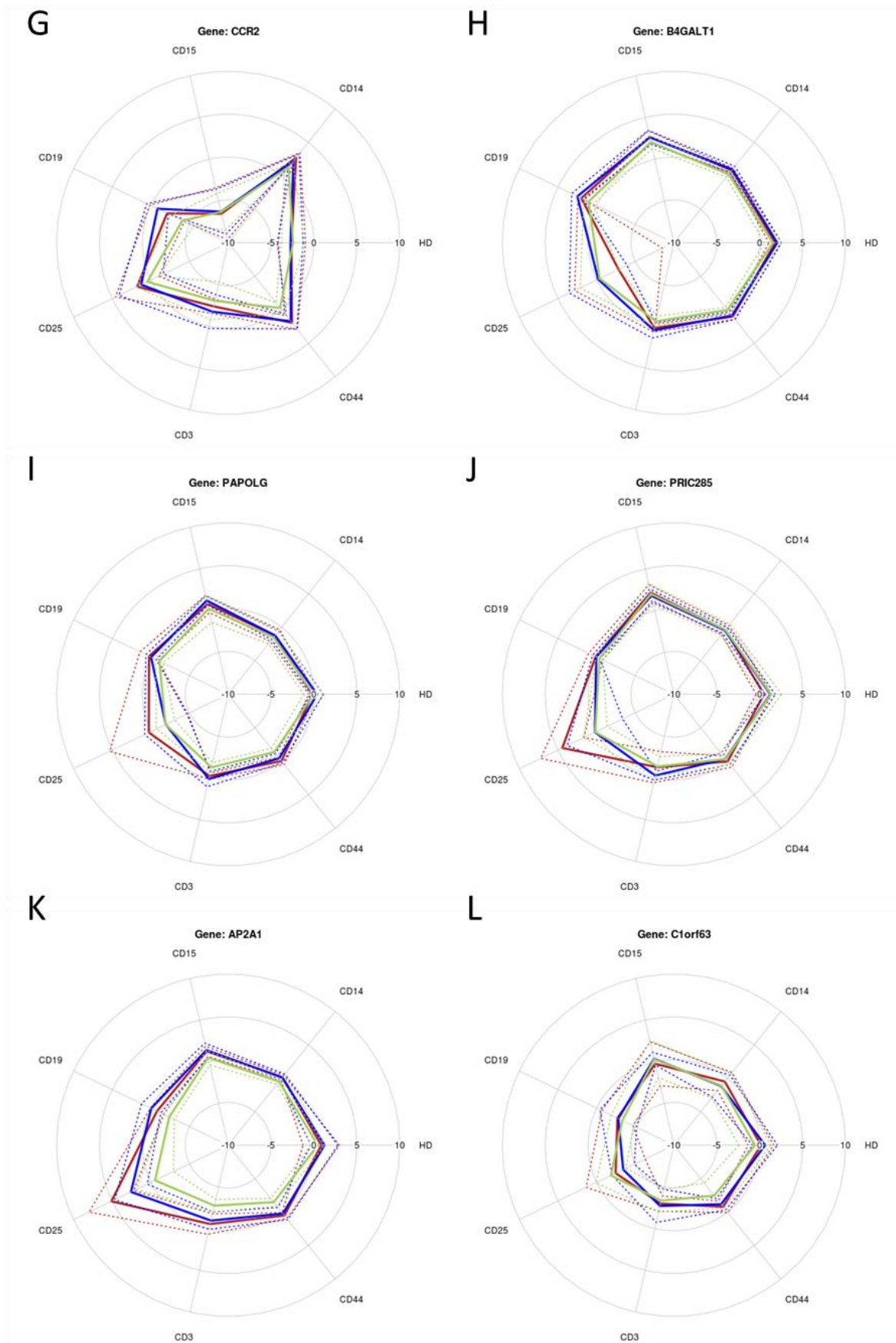
## **3.2 Blood cell gene signatures**

### **3.2.1 Diagnostic panel: heterogeneous expressions and significant differences between patient groups**

The gene expression patterns of the diagnostic 13 gene panel comprising CFP, NOXA1, NEAT1, BC037918, DIS3, ZNF419, CCR2, B4GALT1, PAPOLG, PRIC285, AP2A1, C1orf63 and OSM in the seven fractions, HD, CD3, CD14, CD15, CD19, CD25 and CD44, did not reveal a single blood cell fraction obviously suitable for the determination of this signature. The comparison of the assessed expression values in the seven fractions between individuals showed similar expression patterns among individuals for most genes (data not shown). Most genes were differently expressed in the analyzed blood cell fractions and/or showed different expression patterns according to the three patient groups, EOC patients (OC group), patients with other predominantly malignant diseases except ovarian cancer (M group) and controls comprising patients with benign diseases and healthy individuals (B group) (Figure 5). These similar patterns among individuals indicate that these genes are partially differentially expressed depending on the cell type and/or on the patient group, but fairly independent of the individual.

CFP, AP2A1 and NEAT had the expression peaks in the fractions CD25 and CD15. The latter two genes showed differences between patient groups in many fractions. BC037918 had the highest expression values in the fractions HD and CD15 with several patient group specific differences. OSM showed expression differences among fractions with the highest value for fraction CD15, but equal expression patterns in the different patient groups.





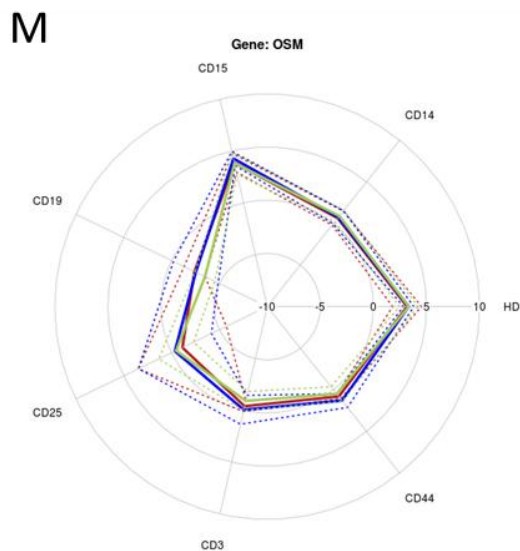


**Figure 5.** Star plots of the expression values of the 13 genes of the diagnostic panel (A – M) in the assessed blood cell fractions. The colors represent the patient groups: green – benign diseases, blue – malignant diseases except ovarian cancer, red – ovarian cancer; HD: high density. The mean expression values are shown as continuous lines. The standard deviations are shown as dashed lines.

DIS3, B4GALT1, PAPOLG and C1orf63 were characterized by similar expression levels without characteristic peaks in the different blood cell fractions. Patient group specific expressions were rare in these four genes, except for PAPOLG. Similarly, PRIC285 showed uniform expression among fractions and patient groups with the exception of slightly higher expression values in fraction CD15 of all three patient groups and higher expression values in fraction CD25 of the patient group OC. CCR2 and NOXA1 were both highest expressed in fraction CD14 followed by the fractions CD25 and CD44, whereby CCR2 additionally showed patient group specific differences. ZNF419 did not show a clear pattern, but was characterized by high standard deviations due to high variations between individuals.

Six of the 13 genes from the diagnostic panel had the expression peaks in the fractions of CD15+, CD25+ and CD44+ enriched cells: CFP, NEAT1, BC037918, PRIC285, AP2A1 and OSM. In contrast, the genes NOXA1 and CCR2 presented a similar expression pattern to most genes of the prognostic panel with the highest expression values in the fractions of CD14+ and CD25+ enriched cells. DIS3, B4GALT, PAPOLG and C1orf63 were characterized by equal expression values in the different fractions. ZNF419 did not show any characteristic pattern.

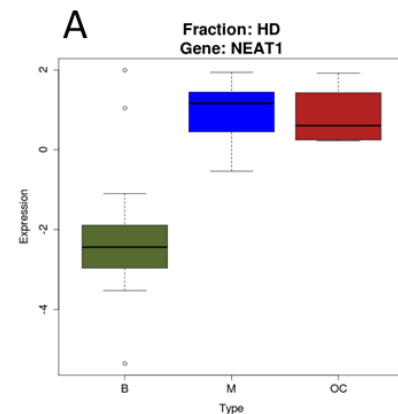
ANOVA comparing the mean expression values of the 13 genes in the seven fractions between the three patient groups OC, M and B and subsequent Bonferroni correction revealed 31 significantly different gene expressions; the more stringent Holm-Bonferroni method revealed 21 significantly different gene expressions. Table 6 shows the mean gene expression

values of the 13 genes in the seven blood cell fractions and significant up- and down-regulations comparing the three patient groups. Figure 6 exemplarily depicts gene expression box plots of significantly differentially expressed genes among the patient groups in the respective fractions. Significant differences were mostly revealed between the control group B and the two malignant groups M and OC, whereas few significant differences were exclusively found between group OC and group B (CCR2 in fraction CD14, NEAT1 in fraction CD25 and DIS3 in fraction CD44). The genes NEAT1, AP2A1 and PAPOLG were characterized by most patient group specific expressions. The fractions with most gene expression differences between patient groups were the fractions CD19 and CD3 corresponding to the lymphocyte fractions (CD19 representing the B cell fraction and CD3 representing the T cell fraction) and the fraction CD44 (representing a mixture of tissue cells, erythrocytes and leukocytes). Interestingly, the fractions CD3 and CD19 were characterized by generally low expression values for the genes of the diagnostic panel. In contrast, the fractions CD15, CD25, CD14 and HD with higher expression values showed no (CD15) or fewer patient group specific gene expressions.

**Table 6.** Comparison of gene expression values of the 13 genes of the diagnostic panel between the patient groups with benign diseases (B), malignant diseases except ovarian cancer (M) and ovarian cancer (OC) in the seven blood cell fractions (A - G).

**A.** High density fraction.

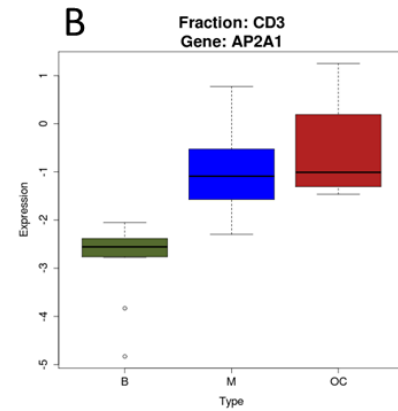
	Patient group					
	B		M		OC	
	Mean	Standard Deviation	Mean	Standard Deviation	Mean	Standard Deviation
CFP	2.16	1.03	2.56	0.52	2.06	0.87
NOXA1	-2.83	1.03	-4.09	1.33	-3.46	1.37
<b>NEAT1*</b>	<b>-2.08</b>	1.91	<b>0.94</b> <b>B</b>	0.88	<b>0.84</b> <b>B</b>	0.79
<b>BC037918*</b>	<b>3.48</b>	1.32	<b>5.09</b> <b>B</b>	1.04	<b>6.10</b> <b>B</b>	0.68
DIS3	-1.19	0.64	-1.29	0.45	-1.35	0.53
ZNF419	-2.76	1.40	-2.69	1.03	-2.47	0.83
CCR2	-2.44	1.35	-2.73	1.46	-2.64	1.66
B4GALT1	1.53	0.99	2.03	0.51	1.80	0.72
PAPOLG	-0.03	1.16	.36	0.73	-0.19	0.43
PRIC285	1.31	1.22	1.24	0.57	0.49	0.91
AP2A1	0.46	0.80	1.21	1.57	0.84	2.12
C1orf63	-0.56	1.86	.62	1.45	0.14	1.48
OSM	3.34	0.87	3.31	0.49	3.17	1.36



HD: high density

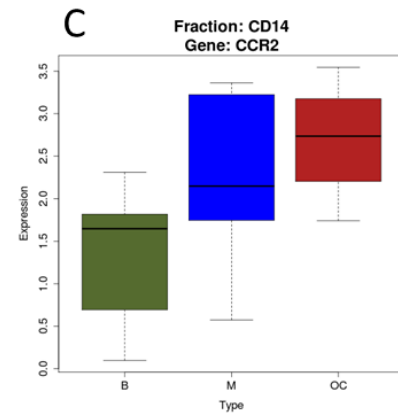
## B. CD3+ enriched cells.

	Patient group					
	B		M		OC	
	Mean	Standard Deviation	Mean	Standard Deviation	Mean	Standard Deviation
<b>CFP*</b>	<b>-4.10</b>	0.66	<b>-2.52</b> <b>B</b>	0.79	-3.34	0.90
NOXA1	-1.86	1.00	-1.29	1.56	-0.65	0.42
<b>NEAT1*</b>	<b>-5.76</b>	0.88	<b>-3.32</b> <b>B</b>	1.61	<b>-3.16</b> <b>B</b>	0.44
BC037918	1.60	1.73	1.47	1.52	2.75	1.97
<b>DIS3*</b>	<b>-1.36</b>	0.51	<b>-0.33</b> <b>B</b>	0.66	<b>-0.57</b> <b>B</b>	0.31
ZNF419	-3.80	3.31	-2.34	3.72	-2.30	3.38
CCR2	-3.06	2.27	-1.76	2.01	-2.40	0.84
<b>B4GALT1</b>	<b>-0.60</b>	0.61	<b>0.46</b> <b>B</b>	0.92	0.19	0.47
<b>PAPOLG*</b>	<b>-1.27</b>	0.56	<b>0.13</b> <b>B</b>	0.92	<b>-0.23</b> <b>B</b>	0.37
PRIC285	-1.37	1.18	-0.27	0.54	-1.28	1.86
<b>AP2A1*</b>	<b>-2.76</b>	0.76	<b>-0.97</b> <b>B</b>	1.04	<b>-0.56</b> <b>B</b>	1.23
C1orf63	-3.36	1.35	-2.73	1.99	-3.01	0.91
OSM	-0.91	0.91	-0.05	1.39	-0.40	0.51



## C. CD14+ enriched cells.

	Patient group					
	B		M		OC	
	Mean	Standard Deviation	Mean	Standard Deviation	Mean	Standard Deviation
CFP	2.08	0.36	2.32	0.27	2.29	0.55
NOXA1	-0.84	0.59	-0.69	0.53	-0.78	0.96
<b>NEAT1</b>	<b>-2.85</b>	0.77	<b>-1.60</b> <b>B</b>	1.03	-1.70	0.94
<b>BC037918</b>	<b>2.29</b> <b>M</b>	1.16	<b>0.30</b>	1.69	0.83	1.56
DIS3	-1.38	0.27	-1.05	0.23	-1.00	0.43
ZNF419	-4.52	1.51	-3.33	0.83	-4.25	2.13
<b>CCR2</b>	<b>1.28</b>	0.78	2.20	1.04	<b>2.69</b> <b>B</b>	0.74
<b>B4GALT1</b>	<b>0.22</b>	0.42	<b>0.93</b> <b>B</b>	0.47	0.80	0.29
PAPOLG	-1.52	0.94	-1.23	0.63	-1.25	0.87
PRIC285	-0.38	0.84	-0.47	0.42	-1.41	0.66
<b>AP2A1</b>	<b>-0.49</b>	0.39	<b>0.12</b> <b>B</b>	0.50	<b>0.14</b> <b>B</b>	0.29
C1orf63	-1.11	1.83	-1.17	1.64	-0.49	1.35
OSM	0.89	0.69	0.74	0.79	0.64	0.84

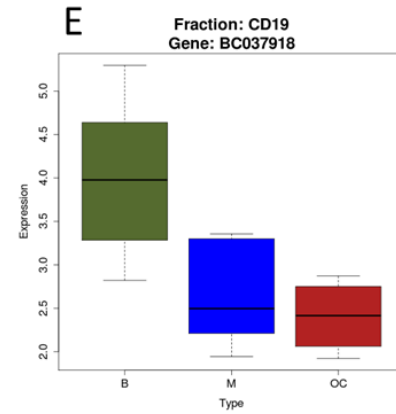


#### D. CD15+ enriched cells.

	Patient group					
	B		M		OC	
	Mean	Standard Deviation	Mean	Standard Deviation	Mean	Standard Deviation
CFP	2.89	0.90	3.13	0.83	3.14	0.86
NOXA1	-5.10	1.26	-6.11	1.53	-4.74	2.75
NEAT1	-0.23	1.20	0.17	1.12	0.72	0.71
BC037918	5.44	1.45	4.59	1.23	5.12	0.96
DIS3	-1.36	0.86	-1.03	0.68	-0.79	0.48
ZNF419	-3.45	2.29	-2.79	3.04	-0.81	0.51
CCR2	-6.30	2.19	-6.28	2.67	-6.52	3.09
B4GALT1	2.04	0.76	2.61	0.83	2.67	0.72
PAPOLG	0.23	1.62	1.21	0.55	0.79	1.03
PRIC285	1.99	1.29	1.79	0.80	2.16	0.93
AP2A1	0.49	0.88	1.40	0.83	1.25	0.61
C1orf63	0.30	2.23	0.36	0.77	-0.24	2.63
OSM	3.80	1.06	4.27	0.68	3.84	0.89

#### E. CD19+ enriched cells.

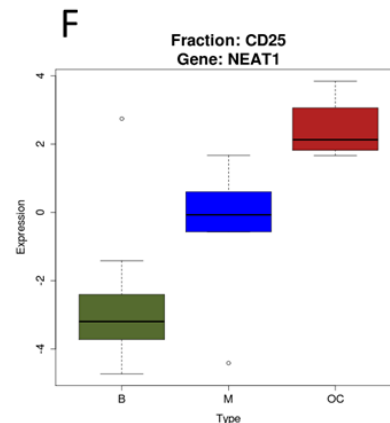
	Patient group					
	B		M		OC	
	Mean	Standard Deviation	Mean	Standard Deviation	Mean	Standard Deviation
CFP	-6.22	1.69	-3.82	3.14	-7.25	1.92
NOXA1	-1.21	0.61	-0.91	1.26	-0.44	0.87
NEAT1*	<b>-5.33</b>	1.14	<b>-3.21</b> <b>B</b>	1.88	-3.45	0.49
BC037918*	<b>4.04</b> <b>M, OC</b>	0.86	<b>2.63</b>	0.60	<b>2.41</b>	0.43
DIS3*	<b>-0.84</b>	0.61	<b>0.02</b> <b>B</b>	0.67	<b>0.23</b> <b>B</b>	0.13
ZNF419	<b>-2.30</b>	2.48	<b>0.49</b> <b>B</b>	1.23	0.08	1.38
CCR2*	<b>-4.07</b>	1.48	<b>-0.86</b> <b>B</b>	1.39	-2.10	2.23
B4GALT1*	<b>1.04</b>	0.63	<b>2.48</b> <b>B</b>	0.73	1.98	0.43
PAPOLG*	<b>-1.10</b>	0.50	<b>-0.03</b> <b>B</b>	0.68	<b>0.23</b> <b>B</b>	1.18
PRIC285	-0.37	0.42	0.04	0.47	0.12	0.90
AP2A1*	<b>-2.39</b>	0.64	<b>-0.05</b> <b>B</b>	1.24	<b>-0.80</b> <b>B</b>	0.83
C1orf63	-3.33	1.44	-2.81	2.37	-2.69	2.00
OSM	-3.50	1.02	-2.54	2.34	-2.40	1.08





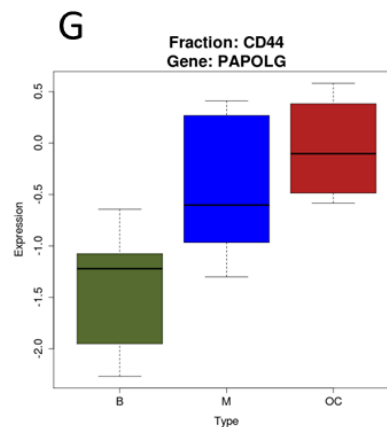
## F. CD25+ enriched cells.

	Patient group					
	B		M		OC	
	Mean	Standard Deviation	Mean	Standard Deviation	Mean	Standard Deviation
CFP	1.85	1.22	2.62	2.78	0.85	2.83
NOXA1	-0.75	1.15	-1.73	1.59	-2.38	0.00
<b>NEAT1*</b>	<b>-2.78</b>	1.88	-0.47	2.08	<b>2.44</b> <b>B</b>	0.97
<b>BC037918</b>	2.73	1.28	<b>1.27</b>	1.44	<b>4.61</b> <b>M</b>	3.06
DIS3	-1.85	0.66	-0.07	1.84	-0.91	2.95
ZNF419	-3.71	2.54	-5.21	1.81	-5.95	0.00
CCR2	0.46	1.40	1.25	2.88	1.77	2.81
B4GALT1	-0.40	2.51	-0.21	3.73	-2.85	5.68
PAPOLG	-1.90	1.18	-1.93	2.74	0.26	5.06
<b>PRIC285</b>	<b>0.16</b>	1.51	<b>0.20</b>	3.57	<b>4.43</b> <b>B, M</b>	2.79
<b>AP2A1*</b>	<b>-0.54</b>	2.38	<b>2.56</b> <b>B</b>	2.10	<b>5.10</b> <b>B</b>	2.89
C1orf63	-1.87	1.95	-3.44	1.45	-2.47	3.82
OSM	-0.49	1.82	-0.35	3.81	-1.14	4.61



## G. CD44+ enriched cells.

	Patient group					
	B		M		OC	
	Mean	Standard Deviation	Mean	Standard Deviation	Mean	Standard Deviation
CFP	0.70	0.49	1.66	1.02	1.31	1.10
NOXA1	-0.81	0.59	-1.45	1.58	-0.36	0.69
<b>NEAT1*</b>	<b>-3.08</b>	1.20	<b>-0.70</b> <b>B</b>	1.41	<b>-0.57</b> <b>B</b>	0.60
BC037918	3.96	1.06	3.25	1.32	2.62	2.06
<b>DIS3</b>	<b>-1.50</b>	0.38	-1.09	0.77	<b>-0.66</b> <b>B</b>	0.11
ZNF419	-3.44	2.35	-3.79	3.59	-2.90	3.55
<b>CCR2*</b>	<b>-0.29</b>	0.77	<b>1.70</b> <b>B</b>	1.14	<b>1.92</b> <b>B</b>	1.00
<b>B4GALT1*</b>	<b>0.01</b>	0.37	<b>0.85</b> <b>B</b>	0.56	<b>1.00</b> <b>B</b>	0.41
<b>PAPOLG*</b>	<b>-1.39</b>	0.56	<b>-0.46</b> <b>B</b>	0.68	<b>-0.05</b> <b>B</b>	0.53
PRIC285	-0.34	0.86	-0.37	0.85	0.02	0.83
<b>AP2A1*</b>	<b>-1.49</b>	0.57	<b>0.22</b> <b>B</b>	0.91	<b>0.51</b> <b>B</b>	0.44
C1orf63	-2.47	1.85	-1.18	0.85	-0.80	0.87
OSM	0.49	0.86	1.29	0.83	0.80	0.26



Significant up- and down-regulations of gene expressions assessed by ANOVA and Bonferroni testing (significant pairs in bold, key of the smaller patient group under the patient group with the larger mean) and by Holm-Bonferroni testing (significance marked with a star)

**Figure 6.** Examples of expression box plots of significantly differently expressed genes of the diagnostic gene panel among the patient groups in the assessed blood cell fractions (A - G). Colors represent the patient groups: green - benign diseases (B), blue - malignant diseases except ovarian cancer (M), red - ovarian cancer (OC).

The relative risk of EOC according to the diagnostic 13 gene panel was computed for each patient for all seven blood cell fractions. The comparison of the relative risk values between the three patient groups assessed in the HD fraction revealed significantly higher values in the two malignant groups OC and M than in the benign group B (Table 7 and Figure 7). The relative risk values of each woman included in the study determined in the HD fraction is listed in Table 4. A trend of higher relative risk values in the OC group compared to the M group was observed which was, however, not significant. In the control group relative risk values of EOC were lower, with the exception of one outlier with a relative risk value of 4.2 that was in the order of the relative risk values in the group OC (mean 4.4) and in the group M (mean 3.3). This woman was 28 years old, diagnosed with CIN II and human papilloma virus – high risk (HPV-HR) negative. She did not present with any histological signs of malignancy. The relative risk values of EOC of the other four CIN patients who were all HPV-HR positive were equal or below the 75<sup>th</sup> percentile of the control group.

Only the expression values obtained from the HD fraction resulted in significantly different relative risk values between the malignant and the benign patient groups, whereas in the other fractions no differences between the patient groups were found with the formula of relative risk of EOC developed for the HD fraction (data not shown).

**Table 7.** Mean of relative risk values of ovarian cancer in patients with benign diseases (B), malignant diseases except ovarian cancer (M) and ovarian cancer (OC) according to the diagnostic 13 gene panel assessed in the high density fraction.

	Patient group		
	B	M	OC
	mean	Mean	mean
<b>Relative risk</b>	<b>-1.28</b>	<b>3.31</b>	<b>4.36</b>
		<b>B</b>	<b>B</b>

Significant differences assessed by ANOVA (significant pairs in bold, key of the smaller patient group under the patient group with the larger mean)

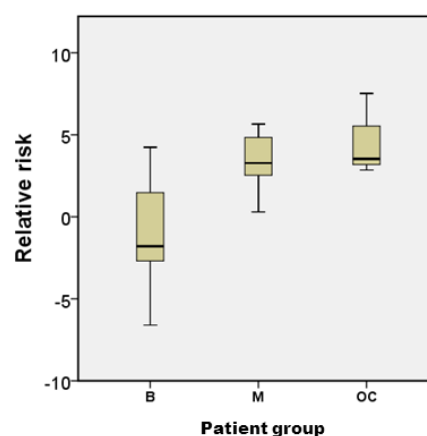


**Figure 7.** Box plots of relative risk values of ovarian cancer in patients with benign diseases (B), malignant diseases except ovarian cancer (M) and ovarian cancer (OC) according to the diagnostic 13 gene panel assessed in the high density fraction.

### 3.2.2 Prognostic panel: peaks in the fractions CD14 and CD25

The analysis of the gene expression patterns of the prognostic seven gene panel comprising SRC, GUCY1B3, TUBB1, GUCY1A3, TUBA8, EGF and TRIM14 in the seven blood cell fractions showed a similar expression pattern for most genes with peaks in the fractions of CD14+ and CD25+ enriched cells and the lowest values in the fraction of CD3+ enriched cells. This expression pattern was similar to the expression patterns of NOXA1 and CCR2 of the diagnostic panel. Figure 8 exemplarily depicts star plots of two genes showing the described expression pattern. SRC, GUCY1B3, TUBB1, GUCY1A and EGF were highest expressed in the fractions CD14 and CD25. GUCY1B3, TUBB1 and GUCY1A additionally showed expression peaks in the fraction of CD44+ enriched cells. In contrast, TUBA8 and TRIM14 were characterized by similar expression levels without characteristic peaks in the different blood cell fractions.

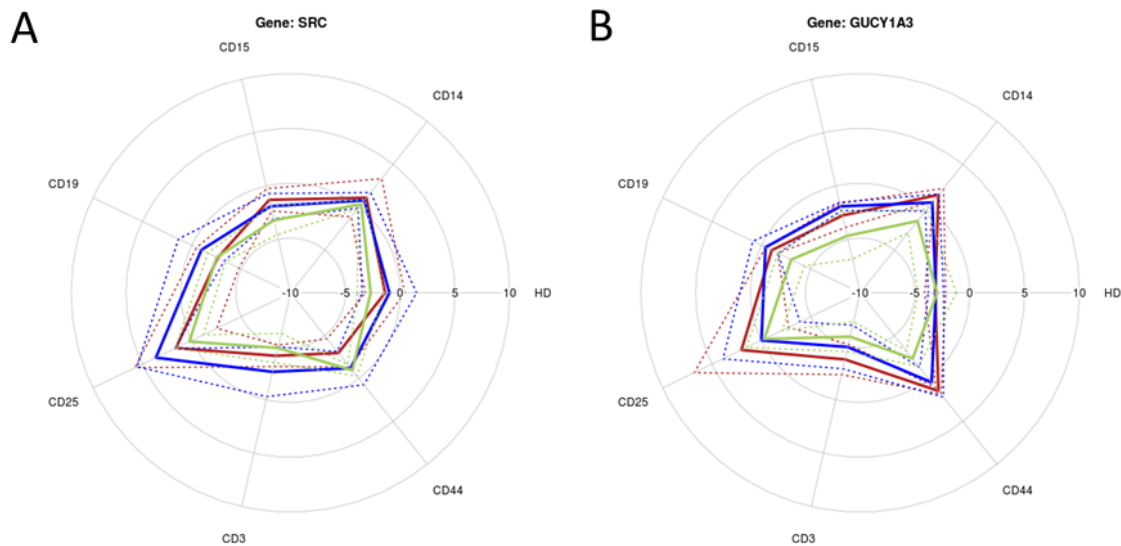


**Figure 8.** Star plots of the expression values of **A** SRC and **B** GUCY1A3 of the prognostic gene panel in the assessed blood cell fractions showing similar expression patterns. The colors represent the patient groups: green – benign diseases, blue – malignant diseases except ovarian cancer, red – ovarian cancer; HD: high density. The mean expression values are shown as continuous lines. The standard deviations are shown as dashed lines.

Gene expression differences between EOC patients with favorable prognosis and those with a worse clinical outcome were not assessed since the number of patients was far too low and at the time of analysis follow-up time was only several months which was not sufficient for analysis of the clinical outcome.

### 3.2.3 Principal Component Analysis of expression patterns in the blood fractions

To reduce the complexity of the gene expression data sets of the genes of the diagnostic and the prognostic gene panel, PCA was performed with the 20 genes as variables. The genes of the two different panels were combined in the PCA to include as many expression data as available for the determination of differences and similarities between the different blood cell fractions.

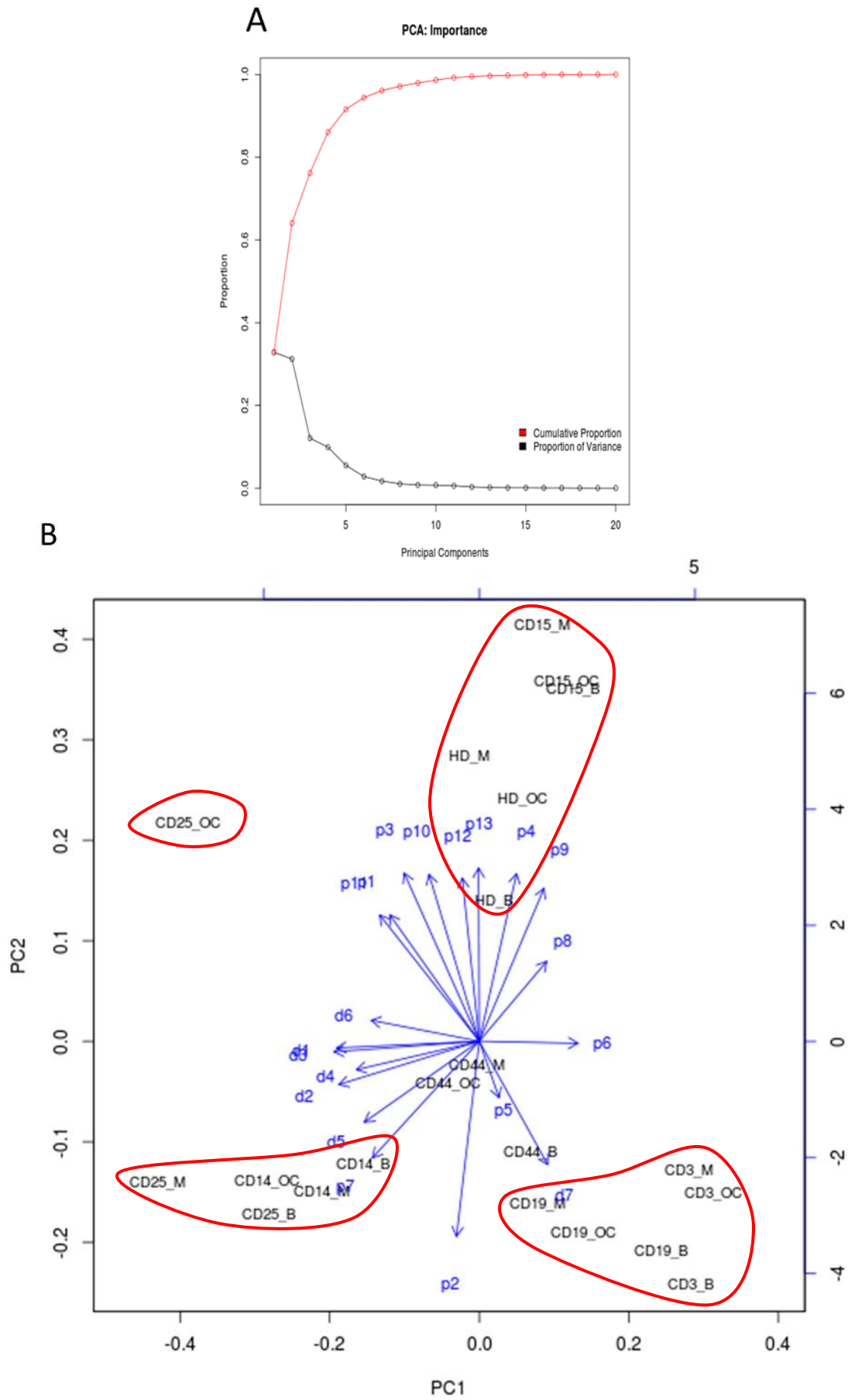
Using the first three PCs, clustering of the fractions of the patient groups B, M and OC and the influences of the gene expressions of the prognostic seven gene panel and the diagnostic 13 gene panel was examined (Figure 9). The importance of the 20 PCs regarding proportion of data variance are presented in Figure 9A.

Figure 9B depicts the first two PCs and shows four clusters of fractions: i) HD and CD15, ii) CD3 and CD19, iii) CD14 and CD25 and iv) CD25\_OC as an outlier far apart from all other fractions. The fractions of CD44+ enriched cells of the three patient groups were localized in the center of the biplot between the three clusters.

Regarding clustering of gene expression values and associated blood cell fractions three clusters were obvious: i) most of the genes from the diagnostic panel (CFP, NEAT1, BC037918, B4GALT1, PAPOLG, PRIC285, AP2A1, C1orf63 and OSM) with the fractions HD and CD15, ii) DIS3 and ZNF419 from the diagnostic panel and TRIM14 from the prognostic panel with the fractions CD3 and CD19 and iii) most of the genes from the prognostic panel (SRC, GUCY1B3, TUBA8, TUBB1, GUCY1A3 and EGF) and NOXA1 and CCR2 from the diagnostic panel with the fractions CD14 and CD25.

The clusters revealed by PCA are in accordance with the expression patterns of the 20 genes in the different blood cell fractions (Figure 4 and 7), which also indicated similarities between most genes of the prognostic panel and NOXA1 and CCR2 of the diagnostic panel. Moreover, DIS3, ZNF419 and TRIM14 were already shown to have differing expression patterns compared to most other genes of the two panels.

The comparison of the blood cell fractions between the different patient groups showed only marginal differences between the three patient groups in the fractions CD14, CD15 and CD19. In contrast, there were substantial differences between the patient groups OC/M and B in the fractions CD44, CD3 and HD. The fraction CD25 showed the greatest difference between the patient group OC in comparison to the patient groups M and B.



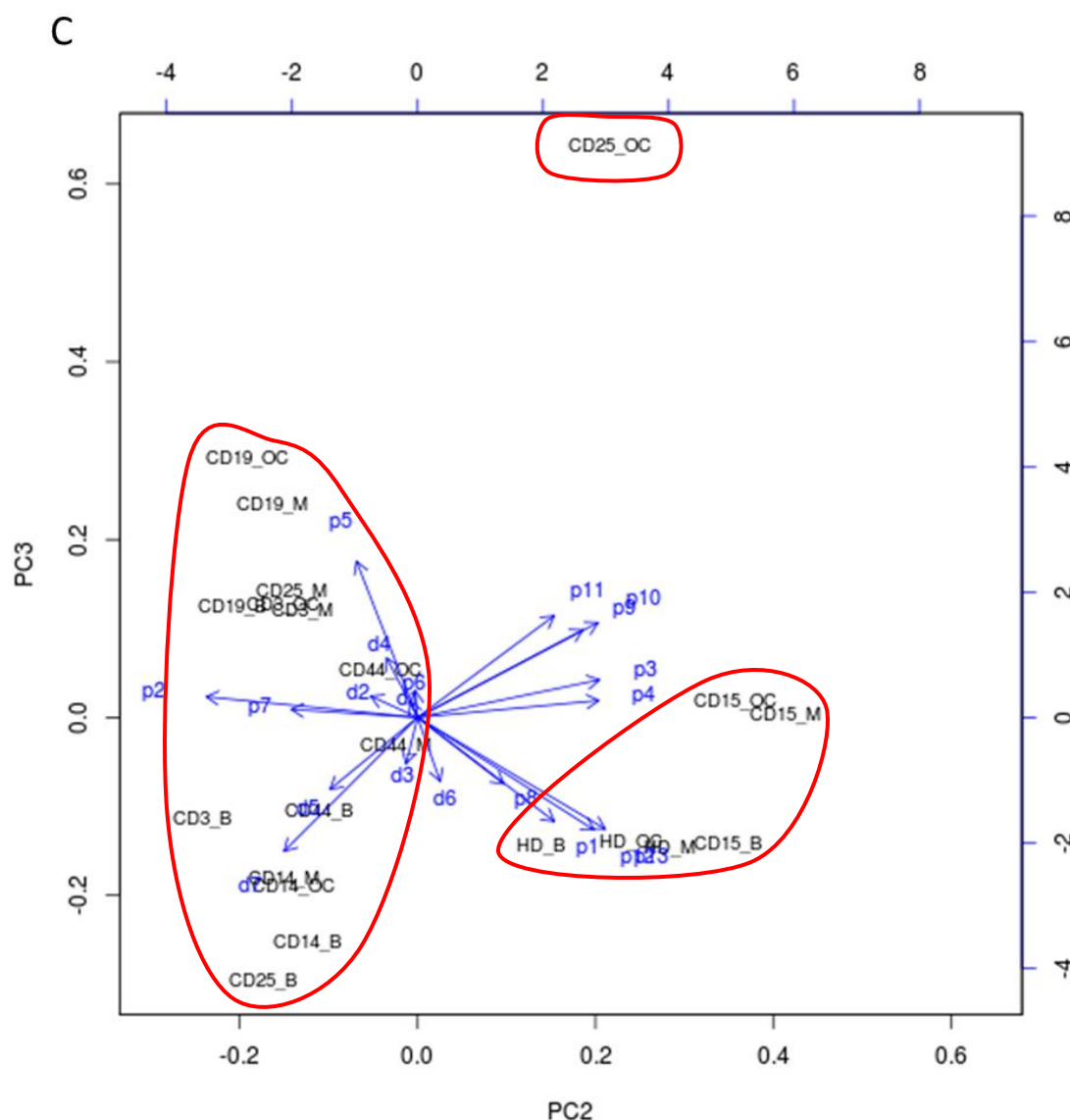


**Figure 9.** Principal component analysis (PCA) using the prognostic seven gene panel (d1-7: SRC, GUCY1B3, TUBA8, TUBB1, GUCY1A1, EGF and TRIM14) and the diagnostic 13 gene panel (p1-13: CFP, NOXA1, NEAT1, BC037918, DIS3, ZNF419, LCCR2, B4GALT1, PAPOLG, PRIC285, AP2A1, C1orf63 and OSM) as variables (blue vectors) for the assessment of clustering of the fractions of the patient groups (benign diseases (B), malignant diseases except ovarian cancer (M) and ovarian cancer (OC)) ; HD: high density. **A** Importance of the 20 PCs regarding proportion of data variance. A proportion of variance of 0.76 were covered by PC1 (0.33), PC2 (0.31) and PC3 (0.12). **B** PC1 and PC2 show four clusters of fractions (marked in red): i) HD and CD15, ii) CD3 and CD19, iii) CD14 and CD25 and iv) CD25\_OC. **C** PC2 and PC3 reveal three clusters (marked in red): i) HD and CD15, ii) CD3, CD14, CD19, CD44, CD25\_M/B and iii) CD25\_OC.

Figure 9C depicting the second and the third PCs showed similar clusters: i) HD and CD15, ii) CD3, CD14, CD19, CD44, CD25\_M and CD25\_B and iii) CD25\_OC.

As in Figure 9B most of the genes from the diagnostic panel clustered with the fractions HD and CD15. All genes from the prognostic panel and NOXA1 and CCR2 from the diagnostic panel clustered with the fractions CD3, CD14, CD19, CD44, CD25\_M and CD25\_B. In contrast to Figure 9B, Figure 9C showed more discriminative power between the

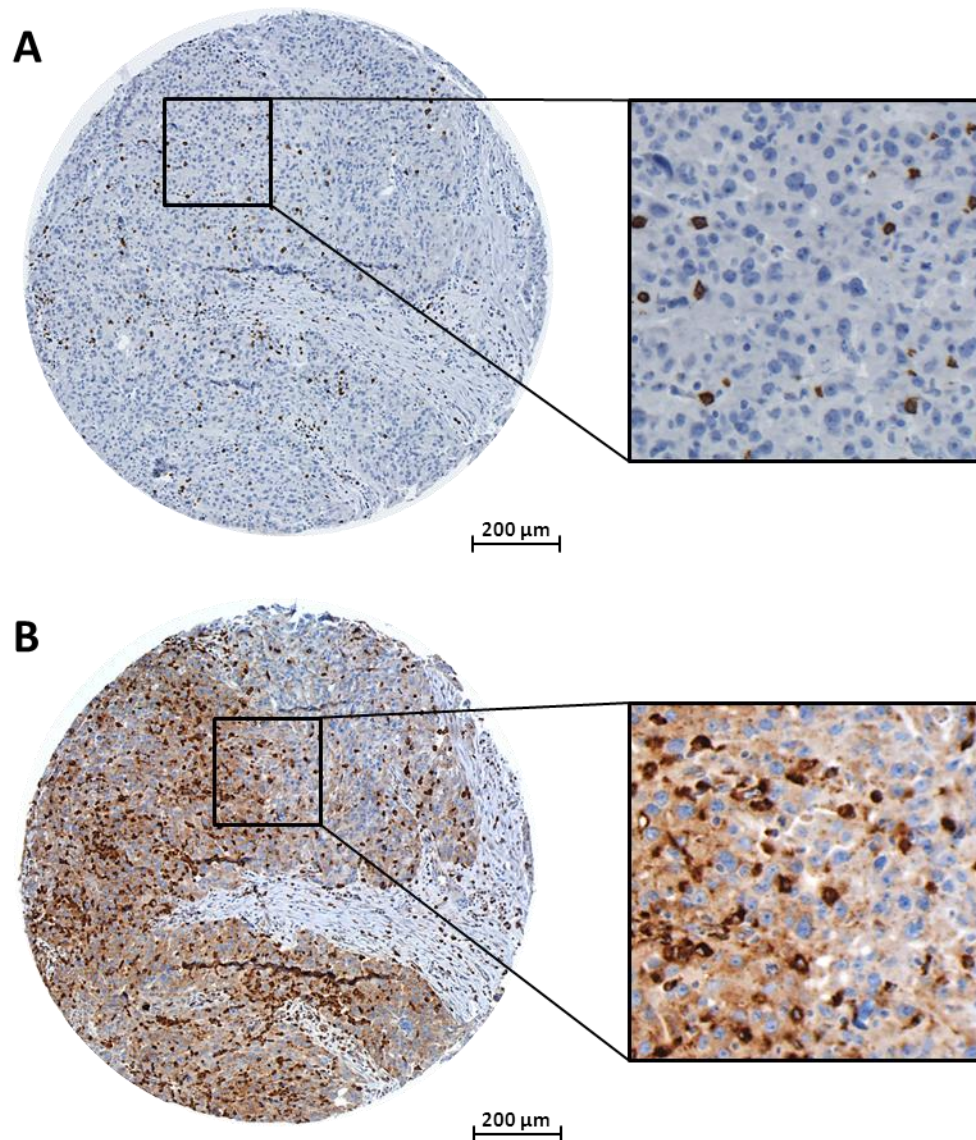


patient groups: The biggest differences were revealed for CD25 where the three patient groups were distributed all over the plot. Smaller, but substantial differences were found for the fractions CD15, CD3 and CD19, whereby the patient groups OC and M clustered closer together than patient group B.

### 3.3 Tumor microenvironment

#### 3.3.1 Immunohistochemical staining

CD8, CD68, CD45 and Ki67 immunohistochemical stainings were performed with tumor tissues of the 209 EOC patients assembled on TMAs. In Figure 10 staining of the four markers are depicted for one exemplary TMA core. Tumor infiltrating leukocytes were observed in the cancer epithelium as well as in the stromal areas (Figure 10).



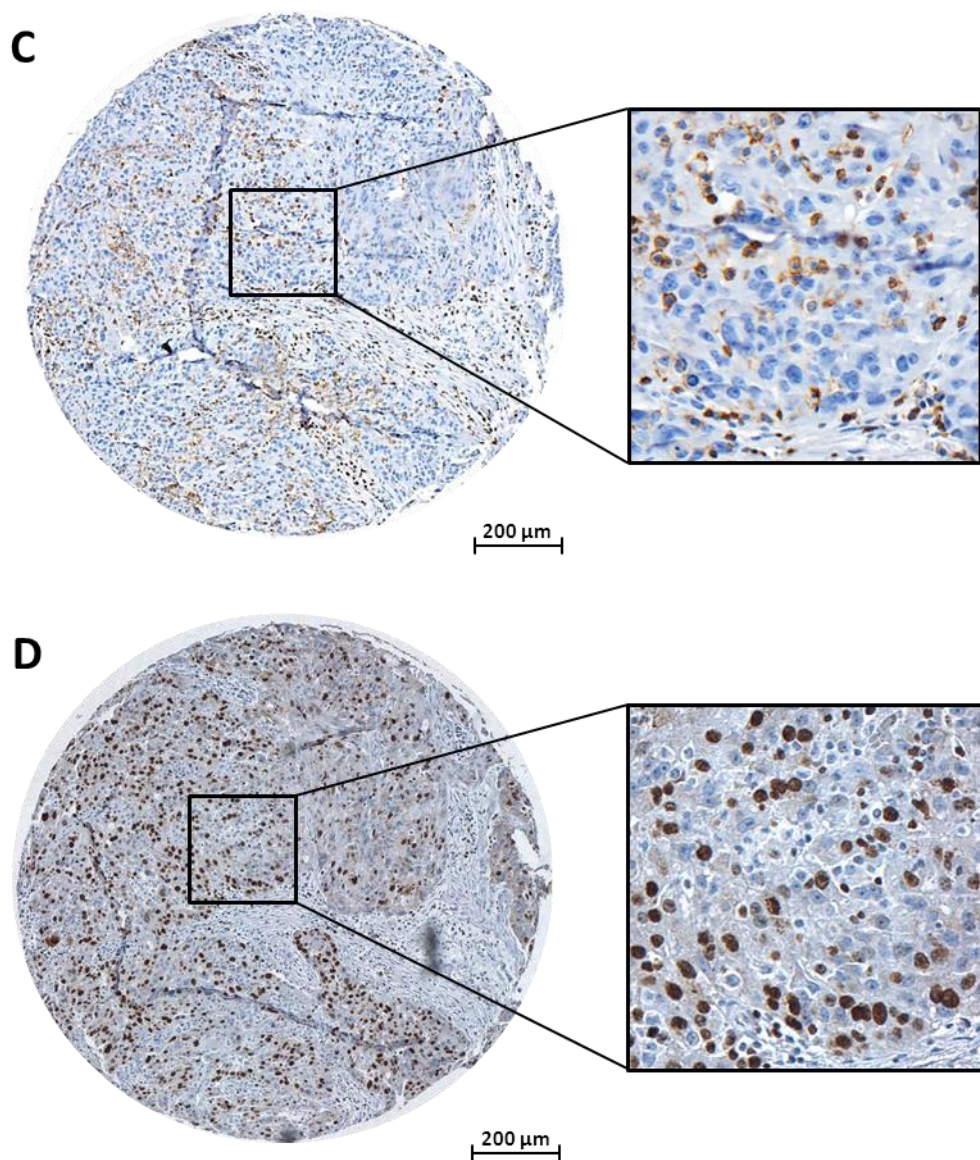


**Figure 10.** Representative example of the CD8, CD68, CD45 and Ki67 immunohistochemical staining of the same tissue microarray core of epithelial ovarian cancer of serous histology; **A** CD8; **B** CD68; **C** CD45; **D** Ki67; optical magnification x200; images acquired with the TissueFAXS/HistoQuest system.

In about 10% of the tumor tissue samples CD8+, CD68+ and/or CD45+ cells clustered together forming leukocyte aggregates (Figure 11). The number and size of aggregates per core varied among the tumor samples from only one cluster of about 50 µm in diameter to more than ten clusters of more than 300 µm in diameter. The aggregates were characterized by high densities of cells with a small, round and regular nucleus and a relatively small cytoplasm. In some cases they comprised almost exclusively one cell type (CD8+ or CD68+ cells); in other



samples clusters contained cells positive for all the assessed leukocyte markers as well as marker negative cells (Figure 11A).

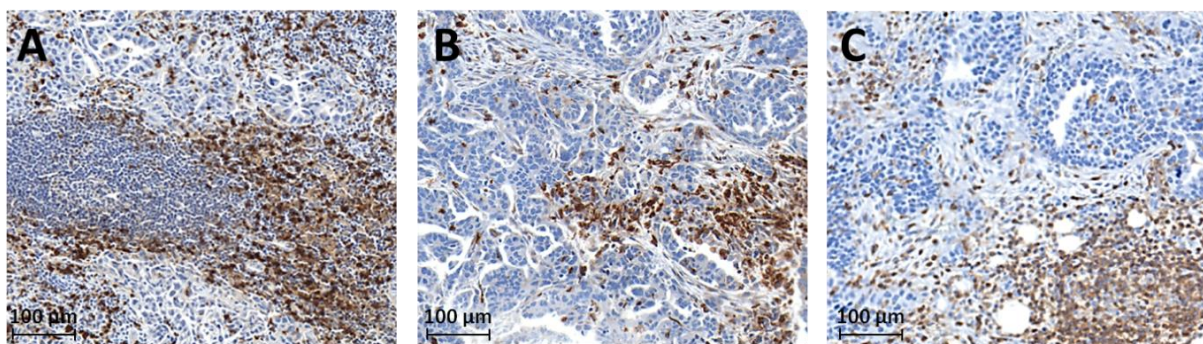


**Figure 11.** Immune cell clusters in epithelial ovarian cancer tissue. **A** CD8; **B** CD68; **C** CD45; optical magnification x200; images acquired with the TissueFAXS/HistoQuest system.

The density of infiltrating immune cells was wide ranging from marginal to about 2,000 cells/mm<sup>2</sup>. Figure 12 shows pictures of representative specimens characterized by a high and low infiltration of CD8+, CD68+ and CD45+ cells as well as a high and low Ki67 labeling index.

Of the 209 patients included in the study IHC data for 190 to 207 patients – dependent on the marker – could be obtained since some of the cores were not evaluable (see 4.2.8). The percentage of tumor tissue present in the cores varied from 30% to 100% with a median of 65% corresponding to an area of approximately 0.65 mm<sup>2</sup>.

CD8 analysis could be performed with 207 samples. CD8+ cells were present in all analyzed samples. CD8+ cells ranged from 1 to 1,931 cells/mm<sup>2</sup> with a median of 126 cells/mm<sup>2</sup> in the whole core (CD8 whole core) and from 3 to 2,257 cells/mm<sup>2</sup> with a median of 137 cells/mm<sup>2</sup> in the cancer epithelium (CD8 cancer epithelium), respectively. CD8 whole core, comprising the whole TMA core with cancer epithelium as well as adjacent stromal areas, and CD8 cancer epithelium, comprising almost exclusively tumor cells, correlated strongly with each other ( $p=0.95$ ,  $p<0.001$ ). Similarly, almost identical correlation coefficients with the other biological markers (data not shown) and HRs in survival analyses (see 3.3.6) were obtained for CD8 whole core and CD8 cancer epithelium. Therefore CD68+ and CD45+ cells were solely analyzed in the whole core. CD68+ cell infiltration could be assessed in 199 patient samples and ranged from 0 to 1,615 cells/mm<sup>2</sup> with a median of 277 cells/mm<sup>2</sup> in the whole core. For 190 samples CD45+ cell infiltration could be determined and ranged from 12 to 2,514 cells/mm<sup>2</sup> with a median of 378 cells/mm<sup>2</sup> in the whole core. As expected, CD45+



cells comprising all leukocytes showed higher values than the more specific leukocyte populations of CD8+ and CD68+ cells. The Ki67 labeling index could be analyzed in 203 samples and ranged from 0% to 90% with a median of 30%. Log<sub>2</sub>-transformed CD8+, CD68+ and CD45+ values showed an acceptable standard distribution.

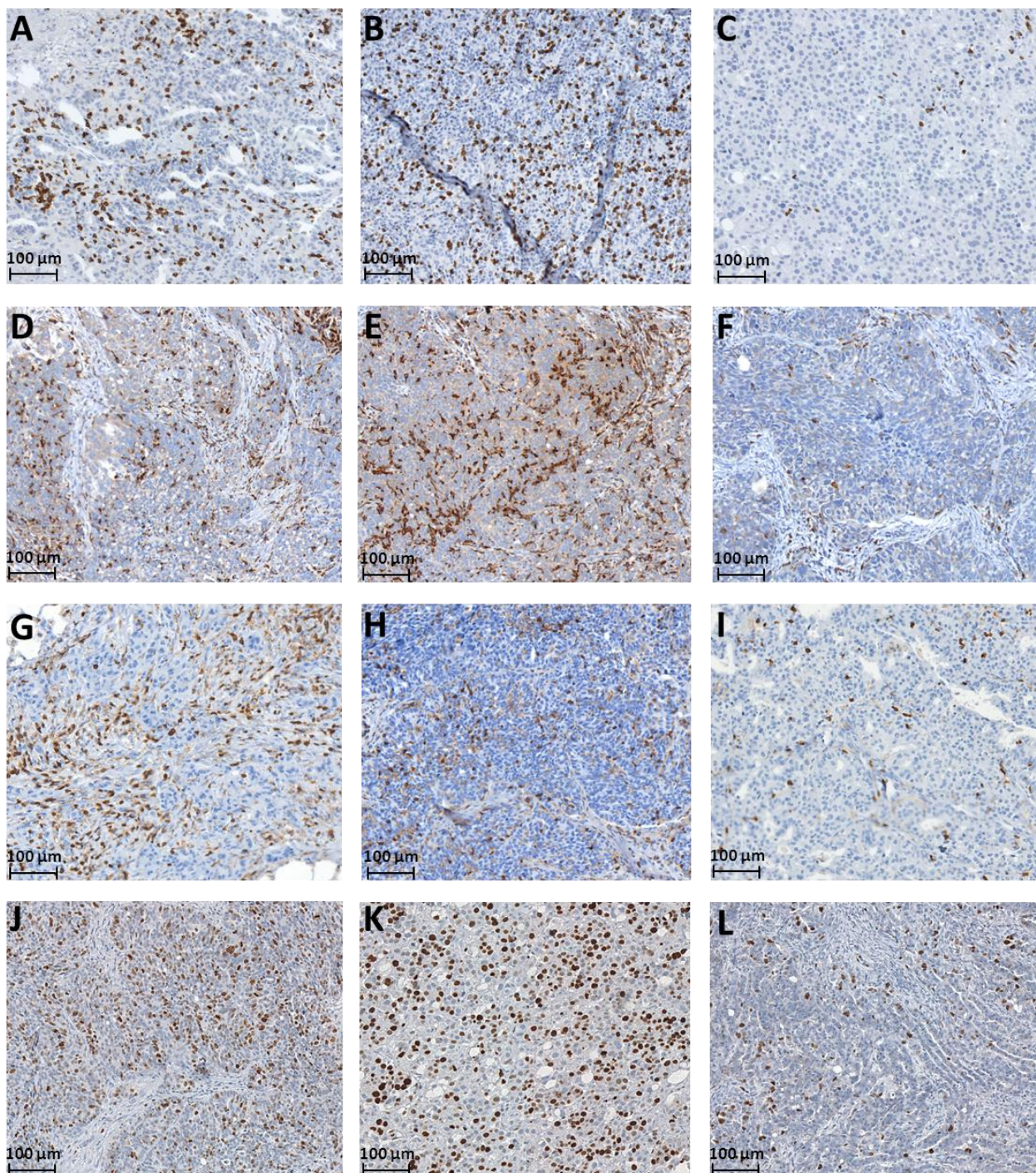


**Figure 12.** Representative epithelial ovarian cancer tissues characterized by high and low infiltration of CD8+ (A, B, C), CD68+ (D, E, F) and CD45+ (G, H, I) cells as well as high and low Ki67 labeling index (J, K, L); A, B, D, E, G, H, J and K high infiltration and labeling index, respectively; C, F, I and L low infiltration and labeling index, respectively; optical magnification x200; images acquired with the TissueFAXS/HistoQuest system.

Table 8 summarizes the correlation coefficients between the densities of CD8+, CD68+ and CD45+ cells in the whole core and the Ki67+ labeling index. Numbers of CD45+ cells correlated moderately with those of CD8+ and CD68+ cells, while CD8+ and CD68+ data did not correlate with each other. As expected, a positive correlation between the presence of immune cell clusters and tumor infiltration of CD8+, CD68+ and CD45+ cells was found ( $p < 0.001$ ,  $p = 0.010$  and  $p < 0.001$ , respectively). The percentage of Ki67+ tumor cells did not correlate with the infiltration of CD8+, CD68+ or CD45+ cells or the presence of immune cell clusters.

**Table 8.** Cell densities of CD8+, CD68+, CD45+ cells (cells/mm<sup>2</sup>) in the whole core and Ki67 labeling index with pairwise correlation coefficients (R).

	Cell densities and labeling index		Correlations				
				CD8	CD68	CD45	Ki67
<b>CD8</b>	Range cells/mm <sup>2</sup>	1-1931	R		<b>0.353<sup>P</sup></b>	<b>0.709<sup>P</sup></b>	-0.083 <sup>P</sup>
	Median cells/mm <sup>2</sup>	126	p		<b>≤ 0.001</b>	<b>≤ 0.001</b>	0.239
	N	207	adjusted p *		<b>≤ 0.001</b>	<b>≤ 0.001</b>	
			N		199	189	201
<b>CD68</b>	Range cells/mm <sup>2</sup>	0-1615	R			<b>0.578<sup>P</sup></b>	<b>0.192<sup>P</sup></b>
	Median cells/mm <sup>2</sup>	277	p			<b>≤ 0.001</b>	<b>0.007</b>
	N	199	adjusted p *			<b>≤ 0.001</b>	<b>0.028</b>
			N			186	196
<b>CD45</b>	Range cells/mm <sup>2</sup>	12-2514	R				0.053 <sup>P</sup>
	Median cells/mm <sup>2</sup>	378	p				0.471
	N	190	adjusted p *				
			N				187
<b>Ki67</b>	Range %	0-90					
	Median %	30					
	N	203					

<sup>P</sup> correlation assessed with Pearson method

\* adjusted p: significant p values were corrected for multiple testing with the Holm-Bonferroni method

### 3.3.2 Immunofluorescent staining

Immunofluorescent double staining with CD68 and MSR1 was performed with tumor tissues of 19 patients on WTSs (Figure 13). TAMs were observed within tumor cells and in the stromal areas (Figure 14). As in the immunohistochemical staining, aggregates of macrophages were observed (Figure 14D). The percentage of CD68+ cells of total cells (DAPI positive) (CD68+/DAPI) ranged from 1% to 19% with a median of 4.5%. The percentage of double positive MSR1+CD68+ cells of total CD68+ cells (MSR1+CD68+/CD68+) ranged from 42% to 95% with a median of 83%. CD68+/DAPI and MSR1+CD68+/CD68+ values showed bimodal distributions. Figure 14 shows representative tumor tissue specimens characterized by high and low infiltration of TAMs as well as high and low percentages of alternatively activated macrophages. CD68+/DAPI and MSR1+CD68+/CD68+ showed a weak correlation, but significance did not hold after correction for multiple testing (Table 9).



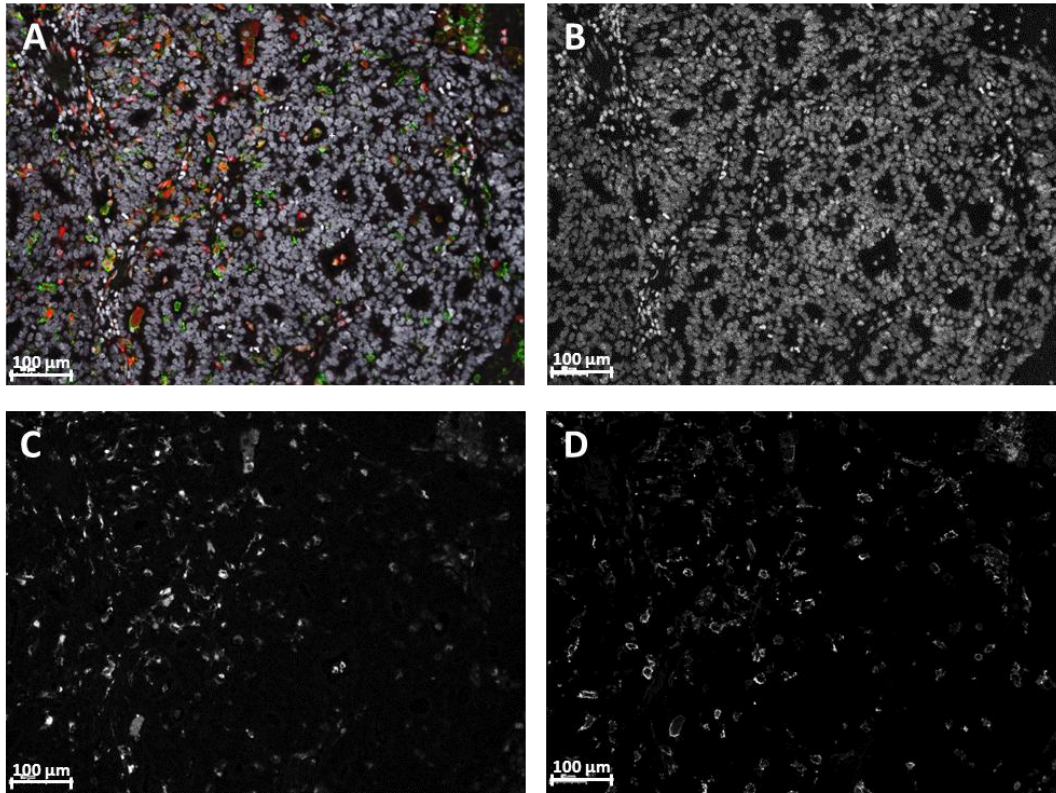


**Figure 13.** Immunofluorescent CD68 MSR1 double staining in epithelial ovarian cancer, DAPI for nuclear counterstaining; **A** three channel overlay: DAPI light grey, CD68 red, MSR1 green; **B** DAPI; **C** CD68; **D** MSR1; optical magnification x200; images acquired with the TissueFAXS/TissueQuest system.

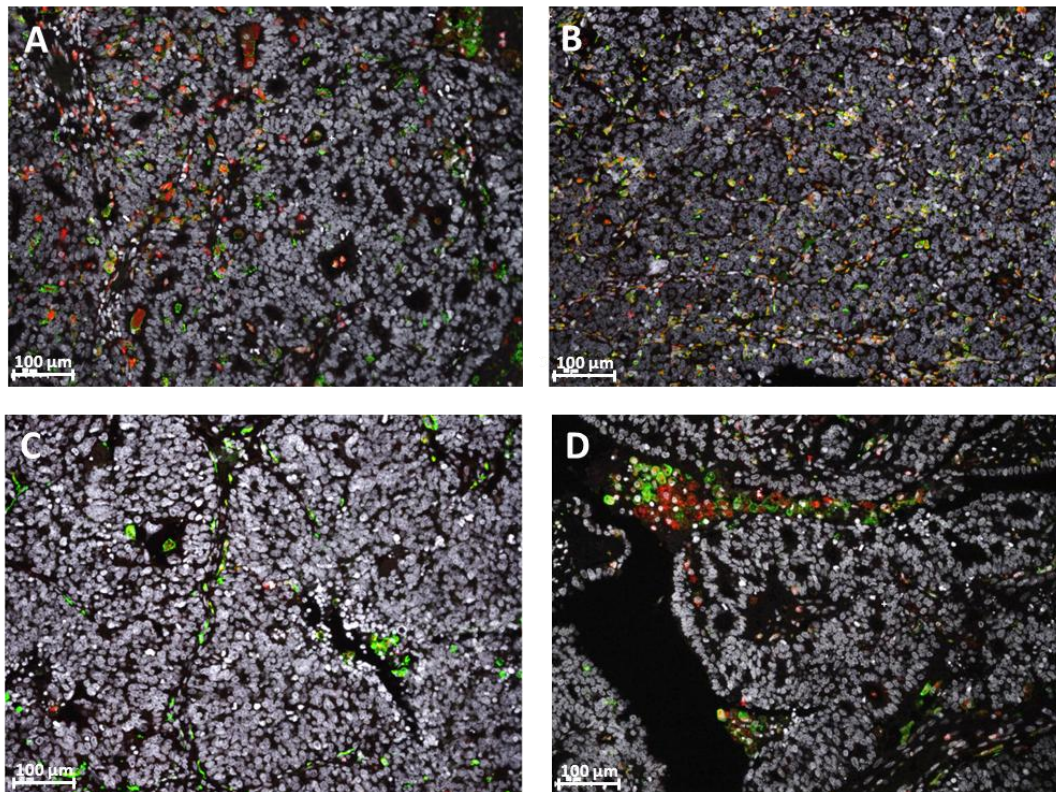


**Figure 14.** Immunofluorescent CD68 (red) MSR1 (green) double staining in epithelial ovarian cancer, DAPI for nuclear counterstaining (light grey); three channel overlay; **A** high macrophage infiltration, ~60% MSR1+CD68+ cells of total CD68+ cells (MSR1+CD68+/CD68+); **B** high macrophages infiltration, >90% MSR1+CD68+/CD68+; **C** low macrophages infiltration, >90% MSR1+CD68+/CD68+; **D** aggregate of macrophages at tumor border, ~50% MSR1+CD68+/CD68+; optical magnification x200; images acquired with the TissueFAXS/TissueQuest system.

**Table 9.** Pairwise correlation coefficients (R) of the percentage of CD68+ cells of total cells (CD68+/DAPI), percentage of MSR1+CD68+ cells of total CD68+ cells (MSR1+CD68+/CD68+), PC1 and PC2 from the prognostic seven gene panel.

		CD68+/DAPI	MSR1+CD68+/CD68+	PC1	PC2
<b>CD68+/DAPI</b>	R		0.533 <sup>S</sup>	0.396 <sup>S</sup>	0.074 <sup>S</sup>
	p		0.019	0.093	0.764
	adjusted p *		0.095		
	N		19	19	19
<b>MSR1+CD68+/CD68+</b>	R			<b>0.709<sup>S</sup></b>	0.018 <sup>S</sup>
	p			<b>0.001</b>	0.943
	adjusted p *			<b>0.006</b>	
	N			<b>19</b>	19
<b>PC1</b>	R				0.162 <sup>P</sup>
	p				0.507
	adjusted p *				
	N				19
<b>PC2</b>					

<sup>P</sup> correlation assessed with Pearson method

<sup>S</sup> correlation assessed with Spearman method

\* adjusted p: significant p values were corrected for multiple testing with the Holm-Bonferroni method

Figure 15 depicts examples of the test staining performed with potential M1 markers (CD80, iNOS and HLA-DR). The used anti-CD80 and anti-iNOS antibodies showed reactivity to tumor cells in some EOC tissue samples and were, therefore, not appropriate for detection of TAMs in EOC tissue. Triple staining performed with CD68, MSR1 and HLA-DR revealed triple positive cells. This observation indicates that M2 polarized macrophages also express HLA-DR and that the marker is not specific for M1 macrophages. Due to the unsatisfying results these tested markers were not used for further staining.

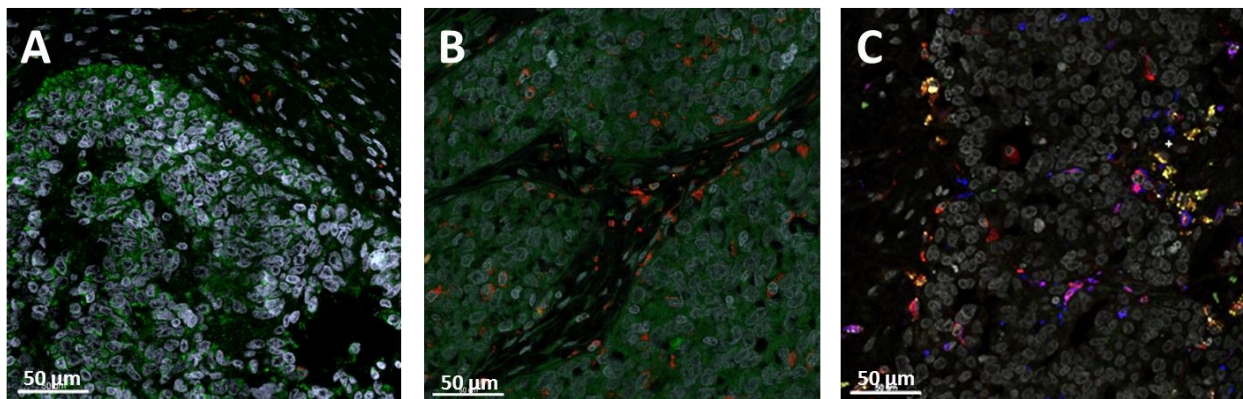


**Figure 15.** Immunofluorescent test staining with CD68 and potential M1 markers in epithelial ovarian cancer, DAPI for nuclear counterstaining (light grey); **A** CD68 (red) CD80 (green) double staining showing CD80+ tumor cells; **B** CD68 (red) iNOS (green) double staining showing iNOS+ tumor cells; **C** CD68 (red) MSR1 (green) HLA-DR (blue) triple staining showing triple positive cells; optical magnification x400; images acquired with a Zeiss laser scanning microscope LSM 700 microscope.



### 3.3.3 Correlation of TAMs and the prognostic blood cell signature

PC1, a linear combination of the expression values of the prognostic seven gene panel associated with reduced OS, correlated with MSR1+CD68+/CD68+ with a Spearman Coefficient of 0.71 ( $p=0.006$ , Table 9, Figure 16C). When the 19 patient cohort was dichotomized into PC1\_high and PC1\_low at the median of the PC1 values (median 0.18), Mann-Whitney-U-test showed that the mean of MSR1+CD68+/CD68+ in the PC1\_high group was significantly higher than in the PC1\_low group ( $p=0.001$ , Figure 16B). PC2, a PC1-uncorrelated linear combination of the expression values of the prognostic seven gene panel and predictive for death within the first two years after EOC diagnosis, did not correlate with macrophage cell numbers, neither with CD68+/DAPI nor with MSR1+CD68+/CD68+ (Table 9).

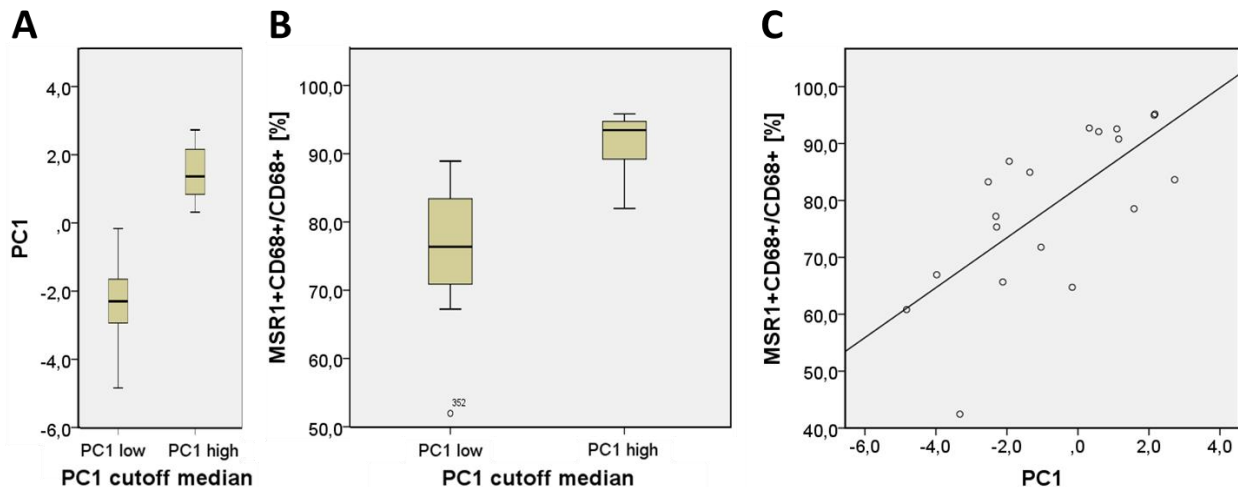


**Figure 16.** Association of PC1 and the percentage of MSR1+CD68+ cells of total CD68+ cells (MSR1+CD68+/CD68+). **A** Box plot of the PC1 values of the patient groups PC1\_low and PC1\_high; **B** box plot of MSR1+CD68+/CD68+ of PC1\_low and PC1\_high patients showing higher MSR1+CD68+/CD68+ values for PC1\_high than for PC1\_low patients ( $p=0.001$ ); **C** scatter plot of MSR1+CD68+/CD68+ and PC1 showing a correlation with a Spearman Coefficient of 0.71 ( $p=0.006$ ).

### 3.3.4 RT-qPCR CD8 relative expression values

Both mRNA expression data and IHC results could be obtained from 160 patients. No correlation between the CD8 gene expression values and the CD8+ density values was found ( $R=0.30$ ,  $p<0.001$ ).

### 3.3.5 Correlation with clinicopathological factors

No associations with the clinicopathological parameters age (continuous), histology (serous, non-serous), FIGO stage (II, III, IV), grade (1, 2 and 3) and residual tumor (yes, no)

were found for CD8 (whole core and cancer epithelium), CD68, CD45 or Ki67 (data not shown). Neither was there an association between immune cell clusters and the clinicopathological parameters or between CD8 gene expression values and the clinicopathological parameters (data not shown). Except for an expected association between FIGO stage and residual tumor ( $p=0.009$ ), no associations between the assessed clinicopathological factors were revealed (data not shown).

### 3.3.6 Survival analyses

Fractional polynomial modeling of the continuous factors age, CD8 (whole core and cancer epithelium), CD68, CD45 and Ki67 confirmed linearity for age, CD8, CD68 and CD45, whereas a non-linear association of Ki67 with survival was revealed. Visualization of the shape of this non-linearity showed that the mortality risk was sharply increased for patients with a Ki67 labeling index lower than 5%, while it was constantly low for patients with a Ki67 labeling index greater than 5% (data not shown). Therefore, it seemed reasonable to dichotomize Ki67 at a cutoff of 5% resulting in eleven patients with Ki67- tumors (<5% Ki67+ tumor cells) and 186 patients with Ki67+ tumors ( $\geq 5\%$  Ki67+ tumor cells). No associations between the 5%-dichotomized Ki67 variable and the clinicopathological parameters were found (data not shown).

This dichotomization was used for OS and PFS analyses. Figure 17 represents the corresponding Kaplan-Meier survival estimates for Ki67 with the cut-off value at 5% (Figure 17A) and the corresponding estimate for Ki67 with the cut-off at the median (Figure 17B).

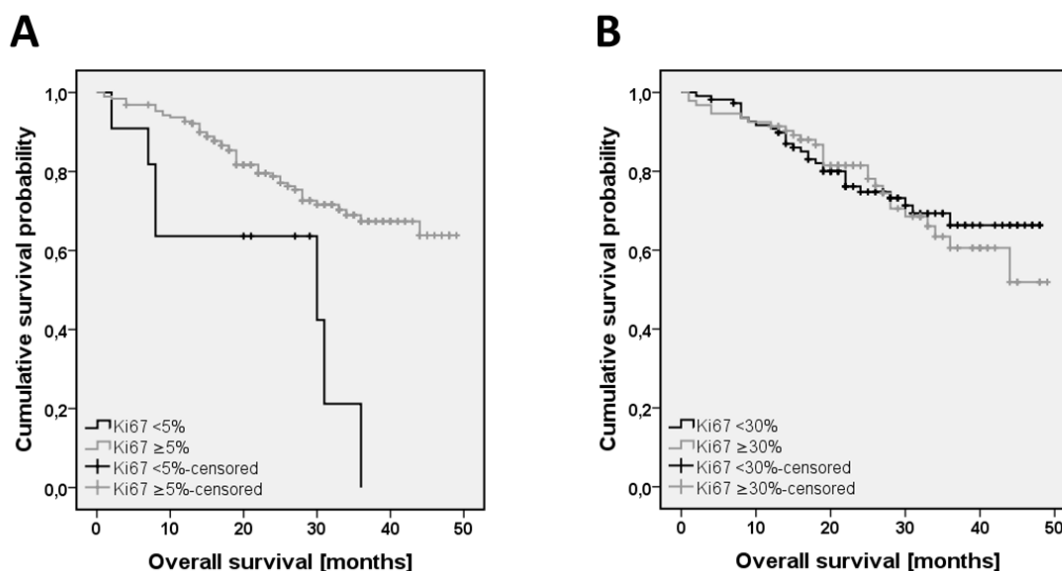


**Figure 17.** Kaplan-Meier curves showing the association between Ki67 and patient overall survival. **A** Ki67 (<5% versus  $\geq 5\%$ ); log-rank test,  $p = 0.002$ ; **B** Ki67 (<30% versus  $\geq 30\%$ ); log-rank test,  $p = 0.747$ .

When dichotomized at 5%, patients with Ki67- tumors had dramatically reduced OS compared to patients with Ki67+ tumors (log-rank test,  $p=0.002$ , Figure 17A), whereas no survival advantage can be seen, when dichotomized at the median (log-rank test,  $p=0.747$ , Figure 17B). Correlation of Ki67 (<5% versus  $\geq 5\%$ ) and refractory disease showed that patients with Ki67- tumors were over-represented in the patient group who suffered from refractory disease (24%) compared to patients with Ki67- tumors in the remaining group of patients (3%) (log-rank test,  $p=0.003$ ).

Multivariable Cox proportional hazards regression analyses including the clinicopathological factors age, histology, FIGO stage and residual tumor after cytoreductive surgery and the immunohistochemical data for CD8 (separate analysis of CD8 whole core and CD8 cancer epithelium), CD68, CD45 and the percentage of Ki67+ tumor cells (<5% versus  $\geq 5\%$ ) revealed age, FIGO stage, CD45 and Ki67 to be significantly and independently associated with survival. In contrast, histology, residual tumor, CD8 (whole core and cancer epithelium) and CD68 did not have any prognostic impact on OS. While the mortality risk increased slightly per each ten years of age (per decade: HR=1.02, 95% confidence interval (CI) 1.00-1.05), it was doubled if the patients had a higher FIGO stage (IV versus III or III versus II: HR=2.09, 95% CI 1.14-3.83). Mortality risk reduced by approximately 16% with each doubling of CD45+ cell density (HR=0.84, 95%CI 0.71-1.00). Moreover, patients with Ki67- tumors (<5% Ki67+ tumor cells) had a significantly poorer OS than those with Ki67+ tumors ( $\geq 5\%$  Ki67+ tumor cells) (HR 3.26, 95%CI 1.43-7.45, Table 10). Univariate analysis showed age, FIGO stage, residual tumor, CD45 and Ki67 to be associated with OS (Table 10).

For PFS, FIGO stage, residual tumor and CD45 were shown to be independent prognostic factors. Similarly to OS analysis, higher FIGO stage corresponded with a more than doubling of risk for recurrent disease (IV vs. III, III vs. II: HR=2.44, 95%CI 1.55-3.85). Patients with residual tumor after surgery had a 70% increased risk (HR=1.70, 95%CI 1.08-2.65). A doubling of CD45+ cell density reduced the risk for disease progression by approximately 13% (HR=0.87, 95%CI 0.76-0.99, Table 11). Univariate analysis showed age, FIGO stage and residual tumor to be associated with OS (Table 11).



**Table 10.** Prognostic significance of clinicopathological parameters, CD8, CD68, CD45 and Ki67 in univariate and multivariable overall survival analysis.**Overall survival**

N = 209				
Univariate			Multivariable	
Characteristics	HR (CI95%)	p	HR (CI95%)	p
Age (continuous, per decade)	<b>1.04 (1.01-1.06)</b>	<b>0.001</b>	<b>1.02 (1.00-1.05)</b>	<b>0.044</b>
Histology (non-serous vs. serous)	1.15 (0.55-2.43)	0.713	*	
FIGO (ordinal, per stage)	<b>1.90 (1.10-3.30)</b>	<b>0.022</b>	<b>2.09 (1.14-3.83)</b>	<b>0.018</b>
Residual tumor (yes vs. no)	<b>1.89 (1.12-3.21)</b>	<b>0.018</b>	*	
CD8 whole core <sup>o</sup> (continuous, per doubling)	0.88 (0.76-1.02)	0.081	*	
CD8 cancer epithelium <sup>o</sup> (continuous, per doubling)	0.88 (0.77-1.01)	0.077	*	
CD68 (continuous, per doubling)	0.95 (0.83-1.10)	0.493	*	
CD45 (continuous, per doubling)	<b>0.82 (0.70-0.96)</b>	<b>0.013</b>	<b>0.84 (0.71-1.00)</b>	<b>0.043</b>
Ki67 (<5% vs. ≥5%)	<b>3.23 (1.46-7.16)</b>	<b>0.004</b>	<b>3.26 (1.43-7.45)</b>	<b>0.005</b>

HR: Hazard Ratio; CI: Confidence Interval; <sup>o</sup> separate analysis of CD8 whole core and CD8 cancer epithelium**Table 11.** Prognostic significance of clinicopathological parameters, CD8, CD68, CD45 and Ki67 in univariate and multivariable progression-free survival analysis.**Progression-free survival**

N = 187				
Univariate			Multivariable	
Characteristics	HR (CI95%)	p	HR (CI95%)	p
Age (continuous, per decade)	<b>1.02 (1.00-1.03)</b>	<b>0.035</b>	*	
Histology (non-serous vs. serous)	0.97 (0.60-1.55)	0.882	*	
FIGO (ordinal, per stage)	<b>2.46 (1.75-3.46)</b>	<b>&lt;0.001</b>	<b>2.44 (1.55-3.85)</b>	<b>&lt;0.001</b>
Residual tumor (yes vs. no)	<b>2.13 (1.52-3.00)</b>	<b>&lt;0.001</b>	<b>1.70 (1.08-2.65)</b>	<b>0.021</b>
CD8 whole core <sup>o</sup> (continuous, per doubling)	1.01 (0.91-1.11)	0.903	*	
CD8 cancer epithelium <sup>o</sup> (continuous, per doubling)	1.00 (0.91-1.10)	0.992	*	
CD68 (continuous, per doubling)	0.97 (0.87-1.07)	0.493	*	
CD45 (continuous, per doubling)	0.93 (0.82-1.05)	0.243	<b>0.87 (0.76-0.99)</b>	<b>0.040</b>
Ki67 (<5% vs. ≥5%)	1.17 (0.43-3.19)	0.753	*	

HR: Hazard Ratio; CI: Confidence Interval; <sup>o</sup> separate analysis of CD8 whole core and CD8 cancer epithelium

To separately assess the influence of each leukocyte marker on the outcome, multivariable Cox proportional hazards regression analyses including only one leukocyte marker (CD8, CD68 or CD45), Ki67 and the clinicopathological factors were performed, while omitting the other two leukocyte markers. Again, CD8 cancer epithelium and CD8 whole core data were separately analyzed. OS analysis with the CD8 intraepithelial data omitting the markers CD68 and CD45 revealed age (HR=1.03, 95%CI 1.00-1.05,  $p=0.019$ ), FIGO stage (HR=1.97, 95%CI 1.09-3.57,  $p=0.025$ ), Ki67 (HR=3.37, 95%CI 1.50-7.57,  $p=0.003$ ) and CD8 cancer epithelium (HR=0.86, 95%CI 0.74-0.99,  $p=0.038$ ) as independent prognostic factors. The corresponding analysis with the whole core data revealed age (HR=1.03, 95%CI 1.01-1.05,  $p=0.015$ ), FIGO stage (HR=1.99, 95%CI 1.10-3.62,  $p=0.024$ ) and Ki67 (HR=3.53, 95%CI 1.57-7.93,  $p=0.002$ ) as independent prognostic factors, whereas CD8 whole core only remained as correcting factor for OS (HR=0.87, 95%CI 0.75-1.01,  $p=0.067$ ). In both analyses, residual tumor remained as correcting factor, but was not significant (HR=1.65, 95%CI 0.94-2.88,  $p=0.079$  and HR=1.69, 95%CI 0.97-2.97,  $p=0.066$  for CD8 cancer epithelium and CD8 whole core, respectively).

For PFS no significant influence of CD8 was observed in analyses omitting CD68 and CD45, neither for CD8 cancer epithelium nor for CD8 whole core data. As in PFS analysis including all assessed markers, FIGO stage (HR=2.11, 95%CI 1.38-3.22,  $p=0.001$ ) and residual tumor (HR=1.68, 95%CI 1.10-2.56,  $p=0.017$ ) were shown to be independent prognostic factors.

The results of the separate analyses for CD68 omitting the markers CD8 and CD45 and for CD45 omitting the markers CD8 and CD68, respectively, were the same as the corresponding results in the analyses including all three leukocyte markers: CD68 did not have any impact on survival, neither on OS nor on PFS (data not shown); CD45 was significantly associated with improved OS (HR=0.83, 95%CI 0.70-0.98,  $p=0.031$ ) and PFS (HR=0.86, 95%CI 0.77-0.97,  $p=0.012$ ); FIGO stage and Ki67 were independent factors for OS, while FIGO stage and residual tumor were associated with PFS.

Interestingly, residual tumor was the only factor significant in univariate OS analysis ( $p=0.018$ ), but losing significance in multivariable OS analysis ( $p=0.157$ ). Therefore and because the tumor mass which is targeted by anti-tumoral infiltrating leukocytes is removed in the cytoreductive surgery, it was assumed that the prognostic impact of tumor infiltrating immune cells might be weaker in optimally debulked patients ( $n=131$ ) compared to patients with residual tumor ( $n=59$ ). Indeed, separate analysis of the influence of CD8+ cell density (low versus high, cut-off value at the median) according to the debulking status revealed a

significantly improved OS associated with high level of CD8+ cell infiltration compared to patients with low CD8+ cell infiltration in the group of patients with residual tumor mass (log-rank test,  $p=0.001$ ). In contrast, no OS difference according to the CD8+ cell density was observed in the group of optimally debulked patients (log-rank test,  $p=0.387$ ). However, an interaction test for CD8+ cell density and residual tumor did not reach significance ( $p=0.102$ ).

The analogous analysis of the prognostic impact of CD45 (low versus high, cut-off value at the median) also showed a stronger positive effect of CD45+ cells on OS time in patients with residual tumor compared to patients without residual tumor. The Kaplan-Meier survival estimates in Figure 18A show the trend of survival advantage associated with high CD45+ cell tumor infiltration compared to low CD45+ cell infiltration in the group of non-optimally debulked patients, which did, however, not reach significance (log-rank test,  $p=0.103$ ). In contrast, in women without residual tumor CD45+ cell infiltration did not influence OS (log-rank test,  $p=0.215$ , Figure 18B). A test of interaction for CD45+ cell density and residual tumor showed significance ( $p=0.006$ ).

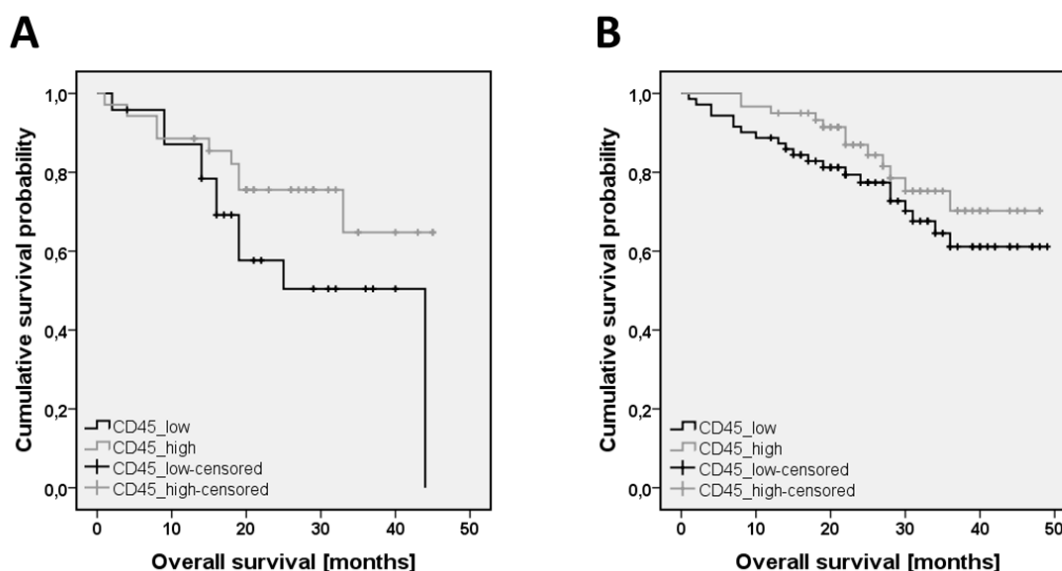


**Figure 18.** Kaplan-Meier curves showing the association between CD45 (low versus high, cut-off value at median) and patient overall survival. **A** Patients with residual tumor; log-rank test,  $p = 0.103$ ; **B** optimally debulked patients; log-rank test,  $p = 0.215$ .

Similarly, the prognostic value of residual tumor was separately assessed according to the tumor infiltration of CD8+ and CD45+ cells (low versus high, cut-off value at the respective median). The Kaplan-Meier survival estimates in Figure 19 show that the presence or absence of residual tumor after the cytoreductive surgery did not significantly influence OS in patients

with high CD8+ cell infiltration (log-rank test,  $p=0.574$ , figure 19A), whereas in patients with low CD8+ cell infiltration optimal debulking was associated with improved OS (log-rank test,  $p=0.001$ , Figure 19B).

The analogous analysis of the prognostic impact of the debulking status according to the infiltration of CD45+ cells showed similar results: a trend of improved OS for optimally debulked patients compared to non-optimally debulked patients in the group of patients with low CD45+ cell infiltration (log-rank test,  $p=0.071$ ). In contrast, no difference in OS time according to the debulking status was observed in the group of patients with high CD45+ cell infiltration (log-rank test,  $p=0.294$ ).

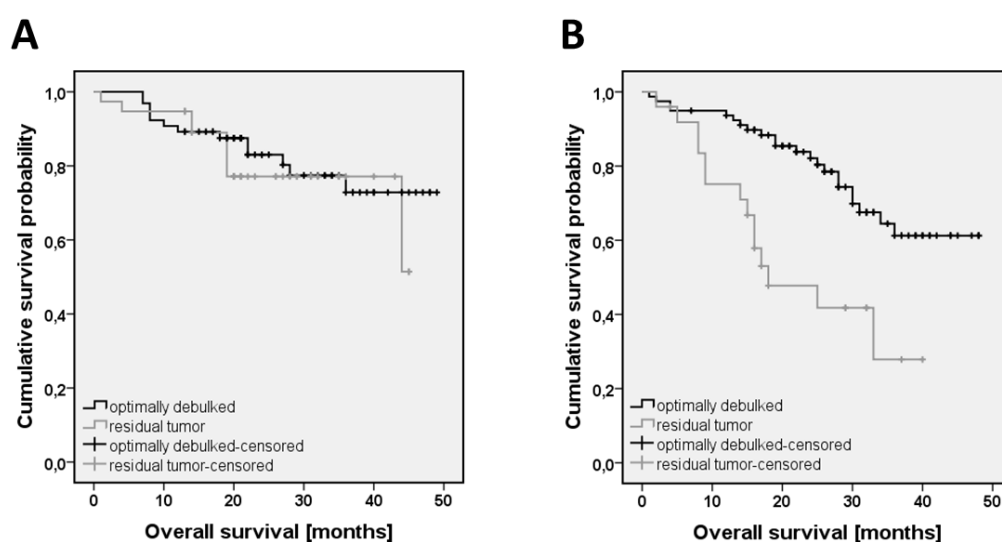


**Figure 19.** Kaplan-Meier curves showing the association between the debulking status and patient overall survival. **A** Patients with high infiltration of CD8+ cells (cut-off value at median); log-rank test,  $p = 0.574$ ; **B** patients with low infiltration of CD8+ cells; log-rank test,  $p = 0.001$ .

The presence of immune cell aggregates (regardless of the number and size) was not significantly associated with OS in univariate or multivariable analyses (data not shown). A trend of improved PFS was found for patients with immune cell aggregates in univariate analysis (HR=1.69, 95%CI 0.86-3.36,  $p=0.130$ ), while this factor was not of independent prognostic value in multivariable PFS analysis (data not shown).

RT-qPCR CD8 relative expression values were not associated with PFS or OS, neither in univariate nor in multivariable analyses (data not shown).

## 4 Discussion

### 4.1 Blood cell gene signatures

So far, no satisfying marker for early detection of EOC or prognosis in EOC patients has been established for routine use. In the search for a sophisticated diagnostic and prognostic peripheral blood biomarker or biomarker panel our working group has described two gene sets in a “high density” leukocyte fraction which is isolated from whole blood using a density gradient: one set for early detection comprising 13 gene expressions and six plasma protein abundances and another panel for prognosis comprising seven genes. For routine use the protocol to isolate the fraction, which is used for the determination of the gene signatures, from whole blood requires simplification. This study was aimed to find blood cell fractions appropriate to substitute the “high density” blood leukocyte fraction. The gene expression values of the genes comprised in these two panels were analyzed in seven different blood cell fractions from four EOC patients, six patients with other predominantly malignant diseases except ovarian cancer and 13 controls in order to identify the best suitable cell fraction(s). The blood cell fraction(s) of choice has(ve) to permit the discrimination of EOC patients and controls with the diagnostic panel and of EOC patients with a favorable outcome and patients with reduced survival time with the prognostic panel. These respective cell types could subsequently be targeted by immune magnetic separation methods to facilitate the protocol of the determination of the blood cell gene signatures.

#### 4.1.1 Diagnostic panel

A single fraction obviously suitable for the evaluation of the diagnostic signature could not be identified. ANOVA and Bonferroni analyses revealed that the genes NEAT, AP2A1 and PAPOLG and the fractions CD19, CD3 (B and T cells, respectively) and CD44 (a mixture of tissue cells, erythrocytes and leukocytes) showed the most significant patient group specific expression patterns. Significantly different gene expression patterns were found between the two patient groups with malignances, EOC and other predominantly malignant diseases, including Krukenberg tumor, signet ring cell carcinoma, borderline tumor, lymphoma and teratoma, compared to the control group, comprising healthy individuals as well as patients with benign gynecological diseases such as hypermenorrhea, myoma, fibroma and CIN I/II.

Analysis of the relative risk of EOC, resulting from the combination of the 13 gene expression values determined in the “high density” leukocyte fraction, showed significantly higher values for the EOC patients and patients with other predominantly malignant diseases compared to the control group. The data generated in this work confirm sensitivity of the described panel determined in the “high density” blood leukocyte fraction to detect malignancy. However, the panel was not found to be EOC specific in this cohort. Only a trend of higher relative risk values for EOC patients compared to patients with other malignancies was found. This could be a result of a lack of specificity, the small patient number or the fact that analysis of the six plasma proteins, which are part of the complete diagnostic panel and which, presumably, contribute to EOC specificity, was not included in this study. A possible failure of the diagnostic gene panel to discriminate between the EOC patients and the patients with other malignancies of this study cohort could be due to the fact that women of the latter patient group predominantly suffered from malignant tumors in the peritoneal cavity. These peritoneal tumors might provoke similar host immune responses as EOC and thus similar blood leukocyte gene expressions. Concerning specificity, comparing EOC patients and controls, one outlier of the control group, a HPV-HR negative CIN II patient, with a relative risk value of about the order of the mean of EOC patients was apparent. Either this can be a result of low statistical specificity of the panel or the patient suffers from a malignant disease which has not been diagnosed yet. The relative risk values of EOC for the three HPV-HR positive patients were equal or below the 75<sup>th</sup> percentile of the control group indicating that a positive HPV-HR status in CIN patients does not result in higher relative risk values.

Solely the relative risk values computed with the gene expression values in the HD fraction were significantly higher for patients with malignant diseases (EOC or other malignancies) compared to the control group. In contrast, the relative risk values computed with expression values in the other fractions did not permit discrimination between the patient groups. This observation was expected since the panel was developed with expression data in the HD fraction. When analyzing the genes separately, other fractions such as the fractions of enriched CD19+ and CD3+ cells were found to exhibit numerous significant gene expression differences between patient groups, while the HD fraction was among the fractions with fewer patient group specific gene expression values. This indicates that the analysis of a blood cell fraction with few significant up- or down-regulations in the single genes can permit better discrimination between patient groups than a fraction with more up- or down-regulations, providing that the genes of the panel in total are expressed differentially in the aforesaid fraction.

The non-uniform expression patterns of the genes of the diagnostic panel in the different blood cell fractions indicate that the panel measures gene expressions of several different cell types. Thus, the heterogeneity of the HD fraction could be suitable for the determination of this gene signature. Nevertheless, the fractions with most and/or highest gene expression differences between patient groups and also fraction CD25 that showed patient group dependent clustering in PCA should be considered for further analyses. The model for the determination of the relative risk of EOC with loadings of the genes developed with gene expression data in the HD fraction could only be used for expression data in another blood cell fraction if this distinct fraction was characterized by a similar cell composition as the HD fraction. Blood cell fractions isolated from whole blood might contain cell types which only marginally overlap with the cells in the HD fraction or which are not even present in the HD fraction. Thus, promising blood cell fractions might require a remodeling of the loadings of the 13 genes in the discriminative model to achieve required sensitivity and specificity. But such an approach is time- and cost-consuming since a large independent sample cohort would be necessary.

#### **4.1.2 Prognostic panel**

In contrast to the diagnostic panel, the genes of the prognostic panel showed much more homogeneous expression patterns with peaks in the fractions of enriched CD25+ and CD14+ cells. The results of this study indicate that among the assessed blood cell fractions the genes of the prognostic panel are mainly expressed by CD14+ monocytes and monocyte derived cells (e.g. activated, thus CD25+) and/or other CD25+ activated immune cells. Interestingly, the two genes from the diagnostic panel NOXA1 and CCR2 showed similar expression patterns indicating similar cell types to be involved. Published microarray data, which have shown that CD25 is also expressed in monocytes, albeit in lower levels than in lymphocytes (Abbas et al., 2005), suggest that cells captured by antibodies against CD14 and CD25 might partially overlap. A further indication for CD25 expression in monocyte derived cells provide an IHC study describing CD25+ macrophages in severe acute respiratory syndrome (SARS) patients (He et al., 2003) and microarray data showing up-regulation of CD25 in M1 polarized macrophages compared to monocytes and to M2 polarized macrophages (Martinez et al., 2006; Solinas et al., 2010). In light of these data, further analyses should be addressed to characterize the composition of the fractions CD14 and CD25.

The study was not designed to analyze gene expression differences between EOC patients according to survival, since a much larger patient cohort would be necessary to analyze

differences between EOC patients regarding survival. Furthermore, at the time of sample collection and analysis follow-up time was too short to assess the clinical outcome. However, the fractions of CD14+ and CD25+ enriched cells seem must promising to be suitable for the determination of the prognostic gene panel. Nevertheless, to evaluate if a certain cell fraction is appropriate to discriminate between EOC patients according to the outcome, blood of a large EOC patient cohort has to be collected and analyzed.

#### **4.1.3 Principal Component Analysis**

Principal Component Analysis, a statistical method to reduce the complexity of multivariable data sets and to assess similarities of parameters, showed the strongest discrimination among all analyzed blood cell fractions between the fraction CD25 of EOC patients, on the one hand, and the fraction CD25 of patients with other predominantly malignant diseases and the controls, on the other hand. As expected, the HD fractions which have been reported to contain mainly granulocytes and lymphocytes (Brandt and Griwatz, 1996) clustered together with the fractions of enriched CD15+ cells, the fractions of predominantly granulocytes and monocytes. Another cluster comprising the fractions CD3 and CD19 reflects the relation of T and B lymphocytes. The cell fractions enriched with an antibody against CD14, a monocyte marker, and the cell fractions enriched with an antibody against CD25, an activation marker expressed in various cell types, predominantly in lymphocytes, also clustered together. The clustering of the fractions CD14 and CD25 represents the similarly high expression values of most genes of the prognostic panel and two genes of the diagnostic panel in these two fractions. As mentioned above, the CD14+ and CD25+ cells might (partially) overlap which could be the reason for the similar expression levels of some genes in the two fractions. As expected, the fractions of CD44+ enriched cells were localized in a central position of the biplot which reflects the composition of this fraction including tissue cells, erythrocytes and leukocytes.

#### **4.1.4 Limitations and outlook**

Regarding the comparison of the gene expression levels in the different blood cell fractions, one has to consider that the expression levels in a certain fraction do not give insight into the relative differences between patient groups or between EOC patients with different clinical outcome. High gene expression values in a certain fraction show that the respective genes are expressed in (some of) the cell types in the fraction which could – but need not – signify the suitability of the respective fraction for the evaluation of the gene signature. It is



also possible that in cell fractions, where a gene is generally expressed on a low level, the expression level is altered due to a malignant disease causing significant gene expression differences. Generally low expression levels, however significant expression differences between patient groups in several genes of the diagnostic panel, were for instance observed in the lymphocyte fractions CD19 and CD3. Therefore, subsequent studies assessing gene expression patterns in promising blood cell fractions require larger patient numbers in the groups to be compared.

The composition of promising fractions could be further analyzed using fluorescence associated cell sorting (FACS) or other marker specific cell sorting methods. The assessment of the expression of markers which have been used to enrich the distinct fractions could reveal eventual overlaps. Moreover, these techniques could be used to obtain higher purity of cells which could improve the gene signatures. However, as the final aim in the search for biomarkers for early detection of EOC and for prognosis in patients with diagnosed EOC is the screening of numerous patients, too advanced and time-consuming protocols requiring special technical equipment and/or know-how have to be avoided for routine applications. In the case of both gene panels the method of choice for cell separation should consist of a possibly short and simple protocol, such as the filtering system used in this study or an immune magnetic separation method.

The main complicacy in the gene expression analysis was that some samples had very low RNA concentrations and gene expression values in some of these samples were below the detection level and were thus imputed for the subsequent analyses.

It was impossible to collect more blood samples of EOC patients in the course of the diploma thesis since EOC is a rare disease. The collection of samples of ten EOC patients was initially planned. In some cases the final diagnosis was only obtained months after taking of the blood samples which complicated subsequent analyses. Among the ten patients with suspected ovarian cancer only four cases were confirmed, while in six patients other predominantly malignant diseases were diagnosed. This lower number of EOC cases diminished the statistical power. However, the unexpected collection of samples of patients with other malignancies allowed the assessment of the diagnostic gene panel regarding its applicability for the discrimination between EOC and other malignancies.

## **4.2 Tumor microenvironment**

In ovarian cancer tumor characteristics such as proliferation and tumor infiltrating immune cells have been addressed in several studies in the last years. However, very little data about the interaction of the local immune system and ovarian cancer growth has been published. Therefore, in this study detailed analyses of the proliferation marker Ki67 as well as CD8+, CD68+ and CD45+ cells in the tumor microenvironment in ovarian cancer patients was performed and the impact on the clinical outcome was studied. The study cohort comprised more than 200 EOC patients for whom a broad and well-described tumor bank and database of the clinicopathological data had been established. A very low percentage of Ki67+ tumor cells was associated with worse OS. Moreover, patients with tumors characterized by high CD45+ cell infiltration were identified to have improved OS and PFS.

### **4.2.1 Study population**

In the OVCAD consortium multiple centers are involved which permitted the collection of this large number of EOC tissue samples, predominantly with advanced stage and mainly of serous histology. In a single center this could not have been accomplished for a rare disease such as EOC. A big and relatively homogeneous study population is essential for a meaningful statistical analysis of interactions of biological markers and especially for survival analyses.

### **4.2.2 Immunohistochemical staining**

The median values of leukocyte cell density and the Ki67 labeling index in this study are similar to data from other studies (Aune et al., 2011; Garcia-Velasco et al., 2008; Hamanishi et al., 2007; Sato et al., 2005). Clusters of immune cells with high numbers of CD8+, CD68+ and/or CD45+ cells were observed in about 10% of the tumor samples. Interestingly, only few studies have described similar aggregates of immune cells – mainly lymphocytes – in human cancer entities: in breast cancer (Liu et al., 2011), non-small-cell lung cancer (Dieu-Nosjean et al., 2008), bladder cancer (Ayari et al., 2009) and ovarian cancer (Anderson et al., 2009; Sato et al., 2005).

Correlation and survival analyses revealed almost identical results for CD8 whole core (HR=0.88, 95%CI 0.76-1.02, p=0.081) and CD8 cancer epithelium (HR=0.88, 95%CI 0.77-1.01, p=0.077), although it is generally recommended to assess only intraepithelial leukocytes in the tumor microenvironment (Hamanishi et al., 2007; Sato et al., 2005). On the one hand, this can be explained by the fact that the analyzed TMA cores comprised mainly tumor cells and putative “stromal contamination” attenuating the statistical significance seemed to be

neglectable. On the other hand, cancer epithelium and stroma could yield similar infiltration values. Considering the very limited – if any – improvement of data and the time-consuming process of the manual selection of cancer epithelium, the other studied leukocytes were quantified solely in the whole TMA core including cancer epithelium as well as stromal areas. However, it is possible that a separate analysis of leukocyte infiltration in the cancer epithelium and in the tumor stroma would slightly change results. For CD8, analyses of positive cells assessed in the cancer epithelium showed slightly smaller p values than analyses of positive cells assessed in the whole core. Thus, separate quantification of intraepithelial cells could have an impact on the prognostic value of CD45 since p values were just below the significance level. However, for CD68 only intraepithelial cells would presumably not change correlation and survival analyses considerably since this marker was far from significance in all survival analyses. Therefore, in studies including numerous markers and/or a large sample size, analysis can be performed with the whole TMA core and – if promising – be repeated with separate quantification of intraepithelial and stromal cells.

As expected, cells positive for the panleukocyte cell marker CD45 were more frequent than cells positive for the more specific cytotoxic T cell and macrophage markers CD8 and CD68. Similarly, total leukocyte numbers correlated with both, cytotoxic T cell and macrophage cell numbers ( $R=0.71$  and  $R=0.58$ , respectively), while the number of cytotoxic T cells and macrophages did not correlate with each other ( $R=0.35$ ). The found association between the presence of immune cell aggregates and the densities of CD8+, CD68+ and CD45+ was also expected.

Inflammation, one of the hallmarks of cancer, contributes to tumorigenesis and tumor progression by inducing cell proliferation, resistance to cell death and angiogenesis via the release of bioactive molecules including growth, survival and pro-angiogenic factors to the tumor microenvironment (Hanahan and Weinberg, 2011). Therefore, the association between tumor infiltrating immune cells and tumor cell proliferation was assessed. In this study cell proliferation, measured by Ki67 expression, did not correlate with tumor infiltrating CD8+, CD68+ or CD45+ cells or the presence of immune cell aggregates. This finding demonstrates that tumor cell proliferation is not essential for the infiltration of leukocytes and that infiltrating leukocytes do not contribute to tumor cell proliferation in human ovarian cancer tissue, respectively.

### 4.2.3 Immunofluorescent staining

Macrophages (CD68+) were detected in all tumor samples with percentages of total cells ranging from very low (1%) up to approximately 20%. Most macrophages in the tumor tissue – between 50% and almost 100% – expressed the alternatively activated macrophage marker MSR1. The bimodal distribution of the percentages of macrophages of total cells and the percentages of alternatively activated macrophages of total macrophages in this data set could be a result of the sample selection of the study only including patients with very high and very low PC1 and PC2 values.

Concerning the analysis of the polarization of TAMs towards M1 or M2, I was aware of the problem of false positive signals with only one marker. However, no description of a M1 marker tested for EOC tissue was found in literature. Thus, M1 markers described for other tissues (CD80, iNOS and HLA-DR) were tested (Escorcio-Correia and Hagemann, 2010; Ma et al., 2010). Nevertheless, no satisfying staining protocol with a specific marker for classically activated macrophages could be established: Two of the three tested corresponding antibodies (CD80, iNOS) showed also reactivity on some EOC tissues. The third tested antibody (HLA-DR) was negative for EOC, but stained some MSR1+CD68+ double positive cells. As these cells were considered as M2 macrophages, HLA-DR was not appropriate to use in combination with MSR1. Due to these practical shortcomings analysis of classically activated macrophages was omitted. Alternatively, CD68+ cells were considered as total macrophages and MSR1+CD68+ cells were considered as alternatively activated macrophages.

### 4.2.4 Correlation of TAMs and the prognostic blood cell signature

To assess a possible interaction between blood cells involved in the prognostic gene panel and tumor infiltrating total (CD68+) and alternatively activated (MSR1+CD68+) macrophages, the small cohort of 19 patients was especially selected according to results from the prognostic gene signature. Patients with very high and very low PC1 and PC2 values indicating risk to die (OS) and risk of death within two years after EOC diagnosis, respectively, were included in the study. Although an interaction between blood leukocytes and leukocytes in the tumor microenvironment was presumed, the high statistical significance of the revealed moderate correlation between PC1 and the percentage of alternatively activated macrophages of total macrophages ( $R=0.71$ ,  $p=0.006$ ) was not expected in this small cohort. Interestingly, no association of the total macrophage data and the alternatively activated macrophage data with PC2 was found. As PC1 and PC2 are independently prognostic for two separate outcome parameters, it can be assumed that they represent two distinct biological features such as cell

type or activation state. Thus, the correlation of alternatively activated macrophages with PC1 and the lack of an association with PC2 indicate that PC1 is related to alternatively activated macrophages at the tumor site, whereas PC2 represents a distinct immunological characteristic.

To my knowledge, this is the first study revealing an association between a prognostic blood cell signature and tumor infiltrating leukocytes. However, a study on mice bearing mammary tumors has reported a similar phenotype for blood monocytes and peritoneal macrophages. Both are neither completely inflammatory nor suppressive and are less differentiated than monocytes and macrophages from normal mice (Caso et al., 2010).

These data indicate a direct or indirect interaction between blood cells involved in the prognostic gene panel and alternatively activated macrophages located in the tumor tissue. It is possible that the prognostic gene panel reflects the polarization of blood monocytes that is related to the polarization of macrophages in the tumor tissue, which was assessed by IF. It remains to be elucidated, whether the blood cell gene signature derives from the same cell line as the M2 macrophages or whether different cell types (blood versus tissue) are measured but responding to the same biological event – ovarian cancer. Moreover, it is unclear if these cells are able to migrate between the tumor tissue and the peripheral blood. To gain more insight into the interaction between blood and tumor tissue immune cells, detailed FACS analyses are planned. Blood samples and single cell suspensions of enzyme-digested tumor tissues will be characterized for their leukocyte composition. Markers specific for total leukocytes, subtypes of T and B lymphocytes, NK cells, granulocytes, MDSCs, monocytes and macrophages as well as activation and differentiation markers will be used to extend the analysis performed in the current study on additional cell types. The ratios of the different cell types will be compared between peripheral blood and tumor tissue.

No further correlation with other biological or clinical factors or survival analysis was performed, since this subproject was designed to correlate the number and polarization of TAMs with the prognostic gene panel in a relatively small patient cohort, but not to provide statistical power for survival analyses. However, the revealed correlation between M2 macrophages and PC1 (associated with decreased OS) indicates a survival disadvantage for patients with high percentages of M2 macrophages. Consistently, high numbers of M2 macrophages have been associated with worse clinical outcome in several cancer entities (Escorcio-Correia and Hagemann, 2010). Thus, the positive correlation of PC1 and M2 macrophages is in accordance with the reported negative effect of M2 macrophages in the tumor microenvironment on tumor regression and survival. For ovarian cancer functional and differentiation studies about macrophages have been published (Kawamura et al., 2009;

Takaishi et al., 2010; Wang et al., 2010), but little is known about the prognostic impact of M2 macrophages for ovarian cancer patients. To approach this question, subsequent analyses including a larger number of tumor tissue samples and sophisticated marker panels for M1 and M2 macrophages would be necessary.

#### **4.2.5 RT-qPCR CD8 relative expression values**

Currently, many studies on prognostic markers are carried out by evaluating mRNA expression. Recent publications, however, have shown little or no correlation between protein and mRNA expression for some genes (Rabiau et al., 2011; Szanto et al., 2011). In this study, the CD8 gene expression values obtained from RT-qPCR did not correlate with the CD8 data generated by IHC. In addition, the prognostic impact of CD8+ cells in the cancer epithelium could not be proven by CD8 gene expression. These differences may be attributed to the fact that the RT-qPCR analysis is based on RNA/cDNA obtained from heterogeneous tumor tissue samples consisting of tumor cells, but also of stromal fibroblasts and blood vessels, whereas for the IHC staining tissue areas with possibly high ratios of tumor cells were selected. Similarly, CD8 assessed in the whole core only showed a trend of improved OS, while the prognostic impact of CD8 data assessed in the cancer epithelium was of significance. These results indicate that when analyzing infiltrating immune cells, gene transcription measurements may not be suitable, at least if tumor tissues are not micro-dissected. RNA in situ assays which permit the assessment of RNA expression on FFPE tissue slides (e.g. QuantiGene® ViewRNA ISH Tissue Assay, Affymetrix, USA) could be a preferable alternative method to RT-qPCR since cancer epithelium and stromal areas can be separately analyzed with this technique. However, two distinct expression levels transcription/RNA stability and translation/protein stability are measured by RT-PCR or RNA in situ assays, on the one hand, and IHC, on the other hand, which per se can lead to uncorrelated results.

#### **4.2.6 Correlation with clinicopathological factors**

No associations with the clinicopathological parameters were found for the assessed leukocytes, leukocyte aggregates, Ki67 and CD8 relative expression values, which is in accordance with other studies also reporting no association of TILs and Ki67 with clinicopathological parameters (Adams et al., 2009; Sengupta et al., 2000). However, other studies reported an association of high Ki67 proliferation index with advanced stage and high grade in ovarian cancer (Aune et al., 2011; Kulkarni et al., 2007). The confirmed association

between FIGO stage and residual tumor ( $p=0.009$ ) is in line with previous studies (Polterauer et al., 2012).

#### 4.2.7 Survival analyses

CD45+ cell infiltration and Ki67 labeling index were found to be independent prognostic factors in multivariable OS analysis. Besides these two biological markers, the well-known clinicopathological prognostic factors high age and advanced FIGO stage were associated with shorter OS, which is in accordance with previous studies (Holschneider and Berek, 2000; Leffers et al., 2009). In PFS analysis, the factors CD45+ cell infiltration, FIGO stage and residual tumor after cytoreductive surgery were found to be of independent prognostic value. The predictive power of FIGO stage and residual tumor for survival is in accordance with literature also reporting these two clinicopathological characteristics to be the most significant prognostic factors (Holschneider and Berek, 2000; Leffers et al., 2009).

Dichotomization of Ki67 at 5% according to the shape of its non-linear association with survival showed a significantly worse survival for a small population of ovarian cancer patients with no or very few Ki67+ tumor cells in their primary tumors compared to patients with  $\geq 5\%$  Ki67+ tumor cells (univariate analysis:  $p=0.004$ ; log-rank test:  $p=0.002$ ). In contrast, no survival advantage was observed when using the median as cut-off value or the continuous values. In multivariable analysis, patients with Ki67- tumors ( $<5\%$  Ki67+ tumor cells) were found to have a more than three times higher risk of death compared to patients with Ki67+ tumors. An association of the proliferative status of ovarian cancer with survival has been reported recently using other proliferation markers such as p21-activated kinase 4 (PAK4) (Siu et al., 2010) or cell cycle-related kinase (CCRK) (Wu et al., 2009). However, there are few reports about the prognostic value of the cell proliferation marker Ki67 for ovarian cancer.

Furthermore, patients with Ki67- tumors were found to be proportionally over-represented in the group of patients who had refractory disease (progression of disease while receiving first line platinum-based therapy or within four weeks after the last chemotherapy cycle) compared to Ki67+ tumors in the remaining group of patients. Similarly, a positive correlation between clinical complete response to first-line chemotherapy and high Ki67 labeling index has been reported (Aune et al., 2011; Garcia-Velasco et al., 2008). All patients included in this study received a platinum-based chemotherapy, in which the platinum complexes cause crosslinking of DNA and trigger apoptosis of the tumor cells. Platinum, like other cytotoxic drugs, is believed to gain its specificity by preferentially killing proliferating

cells. Thus, the dramatically worse clinical outcome of patients with no or very few Ki67+ tumor cells could indicate that these tumor cells may have lower or no response to the platinum-based chemotherapeutic drug. On the other hand, rapidly proliferating tumors are expected to cause poor PFS since these tumors may grow faster to visible recurrent disease. The correlation between Ki67 labeling index and PFS could not be evaluated for the patients with refractory disease who comprised five out of the eleven patients with Ki67- tumors. Hence, the reported correlation between Ki67 labeling index and PFS correlation could only be examined for about half of the patients with Ki67- tumors (and the majority of patients with Ki67+ tumors) and was not confirmed in the current study.

Ovarian cancer patients have a poor prognosis with a less than 40% five year survival for advanced stages (Holschneider and Berek, 2000). About 25% of the patients do not respond to chemotherapy. It is therefore rational to identify the non-responders already at the time of surgery, in order to avoid a harmful but ineffective chemotherapy and to eventually apply alternative therapies. The prevalence of Ki67- tumors is about 5% in the current study including more than 200 EOC patients. If women with Ki67- tumors could be identified at the time of surgery, they could be selected for treatment with alternative drugs, such as angiogenesis inhibitors that reduce tumor growth by inhibiting blood vessel formation rather than targeting rapidly proliferating cells. Studies comprising larger cohorts of patients with Ki67- tumors are needed to further elucidate the clinical relevance of the tumor proliferation marker Ki67 with special focus on response to chemotherapy. Furthermore, the assessment of the Ki67 is well suitable for clinical applications, since standardized, relatively short protocols for Ki67 immunohistochemical staining are available. However, to further elucidate the cause of the worse outcome of patients with Ki67- tumors, the proliferation status of these tumors should be assessed with other proliferation markers specific for proteins which might complement Ki67.

The important role of TILs in human ovarian cancer has recently been investigated in several studies (Curiel et al., 2004; Sato et al., 2005; Zhang et al., 2003). In contrast, there are only few descriptions of CD68+ and CD45+ cells in literature. In the current study high CD45+ cell infiltration was identified as an independent prognostic factor for prolonged survival. The HR per each cell number doubling was reduced by approximately 15% for OS and PFS. This is equal to a reduction of risk to die and risk of disease recurrence of approximately 60% for patients with CD45+ cell infiltrations equivalent to the 75<sup>th</sup> percentile compared to patients with CD45+ cell densities equivalent to the 25<sup>th</sup> percentile infiltration.

Interestingly, CD8+ cytotoxic T cells did not have any prognostic impact in multivariable survival analyses including the clinicopathological factors as well as the other assessed



biological markers. This finding is in contrast to most literature describing CD8+ TILs as an independent prognostic factor in ovarian cancer patients (Leffers et al., 2009; Milne et al., 2009; Sato et al., 2005; Zhang et al., 2003). In the current study high CD8+ T cell infiltration only showed a trend of improved OS in univariate analysis (CD8 cancer epithelium: HR=0.88, 95% CI 0.77-1.01, p=0.077 and CD8 whole core: HR=0.88, 95%CI 0.76-1.02, p=0.081). This apparent discrepancy might be a result of the fact that these earlier studies showing CD8+ cells as an independent prognostic factor did not regard the macrophage marker CD68 and the panleukocyte marker CD45 in multivariable survival analyses. Considering these methodical differences and the positive prognostic trend of cytotoxic T cells in univariate analysis, multivariable analysis was repeated omitting the leukocyte markers CD45 and CD68. Interestingly, in this analysis intraepithelial CD8+ TILs were an independent prognostic factor for OS. This observation indicates inferiority of the prognostic value of CD8+ cytotoxic T cells to that of CD45+ total leukocytes causing the exclusion of CD8+ cell infiltration in the multivariable model comprising CD45. For CD68+ macrophages no impact on patients' survival was found in any of the analyses. This could be due to the expression of CD68 in macrophages with pro- as well as anti-tumoral activities. The much stronger prognostic effect of CD45 compared to CD8 and CD68 suggests that the amount of the total immune cell infiltration is an informative measure of anti-tumoral activity. Due to its panleukocytic reactivity, CD45 indicates most globally, but least specifically an ongoing immune response without revealing the single cell types and their functions. Although the number of CD45+ cells does not provide information about the ratios of the distinct immune cell types with pro- and anti-tumoral functions included in the CD45+ cells, the association of high CD45+ cell infiltration with improved survival, suggest that leukocytes accomplishing tumor regression predominate over immunosuppressive leukocytes favoring tumor progression.

In a successful cytoreductive surgery the major target of anti-tumoral infiltrating immune cells – the tumor mass – is removed as well as the associated infiltrating immune cells. Presumably, different immune cells are involved in inhibiting metastasis formation in the case of optimally debulked patients than the tumor infiltrating immune cells that accomplish the control of tumor outgrowth in patients who suffer from residual tumor. Therefore, it was assumed that in the latter patient group the effect of tumor infiltrating immune cells is more important. Moreover, the factor residual tumor was significant in univariate analysis, but was not significant in multivariable analysis. This led to an additional question regarding the influence of cytotoxic T cells and total leukocytes separately in patients with and without residual tumor. The interaction test and the separate analyses of these two groups of patients

indicated that the positive effect of cytotoxic T cells and total leukocytes on patients' outcome was dependent on the debulking status: a stronger association of CD8+ and CD45+ cell infiltration with improved OS in the group of non-optimally debulked patients compared to the group of optimally debulked patients. The assessment of the prognostic value of the debulking status according to the infiltration of cytotoxic T cells and total leukocytes indicated a dependency of the prognostic impact of the factor residual tumor on the number of cytotoxic T cells and total leukocytes in the tumor mass. The data generated in this study suggest that patients with low CD8+ cell infiltration benefit more from an aggressive cytoreductive surgery than patients with high CD8+ cell tumor infiltration. An explanation for this finding could be that only in the latter patient group the cytotoxic activity of CD8+ T cells limits tumor progression of residual tumor mass, while patients with a low immune cell infiltration have fewer immunological armaments to combat tumor progression. The same trend was observed for CD45+ cells.

These findings are in accordance with a recently published study also reporting a more likely benefit of surgical debulking for patients with aggressive tumor behavior with low CD8+ infiltration and high Ki67 expression (Adams et al., 2009). However, for the latter tumor type the finding was not confirmed in the current study. In accordance with Adams et al., a currently published meta-analysis has shown a varying prognostic impact of CD8 in ovarian cancer patients according to the debulking status. The study has also outlined higher HRs for CD8 in studies comprising optimally and non-optimally debulked patients compared to studies including only optimally debulked patients (Hwang et al., 2012). Together, these results suggest that in non-optimally debulked patients, where tumor infiltrating leukocytes coexist with the residual tumor cells, a higher infiltration presumably correlates with an improved survival due to the contribution of infiltrating leukocytes to tumor regression. In contrast, in optimally debulked patients the tumor and the infiltrating leukocytes are removed and leukocyte cell densities in the primary tumor tissue will have a weaker or no impact on patients' survival. Moreover, CD8 seems a promising marker to predict extent of benefit from extensive surgery for the patients. Quantification of tumor infiltrating cytotoxic T cells could be performed in clinical routine to decide to which extent aggressive cytoreductive surgery should be conducted in patients in whom optimal debulking is difficult and risky to achieve

However, the possible varying prognostic impact of CD8+ and CD45+ cells according to the debulking status and the apparent dependency of the positive effect of optimal debulking on OS according to the infiltration of CD8+ and CD45+ cells described here have to be validated in independent studies.

Concerning residual tumor, inconsistent cut-off values are in use. Several studies define the cut-off value for optimal debulking at 1 or 2 cm (Leffers et al., 2009; Shah et al., 2008; Stumpf et al., 2009), whereas others consider residual tumor as macroscopically visible tumor load as in this study (Clarke et al., 2009; Milne et al., 2009). The question of the influence of residual tumor on the outcome in ovarian cancer patients has recently been addressed in a study stating that for FIGO IV patients macroscopically complete resection was associated with improved survival compared to patients with macroscopically visible residual tumor ( $\geq 0.1$  cm). Categorizing the latter subgroup into patients with minimal residual disease of 0.1 to 1 cm and patients with residual tumor larger than 1 cm, both groups showed similar results (Wimberger et al., 2010). Another study has reported survival advantages for patients without macroscopically visible residual tumor compared to those with minimal visible tumor load ( $\leq 1$  cm) as well as for patients with minimal visible tumor mass ( $\leq 1$  cm) compared to those with residual tumor exceeding 1 cm (Chang and Bristow, 2012). These different definitions of residual tumor have to be taken into account when comparing results.

Clusters of immune cells with high numbers of CD8+, CD68+ and/or CD45+ cells indicate an active immune reaction and might be of prognostic value. No detailed analyses of the cellular composition and the relevance of these aggregates in the anti-tumoral response have been published so far. In this study a trend of improved PFS for the 10% of patients with leukocyte clusters was found suggesting that the presence of immune cell aggregates could be a prognostic factor in ovarian cancer patients. Presumably, a more detailed analysis including the cellular composition, the size and number of such immune cell clusters could increase the prognostic value of these immune cell clusters.

The biological role of tumor infiltrating immune cells in ovarian cancer remains to be further elucidated regarding their pro- and anti-tumoral functions in the complex interplay with tumor cells and stroma cells. For more functional analyses differentiation and activation markers of immune cells should be additionally assessed. Information restricted to cell numbers do not allow interpretation of the actual effector functions or eventual immunosuppressive effects of regulative immune cells such as Tregs or M2 macrophages on anti-tumoral effector cells. Besides the local immune system in the tumor microenvironment, additional mechanisms involved in tumor progression and dissemination such as resistance to cell death, angiogenesis, metastasis or genome instability, which have been reviewed recently (Hanahan and Weinberg, 2011), could be of prognostic value and should be addressed in pursuing studies.

#### 4.2.8 Trouble shooting and limitations

The immunohistochemical analysis revealed information about the prognostic relevance of biological markers such as tumor proliferation and leukocyte infiltration. Nevertheless, the analysis was limited by the use of TMAs comprising only two tissue cores per tumor sample that might not perfectly represent WTSs regarding inhomogeneously distributed tumor infiltrating immune cells. However, for a study comprising hundreds of tumor tissue samples, the use of TMAs provides numerous practical advantages: The TMA technology is relatively inexpensive, preserves patients' material and allows rapid evaluation of different tissues under homogenous conditions. Moreover, if a biological factor of interest has a considerable impact, it should also manifest in TMA analyses. Weighing thoroughly the pros and cons of TMA and WTS, a larger sample size analyzed with TMA technology was preferred over a smaller sample size analyzed with WTSs. However, more reliable data could be obtained when using TMAs with three or even more tissue cores per tumor sample.

Difficulties in the evaluation of the immunohistochemical staining were that some cores did not contain tumor cells (Figure 20A and B) or that they were lost during processing (Figure 20C).

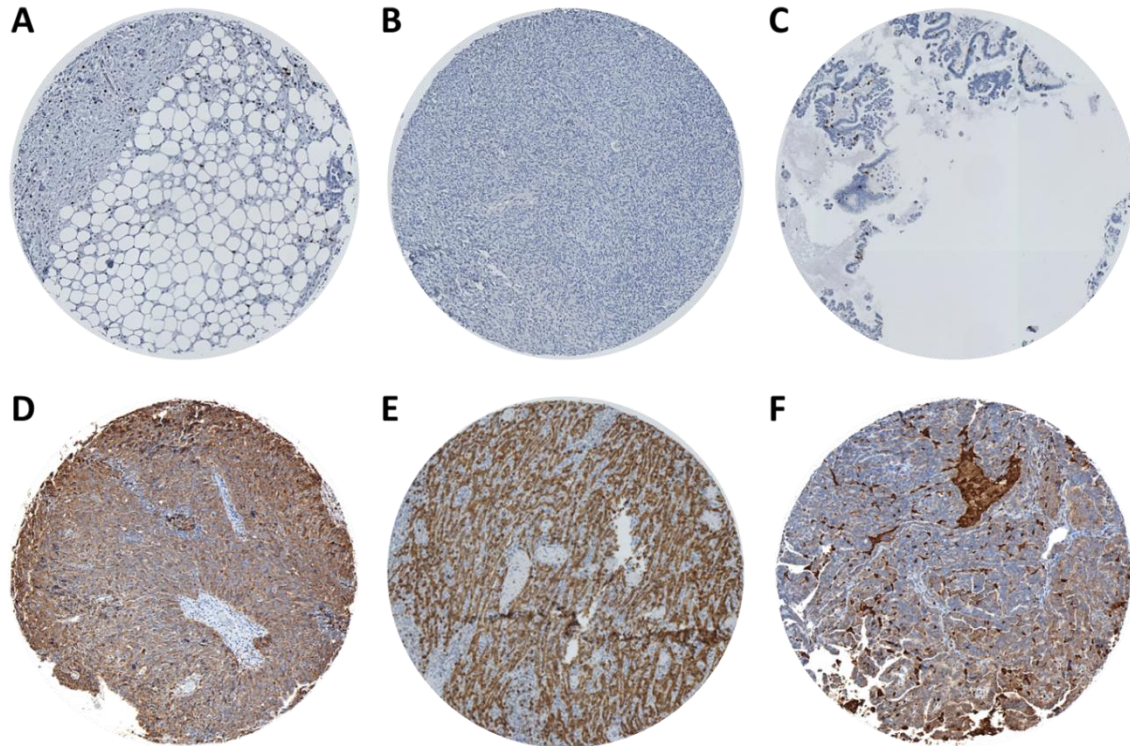


**Figure 20.** Non-evaluative immunohistochemically stained tissue microarray cores of epithelial ovarian cancer due to lack of tumor cells or high background in cancer epithelium and/or necrotic areas; **A** fat tissue; **B** tumor stroma tissue; **C** loss of tissue; **D** high CD68 background in tumor cells; **E** high CD8 background in tumor cells; **F** necrotic areas highly positive for CD68; optical magnification x200; images acquired with the TissueFAXS/HistoQuest system.



Another problem was high background staining: Various tumor samples showed background signals for some of the antibodies either due to expression of the respective antigen or due to unspecific binding of antibodies (Figure 20D and E). Necrotic areas within the tumor tissue also impeded meaningful quantification of marker positive cells since these areas were characterized by unspecific binding and/or high infiltration of immune cells, which were first too dense to be quantified and second might have biased the results. Especially for the quantification of CD68, necrotic areas were problematic (Figure 20F). Therefore, non-evaluable cores or parts of cores lacking cancer epithelium, high background or large necrotic areas were excluded from analysis.

For the analysis of the immunofluorescent staining of WTSs the strong autofluorescence of erythrocytes (Figure 21A and B) was the major problem. As described above, it was impossible to meaningfully analyze necrotic tissue, possibly due to autofluorescence, unspecific binding of antibodies or high macrophage infiltration (Figure 21C and D). Due to difficulties in finding appropriate fields of view without false positive signals, only eight FOVS per WTS were analyzed.

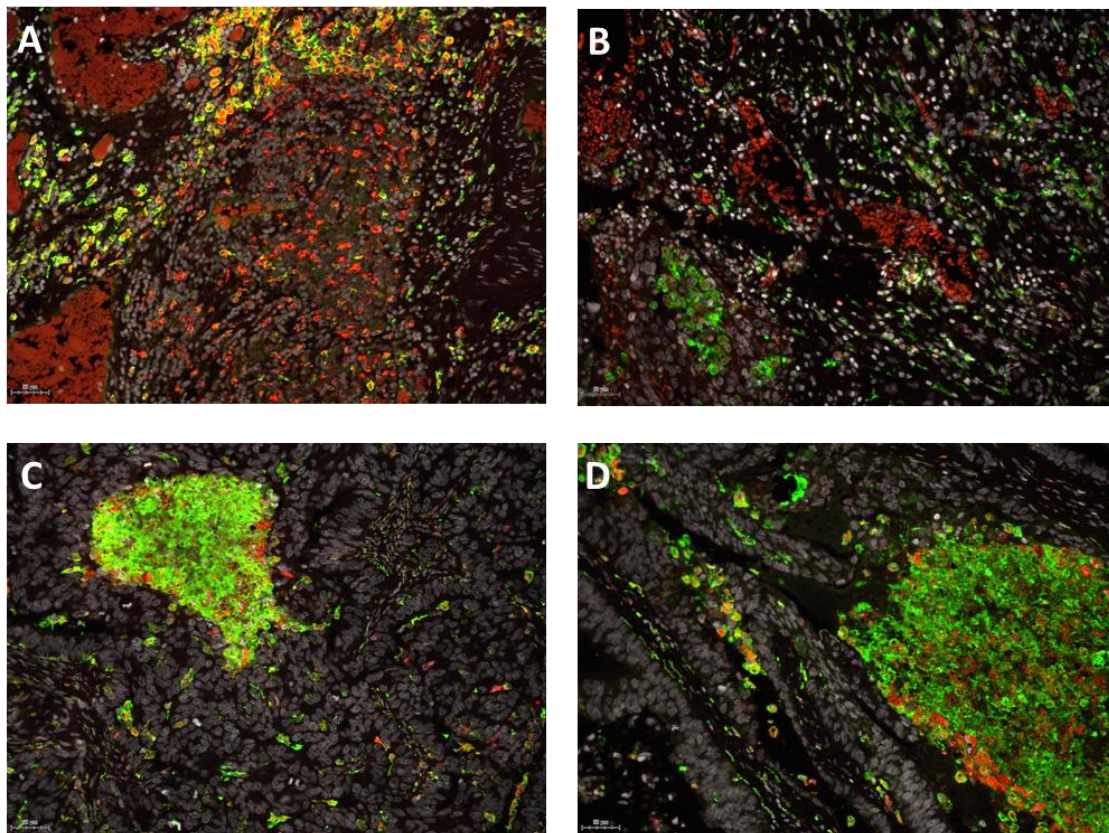


**Figure 21.** Non-evaluable fields of view of immunofluorescence double staining with antibodies against CD68 (red) and MSR1 (green) of epithelial ovarian cancer tissue; DAPI as nuclear counterstaining (light grey); **A** and **B** autofluorescence of erythrocytes; **C** and **D** non-evaluable necrotic areas; optical magnification x200; images acquired with the TissueFAXS/HistoQuest system.

Analyzing the AlexaFluor® 568 detected cells much more false positive signals were observed, whereas hardly any background/autofluorescence complicated the evaluation of AlexaFluor® 647 detected cells. Therefore, a strategy to circumvent the problem of false positive signals might be to use fluorophores emitting in the long-wavelength spectrum. However, the microscope which was used in this study did not provide the filters to use two fluorophores of this kind simultaneously.

### **4.3 Conclusion**

The data obtained from the analysis of gene expression patterns in different blood cell fractions from 23 patients showed heterogeneous expression patterns for the genes comprised in the diagnostic panel. No single cell types obviously suitable for the determination of the diagnostic signature could be identified. However, the fractions of enriched CD3+, CD19+, CD44+ and CD25+ cells seem most promising for patient group specific differences and should be regarded for further analyses. The EOC sensitivity of the diagnostic gene panel determined in the “high density” fraction was confirmed in this study, but the signature was not found to be EOC specific.

For the prognostic panel the gene expression patterns indicate that among the assessed blood cell fractions the genes of this panel are mainly expressed by monocyte derived cells and activated immune cells or from “activated monocytes”.

The immunohistochemical analysis of more than 200 relatively homogeneous EOC samples revealed a dramatically worse clinical outcome for patients with Ki67- tumors, presumably due to poor response to the chemotherapy. Moreover, high CD45+ cell infiltrating of the tumor was associated with prolonged survival, thereby indicating a predominance of anti-tumoral activity over pro-tumoral functions in the total of immune reactions. Interestingly, cytotoxic T cells and total leukocytes were found to have a stronger positive effect on the clinical outcome in patients with residual tumor compared to optimally debulked patients. Similarly, the prolonged overall survival associated with optimal debulking was found to depend on the infiltration level of cytotoxic T cells and total leukocytes. Summarizing, Ki67 and CD8 could be useful clinical tools for the choice of chemotherapy and as a predictive marker for patients’ benefit from an aggressive cytoreductive surgery, respectively. CD45 could be used as a prognostic marker for overall and progression-free survival.

The analysis of the interaction of blood cell leukocytes represented by the two independent prognostic factors PC1 and PC2 derived from the prognostic gene panel and tumor infiltrating macrophages revealed a correlation between M2 macrophages and PC1. This is in accordance with the repeatedly reported positive correlation of M2 macrophages and tumor progression. The observed association indicates a direct or indirect interaction between blood cells involved in the prognostic gene panel and M2 macrophages.

## 5 List of Abbreviations

ANOVA	analysis of variance
CA	cancer antigen
CCRK	cell cycle-related kinase
CI	confidence interval
CIN	cervical intraepithelial neoplasia
CTC	circulating tumor cell
CTLA-4	cytotoxic T lymphocyte antigen 4
DAB	diamino-benzidine
DC	dendritic cell
EGF	epidermal growth factor
EOC	epithelial ovarian cancer
EOK	epitheliales Ovarialkarzinom
FACS	fluorescence associated cell sorting
FIGO	International Federation of Gynecology and Obstetrics
FOV	field of view
GM-CSF	granulocyte macrophage colony-stimulating factor
HD	high density
HE4	human epididymis protein 4
HER-2/neu	human epidermal growth factor receptor 2
HLA	human leukocyte antigen
HPV-HR	human papilloma virus – high risk



HR	hazard ratio
HRP	horseradish peroxidase
IF	immunofluorescence
IFN	interferon
IGF-II	insulin-like growth factor II
IHC	immunohistochemistry
IL	interleukin
iNOS	inducible nitric oxide synthase
JAK	janus kinase
LPS	lipopolysaccharide
MDSC	myeloid derived suppressor cell
MHC	major histocompatibility complex
MIF	macrophage migration inhibitory factor
MSR1	macrophage scavenger receptor 1
NK	natural killer
NO	nitric oxide
OS	overall survival
PAI	plasminogen activator inhibitor type
PAK4	p21-activated kinase 4
PBMC	peripheral blood mononuclear cell
PC	Principal Component
PCA	Principal Component Analysis
PD-L1	programmed death-1 ligand

PFS	progression-free survival
PGE2	prostaglandin E2
RIN	RNA Integrity Number
ROI	region of interest
ROS	reactive oxygen species
RT-qPCR	reverse transcriptase quantitative PCR
SARS	severe acute respiratory syndrome
SMRP	soluble mesothelin-related peptide
STAT	signal transducer and activator of transcription
TAM	tumor associated macrophage
TGF	transforming growth factor
Th	T helper
TIL	tumor infiltrating lymphocyte
TLR	toll-like receptor
TMA	tissue microarray
TNF	tumor necrosis factor
Treg	regulatory T cell
TSP	thrombospondin
VEGF	vascular endothelial growth factor
WTS	whole tissue section

## 6 Abstract

Ovarian cancer is one of the most deadly malignancies in women. Due to a lack of symptoms and a routinely used screening marker most patients are diagnosed at advanced stages and have a five year survival rate below 40%. Thus, to improve overall survival, new diagnostic and prognostic markers are urgently needed. Our working group has developed two gene expression signatures in a blood leukocyte fraction which is isolated using a density gradient: one for early diagnosis of epithelial ovarian cancer (EOC) and another one for prognosis in EOC patients. Besides blood cell gene expressions, tumor proliferation markers and tumor infiltrating leukocytes are promising prognostic biological markers in EOC patients.

In the course of this diploma thesis expression patterns of the genes comprised in the two recently described blood cell signatures were analyzed with reverse transcriptase quantitative PCR in different blood cell fractions. 23 patients including EOC patients, patients with other malignancies and controls with benign gynecological diseases were compared. The study aimed to find blood cell fraction(s) suitable for the determination of the gene signatures to facilitate the current density gradient protocol. The gene expression patterns of the diagnostic panel were heterogeneous suggesting various different cell types expressing these genes. The fractions of CD3+, CD19+, CD44+ and CD25+ enriched cells were the fractions with highest disease specific gene expression differences. Most genes of the prognostic gene panel showed highest expression values in the fractions of CD14+ and CD25+ enriched cells indicating these genes to be mainly expressed by monocyte derived cells and activated immune cells.

Moreover, in more than 200 EOC patients proliferation activity, measured by Ki67 expression, and tumor infiltrating CD8+, CD68+ and CD45+ cells were immunohistochemically analyzed and the prognostic values of these biological markers were assessed. A dramatically diminished overall survival for a small population of patients with no or very few Ki67+ tumor cells was revealed, presumably due to poor response to the chemotherapy. Furthermore, a high infiltration of CD45+ cells was associated with improved overall and progression-free survival. A dependency of the prognostic impact of CD8+ and CD45+ cells on to the debulking status was found. Similarly, a varying prognostic value of residual tumor according to the infiltration of CD8+ and CD45+ cells was revealed.

In addition, in a small EOC patient cohort of 19 women a moderate correlation between the risk to die – according to the prognostic blood cell gene expression panel – and alternatively activated macrophages in the tumor tissue was revealed. This association indicates an interaction between blood circulating immune cells and tumor associated macrophages.

## 7 Zusammenfassung

Ovarialkarzinom zählt zu den Krebserkrankungen mit der höchsten Mortalität bei Frauen. Aufgrund mangelnder Symptome und des Fehlens in der Routine einsetzbarer Screeningmarker wird bei den meisten Patientinnen Ovarialkarzinom in einem bereits fortgeschrittenen Stadium diagnostiziert, mit einer Fünf-Jahres-Überlebensrate von unter 40%. Um das Gesamtüberleben zu verbessern, werden daher neue diagnostische und prognostische Marker dringend benötigt. In unserem Labor wurden eine Genexpressionssignatur für die Frühdiagnose von epitheliale Ovarialkarzinom (EOK) und eine weitere für die Prognostik von EOK-Patientinnen in einer mittels Dichtegradienten isolierten Blutleukozytenfraktion entwickelt. Neben Blutzellgenexpressionen zielen weitere vielversprechende prognostische Marker in EOK-Patientinnen auf Tumorphiliferation und tumorinfiltrierende Leukozyten ab.

Im Laufe dieser Diplomarbeit wurden die Genexpressionen der zwei Blutzellsignaturen mit Reverse Transkriptase quantitative PCR in verschiedenen Blutzellfraktionen von 23 Patientinnen mit EOK, anderen Krebserkrankungen und gutartigen gynäkologischen Erkrankungen analysiert. Ziel war es, Blutzellfraktionen zu finden, die für die Bestimmung der Gensignaturen geeignet sind und die Dichtegradienten-Methode vereinfachen. Die Analyse des diagnostischen Panels zeigte die höchsten krankheitsspezifischen Genexpressionsunterschiede in den CD3+, CD19+, CD44+ und CD25+ angereicherten Zellfraktionen. Die meisten Gene des prognostischen Panels hatten in den CD14+ und CD25+ angereicherten Zellfraktionen die höchsten Expressionswerte, was darauf hindeutet, dass diese Gene vor allem von Zellen der Monozytenlinie und aktivierten Leukozyten exprimiert werden.

Zudem wurden Tumorphiliferation, gemessen durch Ki67 Expression, und tumorinfiltrierende CD8+, CD68+ und CD45+ Zellen in einer immunhistochemischen Analyse mit mehr als 200 EOK-Patientinnen auf ihren prognostischen Wert hin untersucht. Es wurde ein stark verringertes Gesamtüberleben für eine kleine Patientinnenpopulation mit sehr wenigen Ki67+ Tumorzellen festgestellt, vermutlich aufgrund eines schlechteren Ansprechens auf die Chemotherapie. Zudem konnte eine hohe Infiltration von CD45+ Zellen mit längerem Überleben assoziiert werden. Es wurde ein vom Resttumorstatus abhängiger positiver Effekt der CD8+ und CD45+ Zellen auf das Gesamtüberleben aufgezeigt sowie eine Abhängigkeit des prognostischen Werts des Resttumorstatus von der CD8+ und CD45+ Zellinfiltration.

Außerdem wurde in einer kleinen EOK-Patientinnenkohorte von 19 Frauen eine moderate Korrelation zwischen dem mit der prognostischen Blutzellsignatur ermittelten Sterberisiko und alternativ aktivierten Makrophagen im Tumorgewebe gefunden. Dies weist auf eine Interaktion zwischen Blut zirkulierenden Immunzellen und tumorassoziierten Makrophagen hin.

## 8 References

**Aaroe, J., Lindahl, T., Dumeaux, V., Saebo, S., Tobin, D., Hagen, N., Skaane, P., Lonneborg, A., Sharma, P. and Borresen-Dale, A. L.** (2010). Gene expression profiling of peripheral blood cells for early detection of breast cancer. *Breast Cancer Res* **12**, R7.

**Abbas, A. K., Lichtman, A. H. and Pillai, S.** (2007). Cellular and molecular immunology. Edinburgh: Elsevier Saunders.

**Abbas, A. R., Baldwin, D., Ma, Y., Ouyang, W., Gurney, A., Martin, F., Fong, S., van Lookeren Campagne, M., Godowski, P., Williams, P. M. et al.** (2005). Immune response in silico (IRIS): immune-specific genes identified from a compendium of microarray expression data. *Genes Immun* **6**, 319-31.

**Adams, S. F., Levine, D. A., Cadungog, M. G., Hammond, R., Facciabene, A., Olvera, N., Rubin, S. C., Boyd, J., Gimotty, P. A. and Coukos, G.** (2009). Intraepithelial T cells and tumor proliferation: impact on the benefit from surgical cytoreduction in advanced serous ovarian cancer. *Cancer* **115**, 2891-902.

**Anderson, N. S., Turner, L., Livingston, S., Chen, R., Nicosia, S. V. and Kruk, P. A.** (2009). Bcl-2 expression is altered with ovarian tumor progression: an immunohistochemical evaluation. *J Ovarian Res* **2**, 16.

**Apetoh, L., Locher, C., Ghiringhelli, F., Kroemer, G. and Zitvogel, L.** (2011). Harnessing dendritic cells in cancer. *Semin Immunol* **23**, 42-9.

**Augier, S., Ciucci, T., Luci, C., Carle, G. F., Blin-Wakkach, C. and Wakkach, A.** (2010). Inflammatory blood monocytes contribute to tumor development and represent a privileged target to improve host immunosurveillance. *J Immunol* **185**, 7165-73.

**Aune, G., Stunes, A. K., Tingulstad, S., Salvesen, O., Syversen, U. and Torp, S. H.** (2011). The proliferation markers Ki-67/MIB-1, phosphohistone H3, and survivin may contribute in the identification of aggressive ovarian carcinomas. *Int J Clin Exp Pathol* **4**, 444-53.

**Ayari, C., LaRue, H., Hovington, H., Decobert, M., Harel, F., Bergeron, A., Tetu, B., Lacombe, L. and Fradet, Y.** (2009). Bladder tumor infiltrating mature dendritic cells and macrophages as predictors of response to bacillus Calmette-Guerin immunotherapy. *Eur Urol* **55**, 1386-95.

**Bates, G. J., Fox, S. B., Han, C., Leek, R. D., Garcia, J. F., Harris, A. L. and Banham, A. H.** (2006). Quantification of regulatory T cells enables the identification of high-risk breast cancer patients and those at risk of late relapse. *J Clin Oncol* **24**, 5373-80.

**Biswas, S. K. and Mantovani, A.** (2010). Macrophage plasticity and interaction with lymphocyte subsets: cancer as a paradigm. *Nat Immunol* **11**, 889-96.

**Brandt, B. and Griwatz, C.** (1996). Two-layer buoyant density centrifugation gradient for enrichment of prostate-derived cells and cell clusters from peripheral blood. *Clin Chem* **42**, 1881-2.

**Caso, R., Silvera, R., Carrio, R., Iragavarapu-Charyulu, V., Gonzalez-Perez, R. R. and Torroella-Kouri, M.** (2010). Blood monocytes from mammary tumor-bearing mice: early targets of tumor-induced immune suppression? *Int J Oncol* **37**, 891-900.

**Chang, S. J. and Bristow, R. E.** (2012). Evolution of surgical treatment paradigms for advanced-stage ovarian cancer: redefining 'optimal' residual disease. *Gynecol Oncol* **125**, 483-92.

**Clarke, B., Tinker, A. V., Lee, C. H., Subramanian, S., van de Rijn, M., Turbin, D., Kalloger, S., Han, G., Ceballos, K., Cadungog, M. G. et al.** (2009). Intraepithelial T cells and prognosis in ovarian carcinoma: novel associations with stage, tumor type, and BRCA1 loss. *Mod Pathol* **22**, 393-402.

**Cox, C. R.** (1972). Regression models and life-tables (with discussion). *J. R. Statist. Soc. B* **34**, 187-220.

**Curiel, T. J., Coukos, G., Zou, L., Alvarez, X., Cheng, P., Mottram, P., Evdemon-Hogan, M., Conejo-Garcia, J. R., Zhang, L., Burow, M. et al.** (2004). Specific recruitment of regulatory T cells in ovarian carcinoma fosters immune privilege and predicts reduced survival. *Nat Med* **10**, 942-9.

**Dieu-Nosjean, M. C., Antoine, M., Danel, C., Heudes, D., Wislez, M., Poulot, V., Rabbe, N., Laurans, L., Tartour, E., de Chaisemartin, L. et al.** (2008). Long-term survival for patients with non-small-cell lung cancer with intratumoral lymphoid structures. *J Clin Oncol* **26**, 4410-7.

**Escorcio-Correia, M. and Hagemann, T.** (2010). Macrophages in the Tumor Microenvironment. *Journal of Leukocyte Biology*, 371--383.

**Flavell, R. A., Sanjabi, S., Wrzesinski, S. H. and Licona-Limon, P.** (2010). The polarization of immune cells in the tumour environment by TGFbeta. *Nat Rev Immunol* **10**, 554-67.

**Fluge, O., Gravdal, K., Carlsen, E., Vonen, B., Kjellevold, K., Refsum, S., Lilleng, R., Eide, T. J., Halvorsen, T. B., Tveit, K. M. et al.** (2009). Expression of EZH2 and Ki-67 in colorectal cancer and associations with treatment response and prognosis. *Br J Cancer* **101**, 1282-9.

**Friedlander, M., Trimble, E., Tinker, A., Alberts, D., Avall-Lundqvist, E., Brady, M., Harter, P., Pignata, S., Pujade-Lauraine, E., Sehouli, J. et al.** (2011). Clinical trials in recurrent ovarian cancer. *Int J Gynecol Cancer* **21**, 771-5.

**Gabrilovich, D. I. and Nagaraj, S.** (2009). Myeloid-derived suppressor cells as regulators of the immune system. *Nat Rev Immunol* **9**, 162-74.

- Galon, J., Costes, A., Sanchez-Cabo, F., Kirilovsky, A., Mlecnik, B., Lagorce-Pages, C., Tosolini, M., Camus, M., Berger, A., Wind, P. et al.** (2006). Type, density, and location of immune cells within human colorectal tumors predict clinical outcome. *Science* **313**, 1960-4.
- Gao, Q., Qiu, S. J., Fan, J., Zhou, J., Wang, X. Y., Xiao, Y. S., Xu, Y., Li, Y. W. and Tang, Z. Y.** (2007). Intratumoral balance of regulatory and cytotoxic T cells is associated with prognosis of hepatocellular carcinoma after resection. *J Clin Oncol* **25**, 2586-93.
- Garcia-Velasco, A., Mendiola, C., Sanchez-Munoz, A., Ballestin, C., Colomer, R. and Cortes-Funes, H.** (2008). Prognostic value of hormonal receptors, p53, ki67 and HER2/neu expression in epithelial ovarian carcinoma. *Clin Transl Oncol* **10**, 367-71.
- Gimotty, P. A., Van Belle, P., Elder, D. E., Murry, T., Montone, K. T., Xu, X., Hotz, S., Raines, S., Ming, M. E., Wahl, P. et al.** (2005). Biologic and prognostic significance of dermal Ki67 expression, mitoses, and tumorigenicity in thin invasive cutaneous melanoma. *J Clin Oncol* **23**, 8048-56.
- Gooden, M. J., de Bock, G. H., Leffers, N., Daemen, T. and Nijman, H. W.** (2011). The prognostic influence of tumour-infiltrating lymphocytes in cancer: a systematic review with meta-analysis. *Br J Cancer* **105**, 93-103.
- Gordon, S. and Martinez, F. O.** (2010). Alternative activation of macrophages: mechanism and functions. *Immunity* **32**, 593-604.
- Gordon, S. and Taylor, P. R.** (2005). Monocyte and macrophage heterogeneity. *Nat Rev Immunol* **5**, 953-64.
- Hamanishi, J., Mandai, M., Iwasaki, M., Okazaki, T., Tanaka, Y., Yamaguchi, K., Higuchi, T., Yagi, H., Takakura, K., Minato, N. et al.** (2007). Programmed cell death 1 ligand 1 and tumor-infiltrating CD8+ T lymphocytes are prognostic factors of human ovarian cancer. *Proc Natl Acad Sci U S A* **104**, 3360-5.
- Hanahan, D. and Weinberg, R. A.** (2011). Hallmarks of cancer: the next generation. *Cell* **144**, 646-74.
- He, L., Ding, Y. Q., Wang, W., Zhang, Q. L., Zhang, J. H., Geng, J. and Cai, J. J.** (2003). [Expression of immune cells and their roles in the involved tissues of SARS patients]. *Di Yi Jun Yi Da Xue Xue Bao* **23**, 774-6, 780.
- Hefler, L. A., Concin, N., Hofstetter, G., Marth, C., Mustea, A., Sehouli, J., Zeillinger, R., Leipold, H., Lass, H., Grimm, C. et al.** (2008). Serum C-reactive protein as independent prognostic variable in patients with ovarian cancer. *Clin Cancer Res* **14**, 710-4.
- Holschneider, C. H. and Berek, J. S.** (2000). Ovarian cancer: epidemiology, biology, and prognostic factors. *Semin Surg Oncol* **19**, 3-10.
- Hwang, W. T., Adams, S. F., Tahirovic, E., Hagemann, I. S. and Coukos, G.** (2012). Prognostic significance of tumor-infiltrating T cells in ovarian cancer: a meta-analysis. *Gynecol Oncol* **124**, 192-8.

- Jemal, A., Bray, F., Center, M. M., Ferlay, J., Ward, E. and Forman, D.** (2011). Global cancer statistics. *CA Cancer J Clin* **61**, 69-90.
- Kawamura, K., Komohara, Y., Takaishi, K., Katabuchi, H. and Takeya, M.** (2009). Detection of M2 macrophages and colony-stimulating factor 1 expression in serous and mucinous ovarian epithelial tumors. *Pathol Int* **59**, 300-5.
- Kryczek, I., Wei, S., Zhu, G., Myers, L., Mottram, P., Cheng, P., Chen, L., Coukos, G. and Zou, W.** (2007). Relationship between B7-H4, regulatory T cells, and patient outcome in human ovarian carcinoma. *Cancer Res* **67**, 8900-5.
- Kryczek, I., Zou, L., Rodriguez, P., Zhu, G., Wei, S., Mottram, P., Brumlik, M., Cheng, P., Curiel, T., Myers, L. et al.** (2006). B7-H4 expression identifies a novel suppressive macrophage population in human ovarian carcinoma. *J Exp Med* **203**, 871-81.
- Kulkarni, A. A., Loddo, M., Leo, E., Rashid, M., Eward, K. L., Fanshawe, T. R., Butcher, J., Frost, A., Ledermann, J. A., Williams, G. H. et al.** (2007). DNA replication licensing factors and aurora kinases are linked to aneuploidy and clinical outcome in epithelial ovarian carcinoma. *Clin Cancer Res* **13**, 6153-61.
- Lax, S.** (2009). Seröse Genitalkarzinome. *Der Pathologe* **30**, 210-216.
- Lee, H. E., Kim, M. A., Lee, B. L. and Kim, W. H.** (2010). Low Ki-67 proliferation index is an indicator of poor prognosis in gastric cancer. *J Surg Oncol* **102**, 201-6.
- Leffers, N., Gooden, M. J., de Jong, R. A., Hoogeboom, B. N., ten Hoor, K. A., Hollema, H., Boezen, H. M., van der Zee, A. G., Daemen, T. and Nijman, H. W.** (2009). Prognostic significance of tumor-infiltrating T-lymphocytes in primary and metastatic lesions of advanced stage ovarian cancer. *Cancer Immunol Immunother* **58**, 449-59.
- Liu, F., Lang, R., Zhao, J., Zhang, X., Pringle, G. A., Fan, Y., Yin, D., Gu, F., Yao, Z. and Fu, L.** (2011). CD8(+) cytotoxic T cell and FOXP3(+) regulatory T cell infiltration in relation to breast cancer survival and molecular subtypes. *Breast Cancer Res Treat* **130**, 645-55.
- Liu, P., Sun, Y. L., Du, J., Hou, X. S. and Meng, H.** (2012). CD105/Ki67 Coexpression Correlates With Tumor Progression and Poor Prognosis in Epithelial Ovarian Cancer. *Int J Gynecol Cancer*.
- Ma, J., Liu, L., Che, G., Yu, N., Dai, F. and You, Z.** (2010). The M1 form of tumor-associated macrophages in non-small cell lung cancer is positively associated with survival time. *BMC Cancer* **10**, 112.
- Mantovani, A., Sica, A., Allavena, P., Garlanda, C. and Locati, M.** (2009). Tumor-associated macrophages and the related myeloid-derived suppressor cells as a paradigm of the diversity of macrophage activation. *Hum Immunol* **70**, 325-30.
- Mantovani, A., Sozzani, S., Locati, M., Allavena, P. and Sica, A.** (2002). Macrophage polarization: tumor-associated macrophages as a paradigm for polarized M2 mononuclear phagocytes. *Trends Immunol* **23**, 549-55.



- Martinez, F. O., Gordon, S., Locati, M. and Mantovani, A.** (2006). Transcriptional profiling of the human monocyte-to-macrophage differentiation and polarization: new molecules and patterns of gene expression. *J Immunol* **177**, 7303-11.
- Milne, K., Kobel, M., Kalloger, S. E., Barnes, R. O., Gao, D., Gilks, C. B., Watson, P. H. and Nelson, B. H.** (2009). Systematic analysis of immune infiltrates in high-grade serous ovarian cancer reveals CD20, FoxP3 and TIA-1 as positive prognostic factors. *PLoS One* **4**, e6412.
- Moore, R. G., MacLaughlan, S. and Bast, R. C., Jr.** (2010). Current state of biomarker development for clinical application in epithelial ovarian cancer. *Gynecol Oncol* **116**, 240-5.
- Nosho, K., Baba, Y., Tanaka, N., Shima, K., Hayashi, M., Meyerhardt, J. A., Giovannucci, E., Dranoff, G., Fuchs, C. S. and Ogino, S.** (2010). Tumour-infiltrating T-cell subsets, molecular changes in colorectal cancer, and prognosis: cohort study and literature review. *J Pathol* **222**, 350-66.
- Odicino, F., Pecorelli, S., Zigliani, L. and Creasman, W. T.** (2008). History of the FIGO cancer staging system. *Int J Gynaecol Obstet* **101**, 205-10.
- Pollard, J. W.** (2004). Tumour-educated macrophages promote tumour progression and metastasis. *Nat Rev Cancer* **4**, 71-8.
- Polterauer, S., Vergote, I., Concin, N., Braicu, I., Chekarov, R., Mahner, S., Woelber, L., Cadron, I., Van Gorp, T., Zeillinger, R. et al.** (2012). Prognostic value of residual tumor size in patients with epithelial ovarian cancer FIGO stages IIA-IV: analysis of the OVCAD data. *Int J Gynecol Cancer* **22**, 380-5.
- Rabiau, N., Dechelotte, P., Adjakly, M., Kemeny, J. L., Guy, L., Boiteux, J. P., Kwiatkowski, F., Bignon, Y. J. and Bernard-Gallon, D.** (2011). BRCA1, BRCA2, AR and IGF-I expression in prostate cancer: correlation between RT-qPCR and immunohistochemical detection. *Oncol Rep* **26**, 695-702.
- Royston, P. and Sauerbrei, W.** (2008). Multivariable Model-building: A Pragmatic Approach to Regression Analysis Based on Fractional Polynomials for Modelling Continuous Variables: John Wiley.
- Rustin, G. J.** (2003). Use of CA-125 to assess response to new agents in ovarian cancer trials. *J Clin Oncol* **21**, 187s-193s.
- Sato, E., Olson, S. H., Ahn, J., Bundy, B., Nishikawa, H., Qian, F., Jungbluth, A. A., Frosina, D., Gnjjatic, S., Ambrosone, C. et al.** (2005). Intraepithelial CD8+ tumor-infiltrating lymphocytes and a high CD8+/regulatory T cell ratio are associated with favorable prognosis in ovarian cancer. *Proc Natl Acad Sci U S A* **102**, 18538-43.
- Schreiber, R. D., Old, L. J. and Smyth, M. J.** (2011). Cancer immunoediting: integrating immunity's roles in cancer suppression and promotion. *Science* **331**, 1565-70.

**Sengupta, P. S., McGown, A. T., Bajaj, V., Blackhall, F., Swindell, R., Bromley, M., Shanks, J. H., Ward, T., Buckley, C. H., Reynolds, K. et al.** (2000). p53 and related proteins in epithelial ovarian cancer. *Eur J Cancer* **36**, 2317-28.

**Shah, C. A., Allison, K. H., Garcia, R. L., Gray, H. J., Goff, B. A. and Swisher, E. M.** (2008). Intratumoral T cells, tumor-associated macrophages, and regulatory T cells: association with p53 mutations, circulating tumor DNA and survival in women with ovarian cancer. *Gynecol Oncol* **109**, 215-9.

**Sharma, P., Sahni, N. S., Tibshirani, R., Skaane, P., Urdal, P., Berghagen, H., Jensen, M., Kristiansen, L., Moen, C., Zaka, A. et al.** (2005). Early detection of breast cancer based on gene-expression patterns in peripheral blood cells. *Breast Cancer Res* **7**, R634-44.

**Sica, A., Saccani, A. and Mantovani, A.** (2002). Tumor-associated macrophages: a molecular perspective. *Int Immunopharmacol* **2**, 1045-54.

**Siu, M. K., Chan, H. Y., Kong, D. S., Wong, E. S., Wong, O. G., Ngan, H. Y., Tam, K. F., Zhang, H., Li, Z., Chan, Q. K. et al.** (2010). p21-activated kinase 4 regulates ovarian cancer cell proliferation, migration, and invasion and contributes to poor prognosis in patients. *Proc Natl Acad Sci U S A* **107**, 18622-7.

**Solinas, G., Schiarea, S., Liguori, M., Fabbri, M., Pesce, S., Zammataro, L., Pasqualini, F., Nebuloni, M., Chiabrando, C., Mantovani, A. et al.** (2010). Tumor-conditioned macrophages secrete migration-stimulating factor: a new marker for M2-polarization, influencing tumor cell motility. *J Immunol* **185**, 642-52.

**Sorbye, S. W., Kilvaer, T., Valkov, A., Donnem, T., Smeland, E., Al-Shibli, K., Bremnes, R. M. and Busund, L. T.** (2011). Prognostic impact of lymphocytes in soft tissue sarcomas. *PLoS One* **6**, e14611.

**Stumpf, M., Hasenburg, A., Riener, M. O., Jutting, U., Wang, C., Shen, Y., Orlowska-Volk, M., Fisch, P., Wang, Z., Gitsch, G. et al.** (2009). Intraepithelial CD8-positive T lymphocytes predict survival for patients with serous stage III ovarian carcinomas: relevance of clonal selection of T lymphocytes. *Br J Cancer* **101**, 1513-21.

**Szanto, A. G., Nadin-Davis, S. A., Rosatte, R. C. and White, B. N.** (2011). Re-assessment of direct fluorescent antibody negative brain tissues with a real-time PCR assay to detect the presence of raccoon rabies virus RNA. *J Virol Methods* **174**, 110-6.

**Takaishi, K., Komohara, Y., Tashiro, H., Ohtake, H., Nakagawa, T., Katabuchi, H. and Takeya, M.** (2010). Involvement of M2-polarized macrophages in the ascites from advanced epithelial ovarian carcinoma in tumor progression via Stat3 activation. *Cancer Sci* **101**, 2128-36.

**The Cancer Gemone Atlas Research Network.** (2011). Integrated genomic analyses of ovarian carcinoma. *Nature* **474**, 609-15.

**Teng, M. W., Swann, J. B., Koebel, C. M., Schreiber, R. D. and Smyth, M. J.** (2008). Immune-mediated dormancy: an equilibrium with cancer. *J Leukoc Biol* **84**, 988-93.

- Urrea, X., Villamor, N., Amaro, S., Gomez-Choco, M., Obach, V., Oleaga, L., Planas, A. M. and Chamorro, A.** (2009). Monocyte subtypes predict clinical course and prognosis in human stroke. *J Cereb Blood Flow Metab* **29**, 994-1002.
- Vaughan, S., Coward, J. I., Bast, R. C., Jr., Berchuck, A., Berek, J. S., Brenton, J. D., Coukos, G., Crum, C. C., Drapkin, R., Etemadmoghadam, D. et al.** (2011). Rethinking ovarian cancer: recommendations for improving outcomes. *Nat Rev Cancer* **11**, 719-25.
- Vesely, M. D., Kershaw, M. H., Schreiber, R. D. and Smyth, M. J.** (2011). Natural innate and adaptive immunity to cancer. *Annu Rev Immunol* **29**, 235-71.
- Visintin, I., Feng, Z., Longton, G., Ward, D. C., Alvero, A. B., Lai, Y., Tenthorey, J., Leiser, A., Flores-Saaib, R., Yu, H. et al.** (2008). Diagnostic markers for early detection of ovarian cancer. *Clin Cancer Res* **14**, 1065-72.
- Wang, R., Zhang, T., Ma, Z., Wang, Y., Cheng, Z., Xu, H., Li, W. and Wang, X.** (2010). The interaction of coagulation factor XII and monocyte/macrophages mediating peritoneal metastasis of epithelial ovarian cancer. *Gynecol Oncol* **117**, 460-6.
- Wimberger, P., Wehling, M., Lehmann, N., Kimmig, R., Schmalfeldt, B., Burges, A., Harter, P., Pfisterer, J. and du Bois, A.** (2010). Influence of residual tumor on outcome in ovarian cancer patients with FIGO stage IV disease: an exploratory analysis of the AGO-OVAR (Arbeitsgemeinschaft Gynaekologische Onkologie Ovarian Cancer Study Group). *Ann Surg Oncol* **17**, 1642-8.
- Wu, G. Q., Xie, D., Yang, G. F., Liao, Y. J., Mai, S. J., Deng, H. X., Sze, J., Guan, X. Y., Zeng, Y. X., Lin, M. C. et al.** (2009). Cell cycle-related kinase supports ovarian carcinoma cell proliferation via regulation of cyclin D1 and is a predictor of outcome in patients with ovarian carcinoma. *Int J Cancer* **125**, 2631-42.
- Yigit, R., Massuger, L. F., Figdor, C. G. and Torensma, R.** (2010). Ovarian cancer creates a suppressive microenvironment to escape immune elimination. *Gynecol Oncol* **117**, 366-72.
- Zhang, L., Conejo-Garcia, J. R., Katsaros, D., Gimotty, P. A., Massobrio, M., Regnani, G., Makrigiannakis, A., Gray, H., Schlienger, K., Liebman, M. N. et al.** (2003). Intratumoral T cells, recurrence, and survival in epithelial ovarian cancer. *N Engl J Med* **348**, 203-13.
- Zindl, C. L. and Chaplin, D. D.** (2010). Immunology. Tumor immune evasion. *Science* **328**, 697-8.
- Zou, W. and Chen, L.** (2008). Inhibitory B7-family molecules in the tumour microenvironment. *Nat Rev Immunol* **8**, 467-77.
- Zou, W. and Restifo, N. P.** (2010). T(H)17 cells in tumour immunity and immunotherapy. *Nat Rev Immunol* **10**, 248-56.

## 9 Acknowledgements

I thank Robert Zeillinger for giving me the opportunity to work in his laboratory and the whole crew of the Molecular Oncology Group for the supportive collaboration and inspiring working atmosphere. Special thank goes to my supervisors Dietmar Pils, Dan Cacsire Castillo-Tong and Robert Zeillinger who have educated me and provided feedback on this work. Dietmar's advice in statistics, data evaluation and interpretation as well as his creative and intelligent input in numerous research discussions were immeasurably motivating and instructive to me. Dan's scientific support and constructive criticism concerning writing manuscripts were an immense help for me and improved this diploma thesis and the attached manuscripts very much. I especially thank Stefanie Aust for her clinical expertise and friendship. She has been a great support for my work and her enthusiasm was a great motivation.

Furthermore, my appreciation goes to Theresia Thalhammer for the collaboration and for providing the TissueFAXS/TissueQuest/HistoQuest facility as well as to Erika Bajna, Giovanna Bises, Marion Gröger, Radu Rogojanu and Ciprian Husanu for their excellent technical support.

I also want to thank Johannes Schmidt for the inspiring discussions in the course of a thesis seminar, Georg Heinze for the statistical expertise and Weimin Tong for the pathological expertise.

My deepest appreciation goes to my family, especially to my parents, who supported me unconditionally.

## 10 Curriculum Vitae

### Personal data

Name	Anna Bachmayr-Heyda
Date and place of birth	August 3 <sup>rd</sup> 1986, Bregenz, Austria
Nationality	Austria

### Education

2011 – 2012	Diploma thesis at the Molecular Oncology Group, Department of Obstetrics and Gynecology, Medical University of Vienna, Austria
2010	Erasmus: Studies in Biochemistry, Facultad de Ciencias, Universidad Autónoma de Madrid, Spain
Since 2008	Studies in Microbiology and Genetics, University of Vienna, Austria
2006 – 2008	Studies in Biology, University of Vienna, Austria
2005 – 2006	Studies in Mathematics, University of Vienna, Austria
2001 – 2004	BG Gallusstraße, Bregenz, Austria Grammar school focused on modern languages
1996 – 2011	BG Bludenz, Austria Grammar school focused on modern languages

### Working experience

Since 2010	Tutor in students' laboratory exercises "Semicompulsory Lab Course Organic Chemistry" and "Laboratory Course in Organic Chemistry – for the specialization Molecular Biology", Ass.-Prof. Dr. Krois, University of Vienna
------------	---

**Publications (manuscripts see attached)**

**Bachmayr-Heyda A.**, Aust S., Heinze G., Braicu E. I., Sehouli J., Lambrechts S., Vergote I., Mahner S., Pils D., Schuster E., Thalhammer T., Horvat R., Zeillinger R., Cacsire Castillo-Tong D. Prognostic impact of tumor infiltrating CD8+ T cells and Ki67 proliferation index in ovarian cancer patients – A study of the OVCAD consortium. Submitted to: *Clinical Cancer Research*

Aust S., **Bachmayr-Heyda A.**, Pils D., Zhao L., Tong W., Berger A., Fogel M., Thalhammer T., Sehouli J., Horvat R., Zeillinger R., Castillo-Tong D. Determination of tumor infiltrating CD8+ lymphocytes in human ovarian cancer. Submitted to: *International Journal of Gynecological Pathology*

Aust S., **Bachmayr-Heyda A.**, Tong D., Darb-Esfahani S., Denkert C., Chekerov R., Sehouli J., Mahner S., Van Gorp T., Vergote I., Speiser P., Horvat R., Zeillinger R., Pils D. Role of TRAP1 and estrogen receptor alpha in patients with ovarian cancer – A study of the OVCAD consortium. Submitted to: *Molecular Cancer*